

Dissertation zur Erlangung des Doktorgrades
der Fakultät für Chemie und Pharmazie
der Ludwig-Maximilians-Universität München

**The nucleolus: a nuclear compartment
with impact on cytoplasmic mRNA
localization**



Stephan Jellbauer
aus
München

2009

Erklärung

Diese Dissertation wurde im Sinne von § 13 Abs. 3 der Promotionsordnung vom 29. Januar 1998 von Herrn Prof. Dr. Ralf-Peter Jansen betreut.

Ehrenwörtliche Versicherung

Diese Dissertation wurde selbständig und ohne unerlaubte Hilfe erarbeitet.

München, den 16. April 2009

.....

Dissertation eingereicht am 16. April 2009

Erster Gutachter Prof. Dr. Ralf-Peter Jansen

Zweiter Gutachter Prof. Dr. Roland Beckmann

Mündliche Prüfung am 27. Mai 2009

Parts of the present thesis have been published:

Stephan Jellbauer and Ralf-Peter Jansen:
A putative function of the nucleolus in the assembly or maturation of specialized messenger ribonucleoprotein complexes.
RNA Biology **5**(4): 225-229 (2008).

Tung-Gia Du* & Stephan Jellbauer*, Marisa Müller, Maria Schmid, Dierk Niessing
and Ralf-Peter Jansen:
Nuclear transit of the RNA-binding protein She2 is required for translational control of localized *ASH1* mRNA.
EMBO Reports **9**(8): 781-787 (2008).
* these authors contributed equally to this work

A collaboration with the laboratory of Dierk Niessing resulted in the following publication:

Alexander Heuck, Tung-Gia Du, Stephan Jellbauer, Klaus Richter, Claudia Kruse, Sigrun Jaklin, Marisa Müller, Johannes Buchner, Dierk Niessing, Ralf-Peter Jansen and Dierk Niessing:
Monomeric myosin V uses two binding regions for the assembly of stable translocation complexes.
Proceedings of the National Academy of Sciences of the United States of America **104**(50): 19778-19783 (2007).

Contents

Contents	i
Abbreviations	iv
Summary	1
1. Introduction	2
1.1. The nucleolus	2
1.2. Biogenesis of ribosomes	3
1.3. Localization of mRNAs	6
1.4. A simple model system: mRNA localization in yeast	7
1.4.1. Localized mRNAs and <i>cis</i> -acting elements	7
1.4.2. <i>trans</i> -acting factors	9
1.5. The nuclear history of mRNA localization	11
1.6. Aim of this work	12
2. Results	14
2.1. The yeast-specific protein Loc1 localizes mainly to the nucleolus	14
2.2. The PUF family protein Puf6 localizes predominantly to the nucleolus	17
2.3. Loc1 and Puf6 purify with a large protein complex	18
2.4. Loc1 and Puf6 influence mRNA localization	21
2.5. Loc1 and Puf6 participate in ribosome biogenesis	27
2.5.1. Loc1 and Puf6 are large subunit biogenesis factors	27
2.5.2. Deletion of Loc1 delays large subunit rRNA processing	30
2.5.3. Total amount of ribosomes is reduced in Δ loc1 cells	32
2.6. <i>ASH1</i> mRNA is translationally silenced in the nucleolus	33
2.6.1. She2 and <i>ASH1</i> mRNA can be trapped in the nucleolus	33
2.6.2. Cytoplasmic retention of She2 influences Ash1 distribution	35
2.6.3. Cytoplasmic retention of She2 causes premature translation of <i>ASH1</i> mRNA ...	41
2.7. Loc1 does not inhibit <i>ASH1</i> mRNA translation directly	43
2.8. Function of Loc1 in mRNA localization and ribosome biogenesis seems to be coupled	44
2.8.1. Loc1 truncation analysis does not identify separable functional domains	44
2.8.2. Rapid and efficient depletion of Loc1 from yeast cultures is possible with glucose shut-off	49
2.8.3. Depletion of Loc1 affects <i>ASH1</i> mRNA localization and ribosome biogenesis simultaneously	53
2.9. Future directions	56
2.9.1. Translational regulation of <i>ASH1</i> mRNA might be tightened by modifications ..	56
2.9.2. Loc1 might act as a chaperone for RNA folding	58
3. Discussion	62
3.1. The nucleolar protein Loc1 influences mRNA localization	62

3.2. The nucleolus is a site of ribonucleoprotein maturation	63
3.2.1. Signal recognition particle (SRP)	64
3.2.2. The nucleolus and viral infection	65
3.2.3. The nucleolus and cytoplasmic mRNA localization	65
3.2.4. A model of nucleolar function in mRNA localization	67
3.2.5. Implications of a nucleolar role in mRNP formation.....	70
3.3. Loc1 and Puf6 contribute to biogenesis of 60S ribosomal subunits	71
3.4. Loc1 might contribute to remodeling of mRNAs in the nucleolus.....	74
4. Materials.....	77
4.1. Chemicals – Enzymes – Antibodies	77
4.1.1. Enzymes & Proteins	77
4.1.2. Antibiotics & Drugs	77
4.1.3. Special chemicals	78
4.1.4. DNA, RNA & Size Standards	78
4.1.5. Antibodies.....	78
4.2. Strains	79
4.2.1. Yeast strains.....	79
4.2.2. <i>Escherichia coli</i> strains	82
4.3. Plasmids	82
4.4. Oligonucleotides	84
4.4.1. Directly labeled oligonucleotides.....	84
4.4.2. Oligonucleotides for generation of labeled probes	85
4.4.3. Oligonucleotides for gene disruption	85
4.4.4. Oligonucleotides for epitope tagging	86
4.4.5. Oligonucleotides for sequencing or verifying knockouts/taggings	87
4.4.6. Oligonucleotides for cloning	88
4.4.7. Oligonucleotides for site-directed mutagenesis.....	89
4.5. Buffers – Media.....	90
4.5.1. General Buffers	90
4.5.2. Media	90
4.5.3. Consumables.....	91
4.5.4. Devices.....	91
4.5.5. Commercial Kits	92
4.5.6. Stockists	92
5. Methods.....	94
5.1. Methods in molecular biology	94
5.1.1. Agarose gel electrophoresis.....	94
5.1.2. Digestion of DNA with restriction endonucleases	94
5.1.3. Purification of DNA fragments from agarose gels	95
5.1.4. Ligation of DNA fragments.....	95
5.1.5. Polymerase chain reaction (PCR)	95
5.1.6. Extraction and ethanol precipitation of nucleic acids.....	96
5.1.7. RNA extraction for Northern Blots.....	97
5.1.8. Sequencing of DNA	97
5.1.9. Northern Blot.....	97

Contents

5.1.10. Mapping of 2'-O-methylated nucleotides and Ψ residues	98
5.2. Biochemical methods.....	100
5.2.1. SDS-PAGE	100
5.2.2. Denaturing protein extraction	101
5.2.3. Western Blot	102
5.2.4. Sucrose density gradient centrifugation	103
5.2.5. Tandem affinity purification	104
5.2.6. Preparation of glass beads for cell lysis	105
5.3. Working with <i>Escherichia coli</i>	105
5.3.1. Transformation of chemical competent <i>Escherichia coli</i> TOP10	105
5.3.2. Isolation of plasmids from <i>E. coli</i>	106
5.3.3. Overexpression and purification of His ₆ -tagged proteins.....	106
5.3.4. <i>in vivo</i> RNA chaperone assay	106
5.4. Yeast techniques	108
5.4.1. Dot test	108
5.4.2. Transformation of plasmids into yeast	108
5.4.3. Gene disruption and epitope-tagging	108
5.4.4. Mating of yeast strains	109
5.4.5. Sporulation and tetrad dissection.....	110
5.4.6. <i>in vivo</i> pulse labeling.....	110
5.4.7. Time course for combined Western/Northern Blot	110
5.4.8. Long-term storage of cultures	111
5.5. Microscopy	112
5.5.1. Live cell imaging.....	112
5.5.2. Indirect immunofluorescence.....	112
5.5.3. Fluorescent <i>in situ</i> hybridization.....	114
5.5.4. Statistical analysis	116
6. References	117
Acknowledgements	127
Curriculum Vitae.....	129

Note: Throughout this thesis, uppercase italic letters refer to *Saccharomyces cerevisiae* genes and mRNAs; lowercase italic letters refer to temperature sensitive mutants. Gene knockouts are designated by the Greek letter delta (Δ) in front of the gene name in lowercase letters. Proteins are referred to by standard letters, with the initial letter uppercase; the suffix p has always been omitted.

Abbreviations

aa	amino acid
C-terminus	carboxy terminus
Da	Dalton (atomic mass unit)
DFC	dense fibrillar compartment
DNA	deoxyribonucleic acid
et al.	et alii (Latin “and others”)
FC	fibrillar centers
FISH	fluorescent <i>in situ</i> hybridization
GC	granular component
GFP	green fluorescent protein
HO endonuclease	homothallic switching endonuclease
IF	(indirect) immunofluorescence
LE	localization element
LSU	large (ribosomal) subunit
M	molar
mRNA	messenger ribonucleic acid
N-terminus	amino terminus
NLS	nuclear localization sequence
nt	nucleotide
OD	optical density
ORF	open reading frame
RNP	ribonucleoprotein
rRNA	ribosomal ribonucleic acid
S	Svedberg (sedimentation coefficient unit)
snoRNA	small nucleolar ribonucleic acid
snRNA	small nuclear ribonucleic acid
SSU	small (ribosomal) subunit
ts	temperature sensitive
UTR	untranslated region
Ψ	pseudouridine

Δει διαλαβειν ότι και ο πολυς λόγος
και ο βραχυς εις τὸ αυτὸ συντεινει.

Epikur, *Sprüche* 26.

Summary

The nucleolus is the most prominent subnuclear compartment in eukaryotic cells. It has a central function in the biogenesis of ribosomal subunits, but the past decade has revealed that a variety of additional non-ribosomal ribonucleoprotein (RNP) complexes require passage through the nucleolus during their maturation as well. Examples include small nuclear RNPs (snRNPs), the signal recognition particle (SRP), and viral RNPs. Recent data show that also specific localized messenger RNAs (mRNAs) or proteins implicated in their localization either reside predominantly in the nucleolus or accumulate there under certain conditions.

This study presents evidence that two mainly nucleolar RNA-binding proteins of the yeast *Saccharomyces cerevisiae*, Loc1 and Puf6, influence the localization of *ASH1* mRNA as well as the biogenesis of large ribosomal subunits.

In addition, this study shows that block of nuclear mRNA export leads to accumulation of an RNA-binding protein crucial for localization of mRNAs, She2, and *ASH1* mRNA in the nucleolus. Results in this thesis indicate that nuclear exclusion of She2 impairs translational regulation of *ASH1* mRNA, a phenotype also observed for knockouts of *LOC1* and *PUF6*.

Detailed analysis of Loc1 function in this work demonstrates that it contributes to localization of other targeted mRNAs as well, that it does not directly inhibit translation of *ASH1* mRNA and that it is involved in specific steps during biogenesis of the large ribosomal subunit. Data from truncation analysis and rapid depletion of Loc1 indicate coupling of its function in mRNA localization and ribosome biogenesis.

Taken together, the results presented in this study suggest that nucleolar transit of localized mRNAs and of RNA-binding proteins such as She2 is necessary for proper translational control of localizing mRNPs. Loc1 might act in this process as an RNA chaperone, a function that could also explain its contribution to large ribosomal subunit biogenesis.

Die aufmerksame Pflege und Prüfung der wissenschaftlichen Überlieferung (...) [bildet] ein Moment der Erkenntnis (...).

Max Horkheimer & Theodor W. Adorno,
Dialektik der Aufklärung, Vorrede

1. Introduction

1.1. The nucleolus

The nucleus is one of the largest organelles in eukaryotic cells. It is surrounded by a double membrane and its interior is highly organized into a variety of subnuclear domains of specialized functions, such as Cajal bodies, promyelolytic leukemia oncoprotein (PML) bodies, nuclear speckles, and, most prominent, the nucleolus (Handwerger & Gall, 2006). A membrane does not surround any of the intranuclear domains and organelles, which rather form by self-organization (Misteli, 2001), yielding steady-state structures composed of dynamic components without a rigid architectural framework (Colau et al., 2004).

The nucleolus has been discovered by the Italian natural scientist Felice Fontana (Fontana, 1781; for a brief historical overview of science involving the nucleolus see Maggi & Weber, 2005). Electron microscopy (EM) studies have been the basis for the definition of three structural subcompartments, referred to as the fibrillar centers (FC), the dense fibrillar compartment (DFC), and the granular component (GC) (Figure 1).

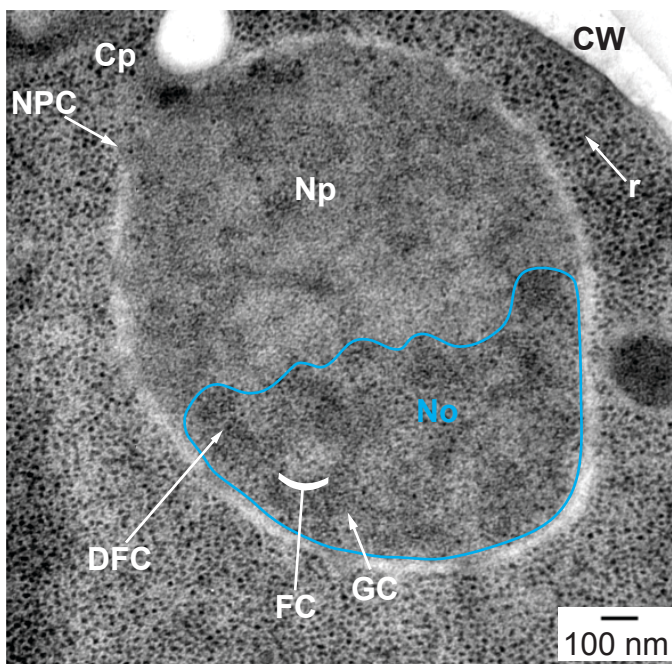


Figure 1 | Nuclear ultrastructure of *Saccharomyces cerevisiae*.

In the electron microscopic image of a yeast nucleus, the nuclear envelope appears as a thin ring. The nucleolus (No, cyan) occupies about one third of the nuclear area. Fibrillar centers (FC) are surrounded by the dense fibrillar compartment (DFC). The remaining nucleolar volume is occupied by the granular component (GC). The image shown was recorded after cryofixation and cryosubstitution from yeast strain S288C. Image courtesy of Isabelle Léger-Silvestre, Université Paul Sabatier, Toulouse, France. Annotation and methodology: I. Léger-Silvestre, personal communication. Abbreviations: Cp – cytoplasm; CW – cell wall; Np – nucleoplasm; NPC – nuclear pore complex; r – ribosome.

This traditional view has been challenged with the suggestion that tripartite nucleoli are only present in amniote vertebrates, whereas most other eukaryotes contain only bipartite nucleoli, composed of fibrillar strands (F) embedded in granules (G) (Thiry & Lafontaine, 2005). However, this hypothesis requires a very strict definition of FCs. A broader definition based on ultrastructural comparative morphology upholds the original allocation I will use throughout this thesis (Trumtel et al., 2000, Isabelle Léger-Silvestre, personal communication). At any rate, proportions and arrangement of nucleolar components are not static, but vary depending on environmental conditions, cell type and species (Raška et al., 2006).

In contrast to higher eukaryotes, the budding yeast *Saccharomyces cerevisiae* (simply referred to as yeast in this study), a unicellular eukaryotic model organism, contains only one nucleolus, which assembles around the rDNA repeats of chromosome XII (Johnston et al., 1997). It has the shape of a crescent and occupies about one third of the nucleus (Figure 1; Carmo-Fonseca et al., 2000). Yeast undergoes closed mitosis, and the nucleolus is separated very late during mitosis, regulated by the FEAR (for *Cdc14* early anaphase release) network (D'Amours et al., 2004; Torres-Rosell et al., 2004).

1.2. Biogenesis of ribosomes

The primary function of nucleoli is to carry out the initial steps of one of the most important cellular processes, ribosome biogenesis. Ribosomes are complex ribonucleoprotein (RNP) particles composed of one large subunit (LSU) and one small subunit (SSU) that are responsible for protein synthesis. In yeast, like in all eukaryotic cells, the small subunit sediments at a rate of 40S, the large subunit at 60S, and the complete ribosome at 80S (Chao, 1957; Chao & Schachman, 1956). 32 ribosomal proteins (rpS) and the 1798 nucleotide (nt)-containing 18S rRNA form the small subunit in yeast, whereas the large subunit is made up of 46 ribosomal proteins (rpL) and three rRNA species – 25S rRNA (3392 nt), 5.8S rRNA (158 nt), and 5S rRNA (121 nt) (Spahn et al., 2001). To ensure adequate supply of newly synthesized proteins, each yeast cell possesses about 200,000 ribosomes (Warner, 1999). This means that rapidly dividing cells have an enormous need of new ribosomes, and in fact a major part of the transcriptional activity in growing cells is dedicated to ribosome biogenesis. RNA polymerase I (Pol I) provides 25S, 5.8S, and

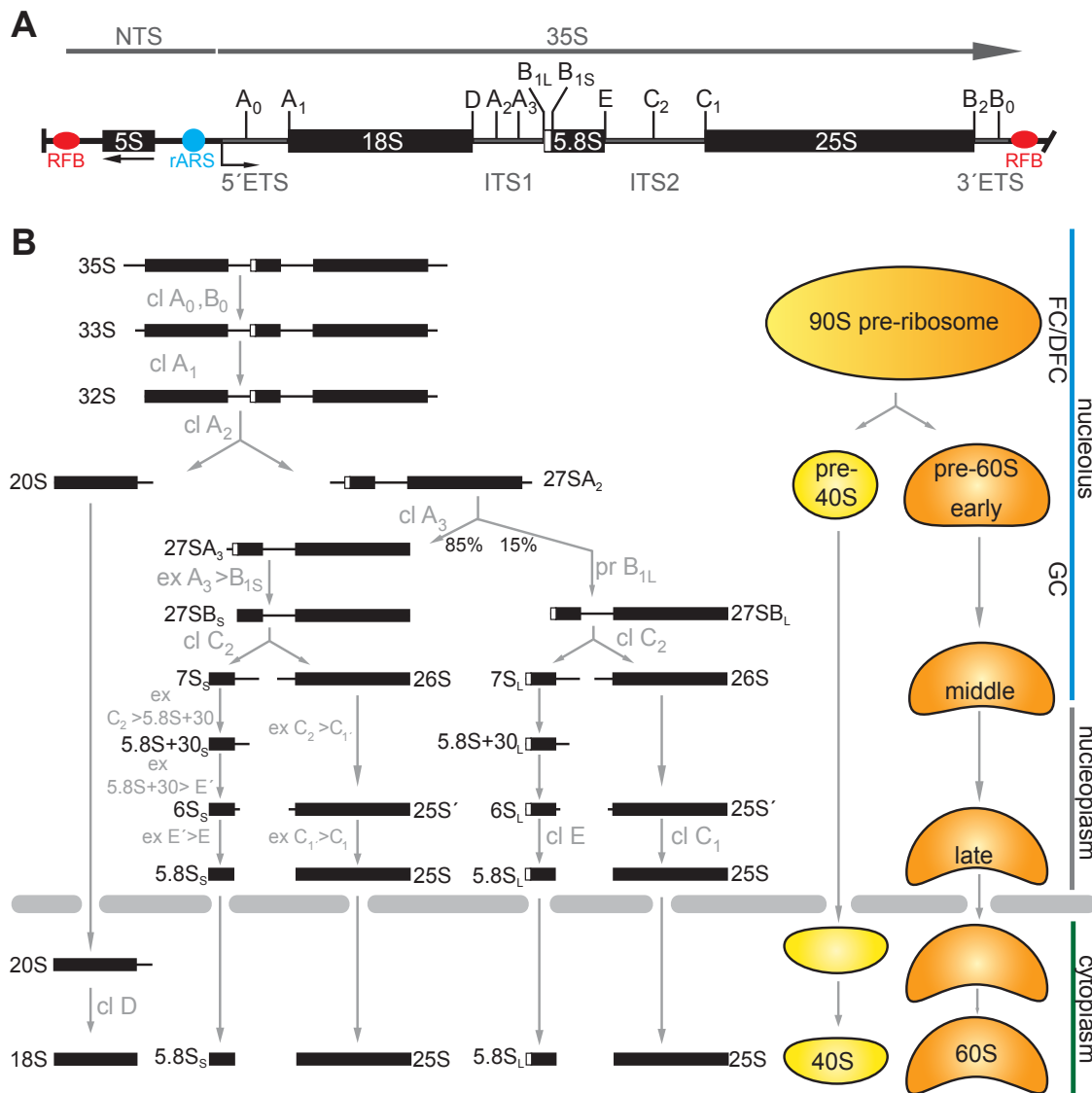


Figure 2 | Ribosome biogenesis in *Saccharomyces cerevisiae*.

A | Structural organization of yeast ribosomal DNA (rDNA) repeats. Each 9.1 kb rDNA repeat is organized into a Pol I transcription unit (35S), and a nontranscribed spacer (NTS). The NTS contains two *cis*-acting elements, a replication fork barrier (RFB), and an autonomously replicating sequence (rARS). A 5S rRNA Pol III transcription unit (5S) is located between rARS and RFB. The transcript of the 35S rDNA contains the 18S, 5.8S, and 25S rRNAs separated by spacer sequences – two external transcribed spacers (ETS) and two internal transcribed spacers (ITS), respectively. Cleavage and processing sites are indicated (see below for details). (Figure adapted from Burkhalter & Sogo, 2004; Fromont-Racine et al., 2003).

B | Processing of pre-rRNAs and assembly of ribosomes. Following initial cleavages at different sites of the primary transcript in the 90S pre-ribosome, cleavage at site A₂ separates pre-40S and pre-60S particles. While small subunit precursors are exported to the cytoplasm relatively fast, pre-rRNAs of the large subunit precursors are subjected to extensive cleavage and processing. The great majority of pre-60S rRNAs are processed starting with cleavage of 27SA₂ rRNA at site A₃, but a substantial part is alternatively processed directly at site B_{1L}. (Figure adapted from Fromont-Racine et al., 2003; Henras et al., 2008). Abbreviations: cl – cleavage; pr – processing; ex – exonuclease processing.

18S rRNA, RNA polymerase II (Pol II) transcribes the ribosomal protein genes, and RNA polymerase III (Pol III) provides 5S rRNA (for review, see Cramer et al., 2008). This coordinated action of all three eukaryotic transcription machineries

accounts for approximately 80% of nuclear transcription in yeast (Moss & Stefanovsky, 2002).

Ribosome biogenesis has been studied in great detail in *S. cerevisiae* over the past 40 years (for a recent review, see Henras et al., 2008). A substantial part of this process takes place inside the nucleolus, whose ultrastructural organization is thought to reflect the vectorial nature of ribosome biogenesis – pre-ribosomes move from the fibrillar to the granular parts and then out of the nucleolus to the nucleoplasm (Thiry & Lafontaine, 2005).

The rRNAs are encoded by ribosomal DNA (rDNA), which is organized in 100 – 200 9.1 kb repeats on the long arm of chromosome XII (Figure 2A; Johnston et al., 1997). Transcription by Pol I and co-transcriptional recruitment of a variety of factors, including the U3 snoRNP, ribosomal proteins and mostly pre-40S ribosome biogenesis factors to the primary transcript yields the first detectable ribosome precursor, termed the 90S pre-ribosome (Figure 2B; Dragon et al., 2002; Grandi et al., 2002). Cleavage at site A₂ leads to formation of pre-40S and pre-60S particles. While the pre-40S subunit is associated with only eight major non-ribosomal proteins and exported to the cytoplasm relatively fast (Schäfer et al., 2003), elaborate processing of rRNA precursors accompanied by rearrangements in protein composition is required for pre-60S subunit maturation (Figure 2B; Harnpicharnchai et al., 2001; Nissan et al., 2002; Saveanu et al., 2003); notably, the number of associated non-ribosomal factors decreases from early to late pre-60S particles (Nissan et al., 2002). The intermediate 27SA₂ pre-rRNA can be further processed following two mutually exclusive paths, finally resulting in two different populations of ribosomes containing a short (S) and a long (L) form of 5.8S rRNA (Henras et al., 2008).

Besides exo- and endonucleolytic cleavage steps, nucleolar processing of rRNAs also involves post-transcriptional modification of nucleotides such as pseudouridylation and 2'-O-ribose methylation (Figure 29A; Reichow et al., 2007). A set of guide snoRNAs target specific nucleotides by direct base pairing. The C/D class of snoRNPs carries out methylation, whereas H/ACA class snoRNPs convert uridine to pseudouridine (for review see Matera et al., 2007). Interestingly, snoRNPs modify not only rRNAs and snRNAs, but probably also other cellular RNAs including mRNAs (Gerbi et al., 2003; Kiss, 2002). Export-competent pre-ribosomal particles are transported to the cytoplasm, where final maturation

occurs. Nuclear export involves a Ran GTPase cycle and a specific subset of nucleoporins (Henras et al., 2008). In total, the astounding number of about 200 non-ribosomal proteins is implicated in ribosome biogenesis.

1.3. Localization of mRNAs

Polarity is a characteristic trait common to nearly all kinds of cells. One important mechanism cells apply to establish polarity is the localization of messenger RNAs coupled to local translation. Recent studies suggest that mRNA localization in eukaryotic cells is much more prevalent than anticipated and serves a large number of biological functions (see for example Lécuyer et al., 2007). Localization of mRNAs has several advantages over localization of proteins. Besides spatial restriction of gene expression that can be easily regulated over time, targeting of mRNAs is economic because it allows production of multiple protein molecules at the target site with active transport of just one mRNA molecule. Finally, proteins may have properties undesirable at sites other than the destination (Martin & Ephrussi, 2009).

Localized mRNAs are probably best known for their role during development in metazoans, with *Drosophila* and *Xenopus* oocytes as the classic model systems. For example, *Vg1* mRNA encodes a TGF- β (for transforming growth factor) family protein that functions in mesoderm induction and is targeted to the vegetal pole of *Xenopus* oocytes after the first stages of their development (Figure 3A; Kress et al., 2004). In *Drosophila* oocytes, *oskar* is an mRNA that localizes to the posterior pole; the corresponding Oskar protein is required for the assembly of an RNP that directs posterior development (Figure 3B; Wilhelm & Smibert, 2005).

A prominent example of a localized mRNA in mammalian cells is β -*actin* mRNA that is delivered to the leading edge of lamellipodia in migrating fibroblasts, where the corresponding protein is required for movement (Figure 3C; Condeelis & Singer, 2005). Stepping back to very simple eukaryotes, *S. cerevisiae* constitutes an excellent model organism to study the basic mechanisms of mRNA localization.

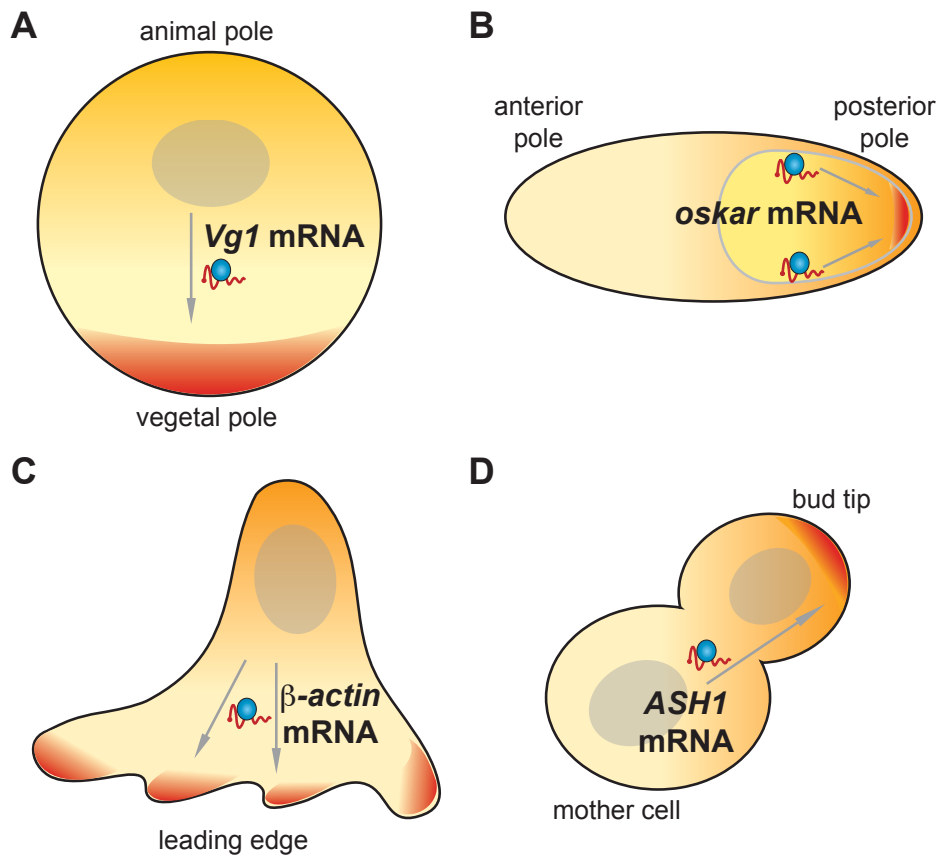


Figure 3 | Examples of localized mRNAs.

RNA-binding proteins (blue) and mRNAs (red) form localizing RNPs that travel along cytoskeletal filaments to their respective destination. Correct localization of all example mRNPs presented depends on their nuclear history (see section 1.5).

A | *Vg1* is a late pathway mRNA that localizes to the vegetal pole of *Xenopus laevis* oocytes at later stages of their development. The RNP is transported along microtubules

B | In *Drosophila melanogaster*, *oskar* mRNA is transported along microtubules to the posterior pole of oocytes.

C | β -actin mRNA is targeted to the leading edge of lamellipodia in chicken and mammalian fibroblasts utilizing actin/myosin dependent transport.

D | mRNPs containing *ASH1* mRNA travel along actin filaments to the tip of the daughter cell in *Saccharomyces cerevisiae*. Figure based on Martin & Ephrussi, 2009.

1.4. A simple model system: mRNA localization in yeast

1.4.1. Localized mRNAs and *cis*-acting elements

Over the past years, around 30 mRNAs have been demonstrated to localize at least partially in yeast; Table 1 shows a selection of mRNAs that strongly accumulate at the bud tip or in the bud (Aronov et al., 2007; Shepard et al., 2003). In addition, there are several mRNAs that are targeted to mitochondria. A significant number of localized mRNAs codes for membrane or membrane-associated proteins (Schmid et al., 2006), for example *IST2* (for increased sodium tolerance), a putative channel, and *WSC2* (for cell wall integrity and stress response component), a

regulator of a signaling pathway (Entian et al., 1999; Takizawa et al., 2000; Verna et al., 1997).

Table 1 | Localized yeast messenger RNAs.

Only mRNAs of verified ORFs with $\geq 60\%$ bud localization are listed under their current standard name (SGDproject, March 2009). Data from Aronov et al., 2007; Shepard et al., 2003.

Gene	Cell cycle regulation	Protein localization
<i>ASH1</i>	M	bud nucleus
<i>BRO1</i>	none	punctae on vacuole
<i>CDC42</i>	n/a	bud tip
<i>CLB2</i>	M	nuclei, spindle pole
<i>CPS1</i>	none	cytoplasmic punctae
<i>DNM1</i>	S	mitochondrial periphery
<i>EAR1</i>	none	endoplasmic reticulum
<i>EGT2</i>	M	membranes, large bud
<i>ERG2</i>	M	endoplasmic reticulum
<i>IRC8</i>	M	membranes, bud
<i>IST2</i>	none	bud plasma membrane
<i>MID2</i>	none	cell periphery, mother-bud junction
<i>MMR1</i>	M	bud sites & tips, mother-bud junction
<i>SEC4</i>	n/a	bud tip
<i>SRL1</i>	G ₁	periphery of small buds
<i>SRO7</i>	n/a	bud tip
<i>TAM41</i>	none	mitochondria
<i>TCB2</i>	none	membranes, bud
<i>TCB3</i>	G ₂	membranes, bud
<i>TPO1</i>	M	bud plasma membrane
<i>WSC2</i>	S	membranes, bud

The most substantial part of the knowledge on mRNA localization in yeast derives from studies on *ASH1*, which encodes a transcriptional repressor (see below) and is probably the best-characterized targeted mRNA.

Four structured *cis*-acting sequences, termed localization elements (LEs) or zip codes, participate in targeting of *ASH1* mRNA. While the E3 LE lies mostly in the 3'-

untranslated region (UTR) of the *ASH1* ORF, the elements E1, E2A, and E2B are entirely located in the coding region (Figure 4A; Chartrand et al., 1999). Each LE alone is sufficient for localization, but they need to cooperate to anchor *ASH1* at the target site (Jansen, 2001). In contrast to metazoans, localization elements that map to the coding sequence seem to be a general theme in yeast (Shepard et al., 2003); *IST2* mRNA contains one LE near the 3'-end of the ORF (nt 2694-2785), *WSC2* mRNA one in the 5'-part (nt 418-471) and one in the 3'-part (nt 1313-1384) of the ORF (Jambhekar et al., 2005; Olivier et al., 2005). The localization elements are predicted to fold into hairpin stem loops as represented schematically in Figure 4A; recognition of an LE by RNA-binding proteins depends on precise three-dimensional structures as well as secondary structure and certain nucleotides in the primary sequence (Jambhekar & DeRisi, 2007).

1.4.2. *trans*-acting factors

Interestingly, a small set of proteins, comprising She proteins and few additional factors, seems to be sufficient to transport all localized transcripts, despite their large number. Five *SHE* (for \underline{S} wi5-dependent *HO* expression) genes have been identified in a screen for mother cell-specific activators of *HO* expression (Jansen et al., 1996). *HO* encodes an endonuclease that allows haploid *S. cerevisiae* cells to switch between the two mating types \mathbf{a} and α ; however, it is only expressed in cells that have previously budded (so-called mother cells). In daughter cells (i.e. former buds that have not yet budded themselves), *HO* transcription is repressed by Ash1, whose corresponding mRNA is localized to the bud tip during cell division (Bobola et al., 1996; Long et al., 1997).

Three of the five She proteins participate directly in transport of *ASH1* and all other localized mRNAs characterized so far (Figure 4B). She2 is the key RNA-binding protein; it binds directly to all four *ASH1* LEs as well as to the LEs of other localized mRNAs (Figure 4; Böhl et al., 2000; Shepard et al., 2003). Structure determination of a truncated version of She2 by X-ray crystallography identified a particular RNA-binding motif termed basic helical hairpin, and additional experiments suggested that dimerization is indispensable for correct function (Niessing et al., 2004).

The motor protein responsible for the transport of localized mRNPs towards the barbed end of actin filaments at the bud tip is a class V myosin, Myo4 (She1;

Haarer et al., 1994; Jansen et al., 1996; for review, see Sellers, 2000). Myo4 does not interact directly with She2-mRNA complexes; instead, it binds with its C-terminal tail and a coiled-coil region to the N-terminal domain of an adapter protein, She3 (Heuck et al., 2007). The C-terminal domain of She3, in turn, interacts with She2 (Böhl et al., 2000).

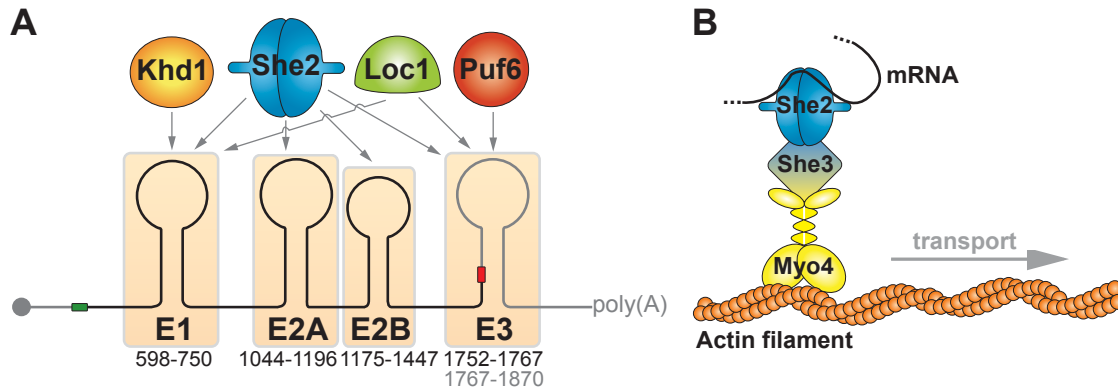


Figure 4 | cis-acting elements and trans-acting factors involved in *ASH1* mRNA localization.

A | *ASH1* mRNA contains four localization elements (LE), E1, E2A, E2B, and E3 (numbers indicate nucleotides relative to start of coding sequence). The first three LE lie within the coding region, indicated by the black line between the Start (green rectangle) and the Stop (red rectangle) codon of the *ASH1* ORF, whereas most of the 118 nt E3 LE is located in the 3'-UTR. She2 binds to all four LE. Loc1 has been shown to bind to E1 and E3, while Khd1 and Puf6 bind to a single LE, E1 and E3, respectively.

B | Core transport components of mRNA localization in yeast. She2 binds directly to the respective mRNA. She3 serves as an adaptor between the RNA-binding protein and the motor protein, Myo4, which transports the mRNP along actin filaments to the bud.

Apart from the She proteins, additional factors are required to ensure correct localization of mRNAs (Figure 4B), at least for *ASH1* mRNA, which is the model mRNA where the major part of data available so far stems from. Khd1 (for hnRNP K homology-domain protein), a protein shuttling between nucleus and cytoplasm, binds to the E1 LE and represses translation of *ASH1* mRNA during transport (Irie et al., 2002). Translational silencing is accomplished through interaction with Tif4631, the yeast homolog of eukaryotic translation initiation factor eIF4G1. At the target site, Yck1 (for yeast casein kinase) phosphorylates Khd1, releases it from the mRNA and thus activates translation (Paquin et al., 2007).

A second translational repressor of *ASH1* mRNA is Puf6, a member of the PUF protein family, named after *Drosophila melanogaster* Pumilio and *Caenorhabditis elegans* Fem-3 mRNA-binding factor (FBF). Contrary to Khd1, it binds the E3 LE and is predominantly located in nuclei (Gu et al., 2004). Likewise, Puf6 adopts a different mechanism to regulate translation. It interferes with translation initiation

through an RNA-dependent interaction with the yeast homolog of eIF5B, Fun12 (for function unknown now; Coleman et al., 1986; Deng et al., 2008). The translational block is lifted via phosphorylation of Puf6 by the casein kinase CK2. The exact function of another *trans*-acting factor, Loc1 (for localization of mRNA), is as yet unclear. Loc1 is exclusively nuclear, binds to two *ASH1* zip codes, E1 and E3, and cells where the *LOC1* gene is deleted show dramatic mislocalization of *ASH1* mRNA (Long et al., 2001). Another study proposed a role for Loc1 in translational regulation (Komili et al., 2007). In addition, there is data indicating that Loc1 does not only function in mRNA localization, but also in the biogenesis of ribosomes (Harnpicharnchai et al., 2001; Urbinati et al., 2006).

1.5. The nuclear history of mRNA localization

Localization of all RNAs necessarily starts in the nucleus, since this is the cellular compartment where transcription takes place. However, it has become clear that the role of the nucleus extends much further. A variety of nuclear or nuclear-cytoplasmic shuttling proteins are indispensable for the formation, translational regulation and correct localization of mRNPs (Figure 5; for review, see Giorgi & Moore, 2007).

Taking the mRNAs from Figure 3 as examples, the proteins Vg1RBP/vera and hnRNP I form a core RNP with *Vg1* mRNA before the complex is exported to the cytoplasm, where it is remodeled and transported to the vegetal cortex (Kress et al., 2004). In fibroblasts, the predominantly nuclear protein ZBP2 associates co-transcriptionally with *β -actin* mRNA to alleviate recruiting of ZBP1, a mammalian ortholog of Vg1RBP that influences localization and translational regulation (Hüttelmaier et al., 2005; Pan et al., 2007). Targeting of *oskar* mRNA to the posterior pole of *Drosophila* oocytes depends on interaction with proteins of the exon junction complex (EJC) in the nucleus (Hachet & Ephrussi, 2004). Finally, *trans*-acting factors of *ASH1* mRNA localization reside transiently or permanently in the nucleus, or more precisely in the nucleolus (see Results; Du et al., 2008). RNP assembly or remodeling steps that occur in the nucleoplasm or subnuclear compartments are not limited to the selected examples, and the nucleolus in particular is involved in the formation of a variety of RNPs other than ribosomes (see Discussion).

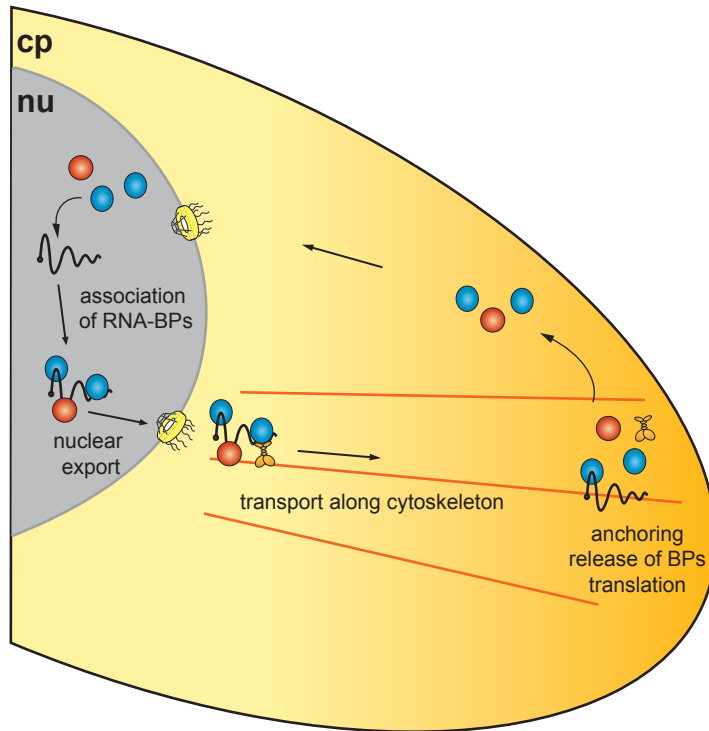


Figure 5 | Nucleo-cytoplasmic shuttling proteins participate in localization of mRNPs.

RNA-binding proteins (RNA-BPs) required for transport (blue) and/or translational regulation (red) associate with the primary transcript (black). Export-competent mRNPs leave the nucleus (nu) through nuclear pore complexes (NPCs, yellow). Subsequently, they are transported along the cytoskeleton with the help of motor proteins (orange) to their destination at the cell periphery. After anchoring, the proteins bound to the transcript are released, the mRNA is translated, and the RNA-BPs shuttle back to the nucleus. (Figure adapted from Farina & Singer, 2002).

1.6. Aim of this work

At the beginning of the project presented in this thesis, little was known about the exact roles of the two nuclear *trans*-acting factors of *ASH1* mRNA localization, Loc1 and Puf6. Thus, an initial goal was to characterize these proteins in more detail, with a focus on exact subcellular localization and possibly well-characterized interacting proteins that might provide insights into function. Besides, I wanted to address the question whether the role of Loc1 and Puf6 is limited to *ASH1* mRNA localization or if they are *trans*-acting factors in the targeting of other mRNAs as well.

With more detailed data on nuclear factors of mRNA localization at hand and findings that the nucleus or a nuclear compartment is involved in correct cytoplasmic localization of certain RNPs, the next goal was set: in a joint project with another Ph.D. student in our laboratory, Tung-Gia Du, we aimed at determination of a possible nuclear function in *ASH1* mRNA localization.

In a further approach, I focused on one *trans*-acting factor. Loc1 had been previously implicated in ribosome biogenesis, but analysis did not go beyond the finding that it participates in large subunit biogenesis. Thus, I wanted to

investigate its role in this central process more closely. Subsequently, I tried to find out if the function of Loc1 in ribosome biogenesis and mRNA localization is coupled or can be separated on a spatial or temporal level.

(...)da me non possa essere fatto maggiore dono che [dare] facultà a potere in brevissimo tempo intendere tutto quello che io, in tanti anni e con tanti mia disagi e pericoli, ho conosciuto e inteso.

Niccolò Machiavelli, *Il Principe*, Widmung.

2. Results

2.1. The yeast-specific protein Loc1 localizes mainly to the nucleolus

The protein Loc1 (for localization of mRNA) has first been described in a study that aimed at identification and characterization of factors involved in *ASH1* mRNA localization in addition to the She proteins (Long et al., 2001). In this study, immunofluorescence demonstrated that Loc1 localizes only to the nucleus (Long et al., 2001). Interestingly, Loc1 has also been found to associate with a nucleolar intermediate of a large ribosomal subunit precursor (Harnpicharnchai et al., 2001). In order to confirm presence of Loc1 in the nucleolus, I analyzed Loc1 distribution by fluorescence microscopy.

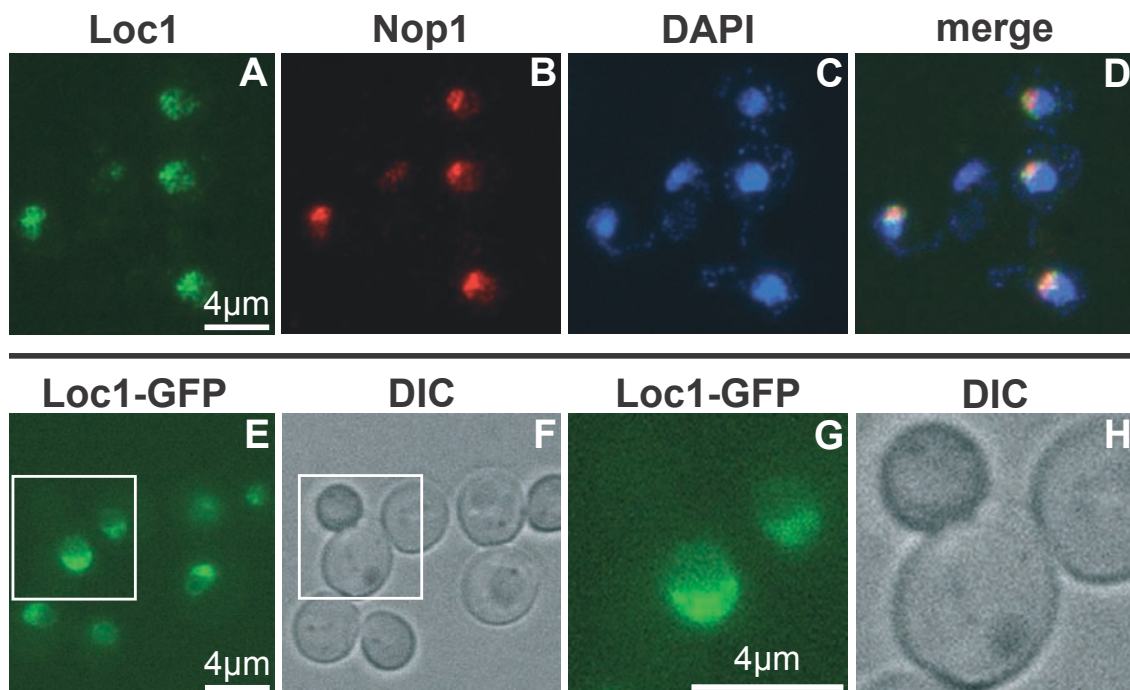


Figure 6 | Loc1 localizes predominantly to the nucleolus.

A-D | Cells expressing a HA₆-tagged version of Loc1 were stained by indirect immunofluorescence with antibodies directed against HA (A) and the nucleolar marker Nop1 (B). Nuclei were visualized with DAPI (C). Overlap of Loc1 and Nop1 staining in a distinct region of the nucleus (D) indicates nucleolar localization of Loc1.

E-H | Live imaging of cells expressing Loc1-GFP. The crescent-shaped GFP-signal (E) in the central region of the cells (F) suggests nucleolar localization of the protein. (G, H) Blow-up of a single cell from images E and F (white square).

With two different approaches, I detected a tagged version of Loc1 either by indirect immunofluorescence or by green fluorescent protein (GFP) live imaging (Figure 6). The Loc1-signal was crescent-shaped in both experiments (Figure 6A, E, G) and entirely confined inside a region of the nucleus stained with DAPI (Figure 6C, D), suggesting nucleolar localization. In addition, the Loc1-HA₆ signal largely overlapped with a nucleolar marker, the yeast homolog to fibrillarin (Nop1, Figure 6B, D).

Since Loc1 is implicated in ribosome biogenesis (Urbinati et al., 2006), a central process in all eukaryotes, I wondered whether it is a conserved protein.

I performed a BLAST search with the *S. cerevisiae* Loc1 amino acid sequence deposited in GenBank (Accession NP_116656; Altschul et al., 1997; Altschul et al., 2005). The amino acid sequence has no regions with high homology to known conserved domains. All sequences with high alignment scores (≥ 80 bits) in the BLAST search were proteins from the order Saccharomycetales (Hibbett et al., 2007) and are mostly hypothetical proteins. The eight closest homologs (bit score ≥ 150) were aligned using Clustal W (Figure 7; Larkin et al., 2007). The majority of absolutely conserved amino acids are charged either positively or negatively. Conserved amino acids are found over the entire protein sequence, with an accumulation around amino acids 90 to 130. Secondary structure prediction with Jpred (Cole et al., 2008) suggests α -helical stretches in the C-terminal half of the protein, but no β -sheets at all, since the detected regions are too short to form β -sheets (Figure 7). Judging from the prediction, especially the central third of Loc1 appears to be largely unstructured.

In summary, I confirmed the predominantly nucleolar localization of Loc1. The protein lacks conserved domains and seems to have no sequence homologs in eukaryotes other than yeasts.

Results



Sce MAPKKP---SKR--QNLRRREVAP~~EVFQDSQARNQLANVPHL~~TEKSAQRKPSKT 48
Cgl MGSIKK---TKGKSQSTKR~~VVTP~~EVFADQQARNQLANAPNLTEKSERRKANKL 50
Vpo MAVKKS---SKG--QOTREVRPE~~EVFQDKQARNQLANVPQL~~TEKSAHKKPNKL 48
Ego MAGKQTKTAKRAKTQ~~NRTREVTSEVFQDSQARNQLANAPKV~~-EKPSARKATKR 52
Kla MAPKQSKTAKRSKQ~~NGTREVRSEVFE~~DSIAKNQMANVPKMTEKSDTKKPTKL 53
Lel MAPRQSQTAKRNKTQ~~NKTR~~ENESEVFLDSAARNLLENQPKLAAKSKVKKLSKL 53
Cal MAPRQSKTAKRNKTQ~~NKTR~~TVDS~~EVFSDSA~~AKNLLADQPKLTPKSKVKKISKL 53
Dha MAPRQSKTAKRSKVQ~~NKTR~~TVES~~EVGSDSA~~ARNLLMSQPKLTPKSIVKAPSKA 53
Pst MAPRQSKTAKRSKTQ~~NKTR~~ANES~~EVFSDA~~SARNL~~MANQ~~PKLTEKSKVKKLSKR 53
* . : . : * . * . ** * * : * : . * : : * . : . *



Sce KVKKEQSLARLYGAKKDKKGYSEKDLNIP~~TLNRAIVPGVKIRRGKKGKFFIA~~ 101
Cgl QVKKEQARARLYGKKK-KESTYSEKDL~~DLPSLNKAVNPGVKLRRGKKGKFFID~~ 102
Vpo QVSKGQFKARLYGTTK-KDRKYTEKEL~~DIPTLNKAVIPGVKIKRGKKGKFFID~~ 100
Ego QVKKEQAVRRLYGTRKK-EKTYSEKEL~~NIPTLNRAIVPGV~~KIKTGKKGKFFVD 104
Kla QVKKDNFKARLYGSQKKKERRYTEKEL~~NIPTLNRAIVPGV~~KIKKGKKGKFFIG 106
Lel QVKKQQAKIRLYGAKNG--KEYREEQ~~LSIPDLNKAIVPGV~~KAKRGKKGKFFVD 104
Cal ALKKQQAKIRLYGAKNG--KEYREDQ~~LNIPTLNKAIVPGV~~KAKRGKKGKFFVD 104
Dha AVKKQQAKIRLYGARG--KEYREDQ~~LIPALNKAITPGV~~KAKKGKKGKFFVE 104
Pst VVKKQQAKIRLYGAKNG--KEYREDQ~~LIPTLNKAIPGV~~RAKKGKKGKFFVD 104
:. * : **** : . * * . : * . : * * * : * * : : * * * * * :



Sce DNDTLTLNRLITTIGDKYDDIAESKLEKAR~~RLEEIRELKRKEIERKEALKQDK~~ 154
Cgl DHDSLTLHRLIKTIGDKYDDITESKLEK~~DRRLEVIRELKRQEI~~ERKEAAKQSQ 155
Vpo DHDTLALNRLIKTIGDKYDDITESKLEK~~ARLEEIREIKRKEI~~EMKESLKNDK 153
Ego DHDLTLNRLIKTIGDKNDEVTE~~SKLEKAKRLEEIRELKKQ~~ELERKEQAKKEK 157
Kla DHDLIALNRLIKTIGDKNDEITE~~SKLEKTRLEEIRD~~LKRQEMERKETEKKEQ 159
Lel DNDSLTLNRLVKSINDKYDQVNE~~SKLEKSRLEEIRELKRQ~~EMERKEQM~~KKDK~~ 157
Cal DNDTLTMNRLVKSINDKYDQVNE~~SKLEKSRLEEIRD~~LKRQEI~~ERKEQQ~~KKDK 157
Dha DNDALTLNRLVKSINDKYDQANE~~SKLEKSRLE~~IRELKKQELERKEEQKENK 157
Pst DNDTLTSLRLVKSINDKYDVVNE~~SKLEKSRLEEL~~RELKKKEIERKEQQKMDK 157
* : * : : * * . : * . * * * * * : * * : : * : * : * : * * * * * . :



Sce LEEKKDEIKKKSSVARTIRRNKR~~DMLKSEAKASESKTEGRKVKKVSFAQ~~ 204
Cgl LEEKKDELKKKKS~~IARSMRRKNRRDQER-DLHTTSNDKVQR~~KKKSVSFA- 203
Vpo LEEKKNEIRSKASLARS~~MRRKNRRD~~TVRADVEEKSTNANKPKK~~VSFA-~~ 202
Ego LDDKMDELKRKASVARTL~~RRNKRHEKKLEDVP-KSS-~~-----K~~VSFA-~~ 199
Kla LEGKKDEIKKKASVARTIRRN~~TKRQELKQETLA-AQSEPI~~KKKSVSFA- 207
Lel LDGKKDELRSKASVARA~~ARRKNAKAR~~KADEVD-EGENTVP~~KKK-~~VSFA- 204
Cal LEGKKDELRSKASVAR~~STRRN~~AKARRADEESQE~~QEEES~~PKKK~~VSFV-~~ 206
Dha LEGKKNEVKSASLARAN~~RKSAKSQKNEESK--AASN--~~KGK~~VSFA-~~ 202
Pst LEGKKSELKNRASVAR~~SRRN~~AKAAK~~IEDE--ETDQPR~~KKTS~~VSFA-~~ 204
* : * . * : : : * : * * : * * . : : : : * * * * .

(previous page:)

Figure 7 | **Loc1 is predicted to contain α -helices and shows sequence conservation within mostly hypothetical proteins of the Saccharomycetales.**

Secondary structure prediction for the *Saccharomyces cerevisiae* Loc1 amino acid sequence (Sce, in bold; GenBank accession NP_116656) has been carried out using Jpred 3 (Cole et al., 2008). Predicted β -sheets are shown as orange arrows, predicted α -helices as red bars. Sequences were aligned with Clustal W2 (Larkin et al., 2007), using the eight most closely related proteins. These were identified by a BLAST search against the nr database (BLASTP2.2.19+, Score \geq 150 bits; Altschul et al., 1997; Altschul et al., 2005) and most of them are hypothetical proteins. Conserved aminoacids are shown in blue and marked by an asterisk below the sequences. In addition, conserved substitutions are indicated by a colon, and semi-conserved substitutions by a dot.

Cgl *Candida glabrata* (XP_446071); Vpo *Vanderwaltozyma polyspora* (XP_001645367); Ego *Eremothecium gossypii* (NP_986666); Kla *Kluyveromyces lactis* (XP_454593); Lel *Lodderomyces elongisporus* (XP_001526360); Cal *Candida albicans* (XP_721719); Dha *Debaryomyces hansenii* (XP_459244); Pst *Pichia stipitis* (XP_001387044).

2.2. The PUF family protein Puf6 localizes predominantly to the nucleolus

Proteins of the PUF family, named after *Drosophila melanogaster* Pumilio and *Caenorhabditis elegans* Fem-3 mRNA-binding factor (FBF) have been found in a great variety of eukaryotic species (Wharton & Aggarwal, 2006). The family consists of at least five subfamilies (Spasov & Jurecic, 2003). By binding to sequences in the 3' untranslated region (3'-UTR) of specific target mRNAs, PUF proteins regulate translation and stability of these mRNAs. The *S. cerevisiae* genome encodes six PUF proteins (Puf1-Puf6), which greatly differ in localization and RNA specificity (Gerber et al., 2004; Gu et al., 2004). In a pioneering study on Puf6, it was shown that Puf6 associates with the *ASH1* mRNP and is necessary to inhibit translation of the mRNA (Gu et al., 2004). In immunofluorescence and live imaging experiments in this study Puf6 was detected mainly in the nucleus.

Interestingly, Puf6 has also been found to associate with an early nucleolar pre-ribosomal particle, which was affinity-purified by a tagged version of Cic1/Nsa3 (for core interacting component; Jäger et al., 2001; Nissan et al., 2002). To verify nucleolar localization of Puf6, I performed fluorescence microscopy with tagged versions of the protein (Figure 8). Similar to Loc1, the Puf6-GFP signal is confined to a crescent-shaped region in the center of the cell (Figure 8, lower panel). Indirect immunofluorescence with Puf6-HA₆ proves that the signal is completely inside the nucleus (Figure 8C, D) and that it largely overlaps with the signal of the nucleolar marker Nop1 (Figure 8B, D). Thus, Puf6 indeed localizes predominantly to the nucleolus.

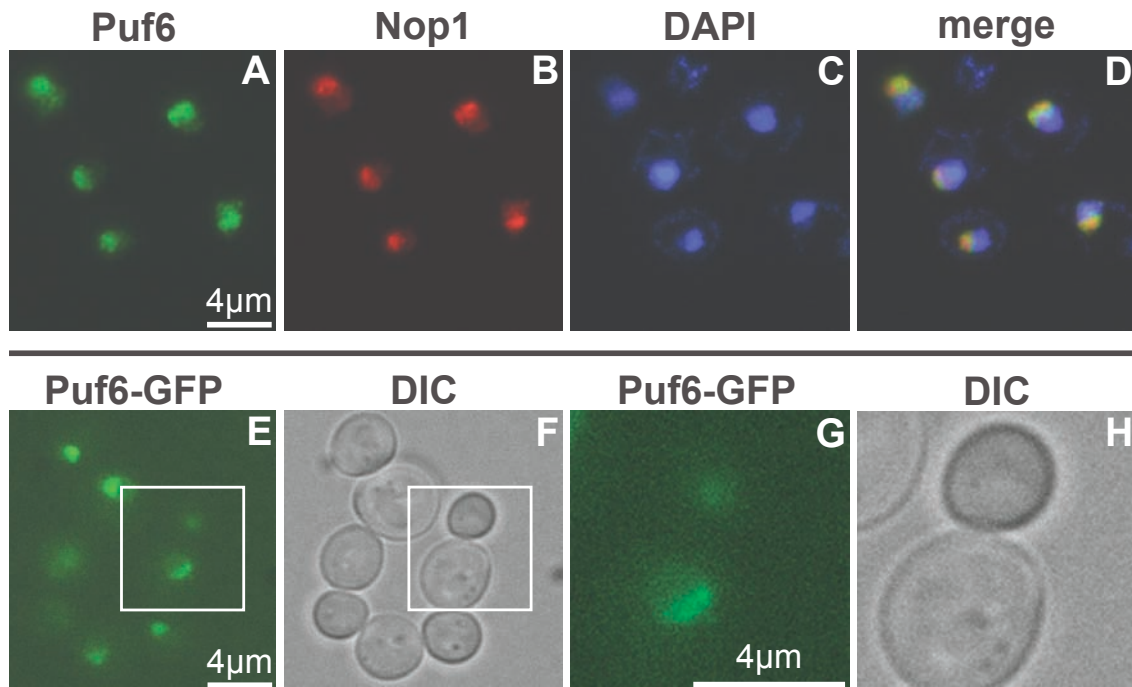


Figure 8 | Puf6 localizes predominantly to the nucleolus.

A-D | Cells expressing a HA₆-tagged version of Puf6 were stained by indirect immunofluorescence with antibodies directed against HA (A) and the nucleolar marker Nop1 (B). Nuclei were visualized with DAPI (C). Overlap of Puf6 and Nop1 staining in a distinct region of the nucleus (D) indicates nucleolar localization of Puf6.

E-H | Live imaging of cells expressing Puf6-GFP. The crescent-shaped GFP-signal (E) in the central region of the cells (F) suggests nucleolar localization of the protein. (G, H) Blow-up of a single cell from images E and F (white square).

2.3. Loc1 and Puf6 purify with a large protein complex

In the preceding paragraphs, I have shown that both Loc1 and Puf6 are predominantly nucleolar proteins. There is evidence that both proteins are implicated in mRNA localization as well as in ribosome biogenesis. To obtain indications about the involvement of Loc1 and Puf6 in these processes, I decided to perform an indirect approach first. Therefore, I tried to identify proteins that interact with Loc1 and Puf6, respectively.

A well-established method to purify native protein complexes in yeast is tandem affinity purification (TAP; Rigaut et al., 1999). Addition of a tag to the C- or N-terminus of the ORF of interest allows two-step purification. First, protein complexes are bound to IgG sepharose by two IgG binding domains. Cleavage with tobacco etch virus (TEV) protease releases the complexes. The second purification step involves binding of the calmodulin binding peptide (CBP) to a calmodulin resin and subsequent elution with a chelating agent.

In order to identify protein interactors of Loc1 and Puf6, respectively, I added the TAP-tag to the C-terminus of either protein. While Puf6-TAP grows at wild type levels, Loc1-TAP shows temperature sensitivity at 37°C (Figure 9A). Therefore, I added the TAP-tag to the N-terminus of Loc1, which restored growth at 37°C, but lead to a mild growth defect at all temperatures tested (Figure 9A). Purification of Puf6- and Loc1-, but not of Hpr1-associated complexes under low salt conditions yielded a large number of interacting proteins (Figure 9B, left). The Puf6- and Loc1-associated complexes were very stable at higher salt concentrations and could only be disassembled with 1 M salt (Figure 9B, right). Bait proteins were identified by mass-spectrometry (except for Hpr1 and Loc1 (low salt)). For Puf6, I could additionally confirm two published interacting proteins, Drs1 and Cbf5 (Table 2; Gavin et al., 2006).

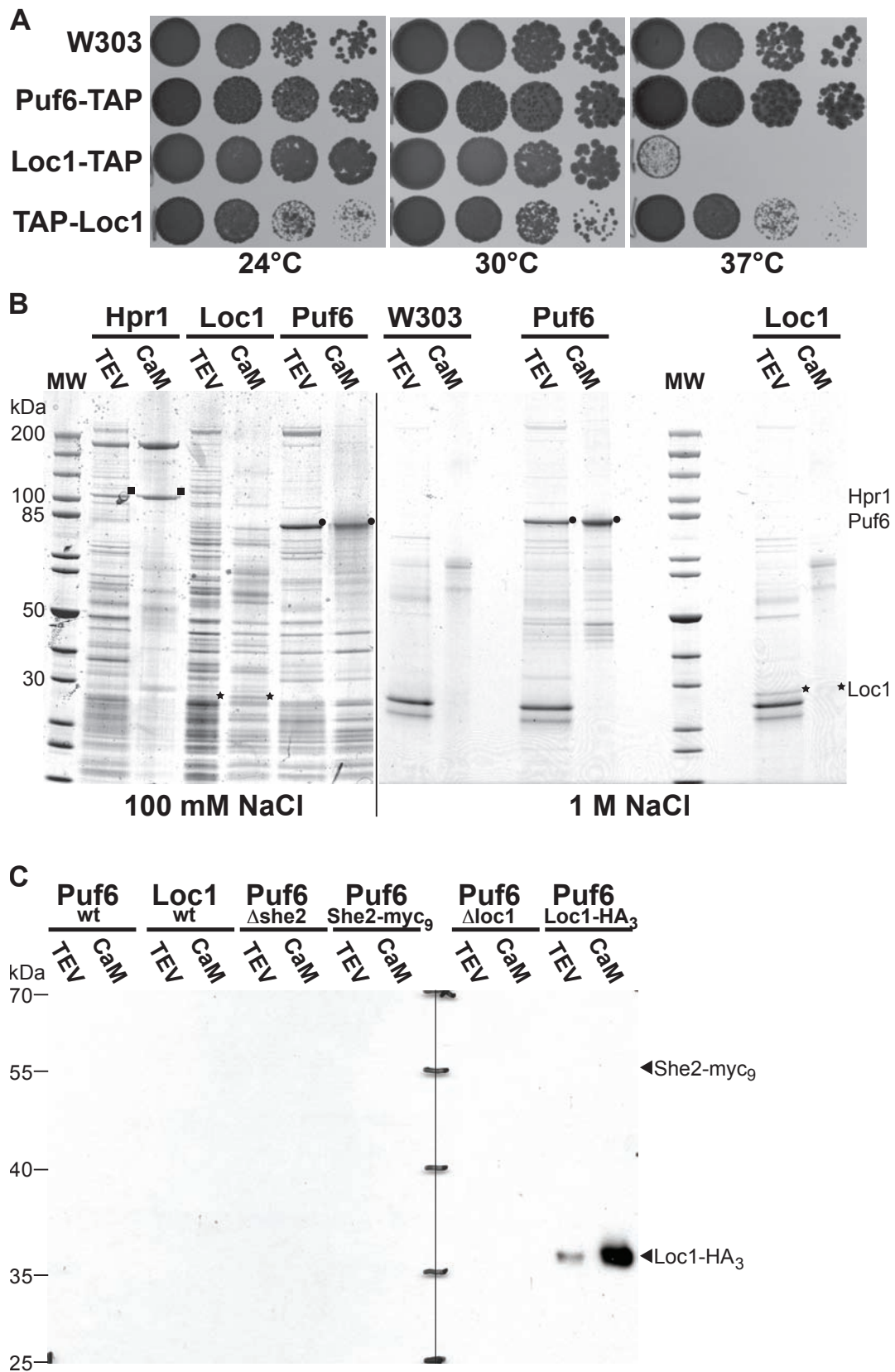
Table 2 | Proteins from tandem affinity purifications identified by mass spectrometry.

Purification	identified proteins
Loc1-TAP (1 M NaCl)	Loc1
Puf6-TAP (0.1 M NaCl)	Puf6
	Drs1
	Cbf5

Since the large number of bands, especially below 50 kDa, was not visible in the control purification of Hpr1-TAP (for hyperrecombination; Aguilera & Klein, 1990; Strässer et al., 2002), I concluded that they are not contaminations, but likely represent ribosomal proteins of the large subunit, which is in agreement with purifications of other nucleolar factors (e.g. Rlp24; Saveanu et al., 2003; see discussion) and large scale TAP of Loc1 and Puf6 (Gavin et al., 2006; Gavin et al., 2002).

Given that by SDS-PAGE it was impossible to detect interaction of Puf6 and Loc1 with each other and with components of the mRNA localization machinery such as She2, respectively, I analyzed Puf6 tandem affinity purifications by Western blot. To this purpose, I created strains where HA- or myc-epitopes were fused to the C-terminus of either She2 or Loc1. While interaction between Puf6 and Loc1 could clearly be detected, this was not the case for a Puf6-She2 interaction (Figure 9C).

To summarize, I have demonstrated that Puf6 and Loc1 interact at least indirectly on protein level, and both copurify with large, highly stable protein complexes.



(previous page:)

Figure 9 | Loc1 and Puf6 purify a large protein complex.

A | Initial characterization of TAP-strains. A strain expressing Puf6 with a C-terminal TAP-tag grows like wild type (W303) at all temperatures tested. In contrast, a strain expressing Loc1 with a C-terminal TAP-tag is temperature-sensitive at 37°C; N-terminal tagging results in a mild growth defect at all temperatures tested. This strain was used for all Loc1 purifications. For dot tests, cells were spotted in serial dilutions onto YPD and incubated at the respective temperature for 3 days.

B | Tandem affinity purification of Loc1 and Puf6 at 100 mM NaCl (low salt, left) and 1 M NaCl (high salt, right), respectively. Unlike the control Hpr1 (bait marked with squares), both Puf6 (circles) and Loc1 (asterisks) purify with several proteins that most likely represents a 60S ribosomal subunit precursor (see e.g. Horsey et al., 2004 for comparison). This complex dissociates from the respective bait proteins only under high salt conditions. Novex Bis-Tris 4%-12% gradient gels were used for SDS-PAGE and stained with colloidal Coomassie blue.

C | Western blot analysis shows interaction of Puf6 with Loc1, but not with She2. Tandem affinity purification of Puf6; *SHE2* and *LOC1* have either been deleted or tagged at the C-terminus. While the Loc1-HA₃ signal is clearly visible in the Western blot, no signal for She2-myc₉ can be detected. Vertical line indicates cutting of membrane for different antibody incubations.

2.4. Loc1 and Puf6 influence mRNA localization

Both Loc1 and Puf6 were first identified as RNA-binding proteins that are implicated in localization of *ASH1* mRNA. Puf6 was found in tandem affinity purifications of She2-TAP (Gu et al., 2004), and Loc1 was identified in a yeast three-hybrid screen using the *ASH1* localization element E3 as bait (Long et al., 2001). In a first approach, I wanted to confirm the published data on the participation of Loc1 and Puf6, respectively, on *ASH1* mRNA localization.

I created strains with deletions of either *LOC1* or *PUF6*, carrying a high-copy number plasmid expressing *ASH1* to alleviate finding cells with *ASH1* mRNA signals, and performed fluorescent *in situ* hybridization (FISH, see section 5.5.3). I counted late anaphase cells, where nuclei of mother and daughter cell are already largely separated, and clustered them into three groups: cells where a clear mRNA signal could be observed at the tip of the daughter cell (bud-tip localized, Figure 10A), cells where the mRNA signal was enriched in the daughter cell, but not anchored at the tip (bud enriched, Figure 10B), and cells with no detectable enrichment of RNA anywhere in mother and daughter cell (delocalized, Figure 10C). The first category was scored as localized, the other two as delocalized. Statistical analysis showed that deletion of *PUF6* leads to a moderate decrease of cells correctly localizing *ASH1* mRNA from about 70% in wild type cells to approximately 50% in Δ puf6 cells (Figure 10G). In contrast, deletion of *LOC1* has a dramatic effect on *ASH1* mRNA localization. In Δ loc1 cells, only one fifth of all cells counted have *ASH1* mRNA localized correctly at the bud tip, whereas in about 80%

of the cells the signal was uniformly distributed over mother and daughter cell (Figure 10G).

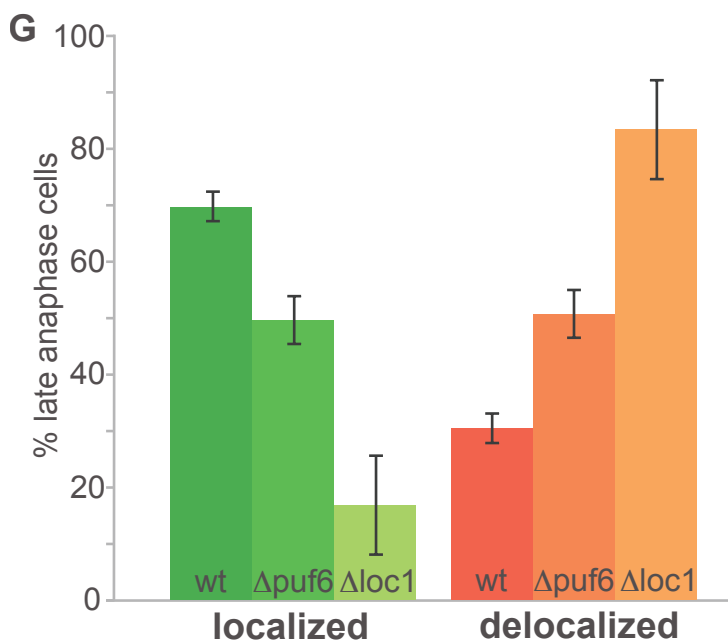
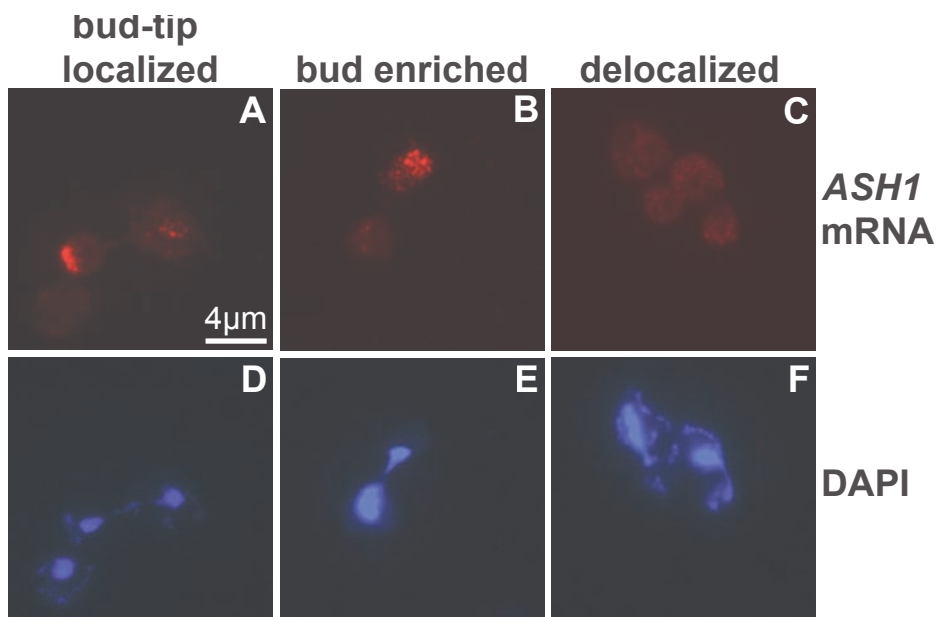


Figure 10 | Deletion of *LOC1* or *PUF6* has an effect on localization of *ASH1* mRNA.

A-F | Fluorescent *in situ* hybridization (FISH) of cells carrying *ASH1* on a high-copy number plasmid. The signal strongly accumulated at the bud tip (A), was enriched in the bud (B), or uniformly distributed over mother cell and bud (C). Nuclei were visualized with DAPI (D-F). Only cells in late anaphase, i.e. cells with large buds, where nuclei are separating (as in F) or have already separated (as in D), were counted.

G | Efficiency of *ASH1* mRNA localization as determined by FISH in wild type (wt), *loc1* knockout ($\Delta loc1$), or *puf6* knockout ($\Delta puf6$) cells. In $\Delta puf6$, percentage of cells with correctly localized *ASH1* signals decreases moderately from $70 \pm 2.6\%$ to $50 \pm 4.2\%$ ($n(\text{wt})=300$; $n(\Delta puf6)=83$; $P < 0.001$). In contrast, correct *ASH1* mRNA localization can be observed in only $17 \pm 8.8\%$ of $\Delta loc1$ cells ($n(\Delta loc1)=105$, $P < 10^{-20}$). Cells with a signal enriched in the bud could be clearly discriminated from bud-tip-localized cells and therefore have been scored as delocalized.

Both observations are in accordance with the mentioned studies, where $42\pm 5.1\%$ of $\Delta puf6$ cells and 13% of $\Delta loc1$ cells have been shown to localize *ASH1* mRNA properly at the bud tip (Gu et al., 2004; Long et al., 2001).

In conclusion, I could confirm the available data on *ASH1* mRNA localization in $\Delta loc1$ and $\Delta puf6$ cells.

It was shown above that *Loc1* and *Puf6* are predominantly nucleolar proteins (Figure 6; Figure 8), and there is data connecting both proteins to ribosome biogenesis (Nissan et al., 2002; Urbinati et al., 2006; see section 2.5). I hypothesized that other nucleolar, nonessential ribosome biogenesis factors might participate in localization of *ASH1* mRNA as well. Therefore, I created strains with deletions of *MRT4* (for mRNA turnover) and *NOP16* (for nucleolar protein), respectively (Harnpicharnchai et al., 2001; Zuk et al., 1999). Counting and scoring of cells after FISH of *ASH1* mRNA was performed as described above. Data analysis showed that in contrast to *Puf6* and *Loc1*, *Mrt4* and *Nop16* do not seem to play a significant role in localization of *ASH1* mRNA. Deletion of *MRT4* leads to a reduction of cells correctly localizing *ASH1* mRNA by approximately 10%. Deletion of *NOP16* has no effect at all, though data derives from a single experiment (Figure 11).

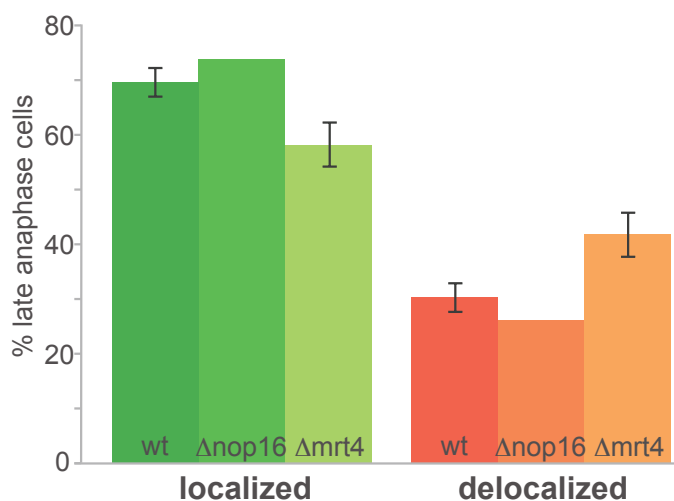


Figure 11 | Deletion of *MRT4* has a mild, deletion of *NOP16* no effect on localization of *ASH1* mRNA.

Efficiency of *ASH1* mRNA localization as determined by FISH in wild type (wt), *nop16* knockout ($\Delta nop16$), or *mrt4* knockout ($\Delta mrt4$) cells. In a $\Delta mrt4$ background, percentage of cells with correctly localized *ASH1* signals decreases slightly from $70\pm 2.6\%$ to $58\pm 4.0\%$ ($n(\text{wt})=300$; $n(\Delta mrt4)=181$; $P<0.007$). In contrast, a single experiment with $\Delta nop16$ cells showed nearly no effect on *ASH1* mRNA localization ($n(\Delta nop16)=115$).

Having analyzed additional protein factors, I stepped back to Loc1 and Puf6. *ASH1* mRNA is the paradigm of a localizing mRNA, but in total there are about 30 localized mRNAs in yeast (see Table 1, Aronov et al., 2007; Shepard et al., 2003). So far, a role for Loc1 has only been demonstrated in localization of *ASH1* mRNA, and it is unclear if localization of other mRNAs depends on Loc1 as well.

Therefore, I decided to investigate localization of two other mRNAs in wild type and Δ loc1 cells, because a deletion of *LOC1* showed the most dramatic effect in *ASH1* mRNA localization (Figure 10).

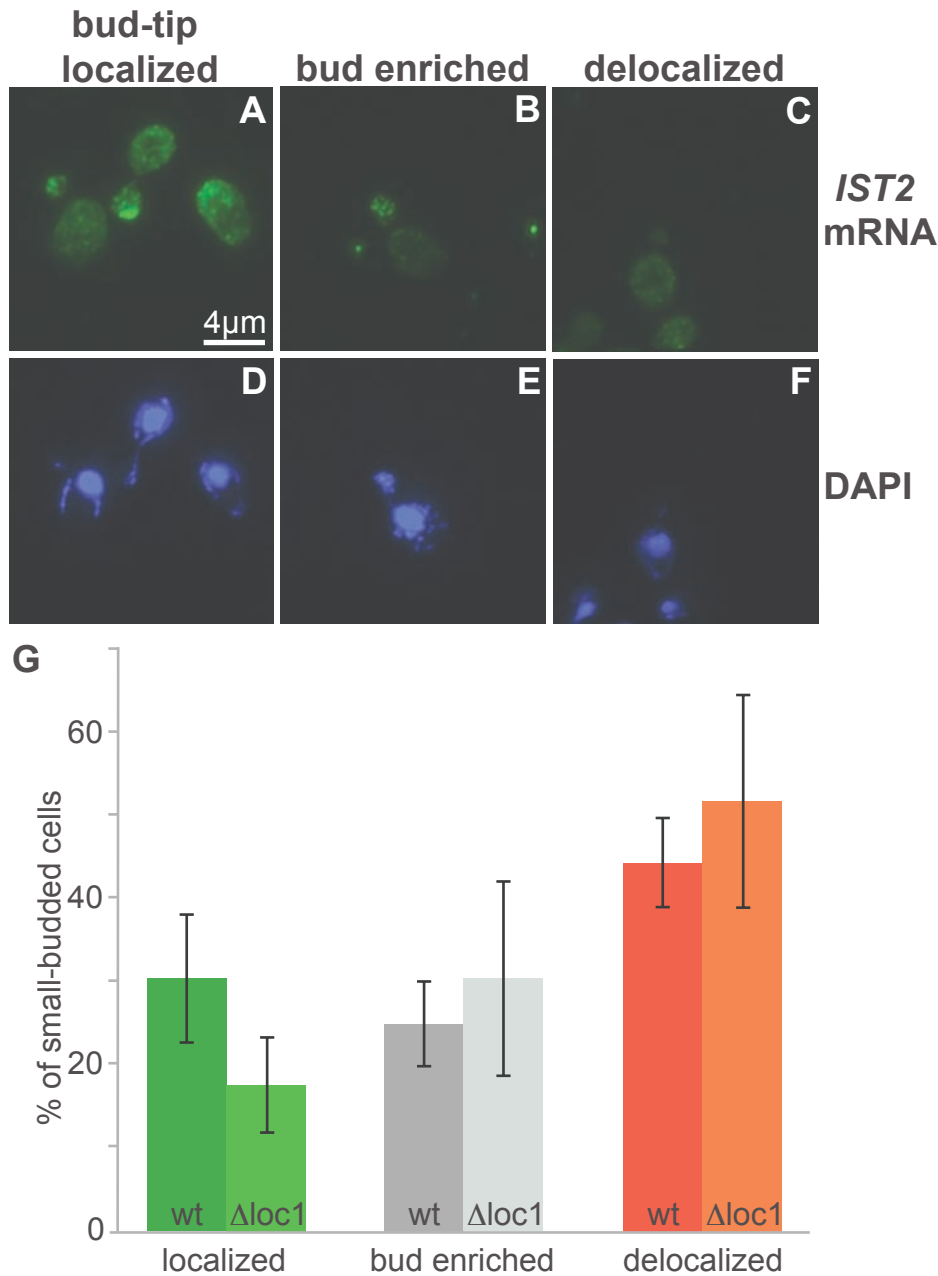
IST2 mRNA (for increased sodium tolerance; Entian et al., 1999) has been identified in a whole-genome analysis of transcripts associating with She2, She3, and Myo4 (Takizawa et al., 2000). In contrast to *ASH1* mRNA, which is expressed only during mitosis, *IST2* mRNA is not regulated during cell cycle. The mRNA encodes a protein that localizes to the plasma membrane of the daughter cell and not to the nucleus (Shepard et al., 2003; Takizawa et al., 2000).

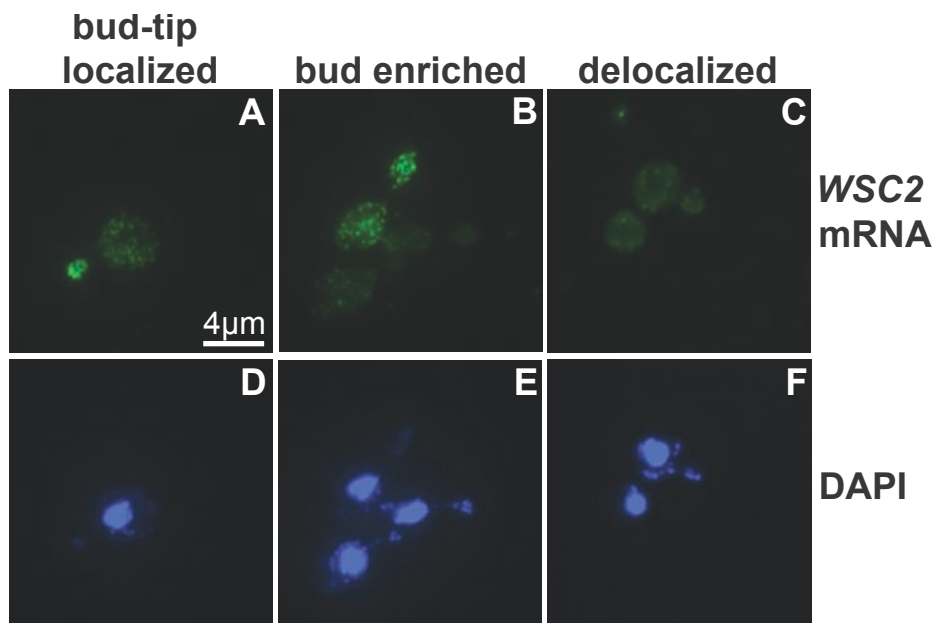
I created the required strains by transforming either wild type or loc1 knockout cells with a high-copy number plasmid expressing *IST2* under its own promoter to facilitate microscopy; *IST2* overexpression did not influence cell growth (data not shown). Subsequently, I performed FISH analysis of wild type and Δ loc1 cells. Here, only small buds with a size of up to one third of the mother cell were counted, since the *IST2* mRNA signal was not detectable in large-budded cells (Figure 12A-F).

In contrast to FISH analysis of *ASH1* mRNA, cells displaying signals enriched in the bud were not scored as delocalized because it was often difficult to discriminate between bud-tip localized and bud enriched signals (Figure 12G). Scoring of signals into the described categories showed that although the overall effect of *LOC1* deletion on localization of *IST2* mRNA is less prominent as compared to *ASH1* mRNA, a clear reduction of cells with a correctly localized *IST2* signal from about 30% in wt cells to about 18% in Δ loc1 cells can be observed (Figure 12G).

The third mRNA I tested for localization defects in Δ loc1 cells is *WSC2* mRNA (for cell wall integrity and stress-response component; Verna et al., 1997). It was identified as a bud-localized transcript in a study that further developed the microarray-based screen method mentioned previously (Shepard et al., 2003;

Takizawa et al., 2000) and codes for an integral membrane protein. *WSC2* mRNA differs from *IST2* mRNA in that it is cell cycle-regulated, and from *ASH1* mRNA in that it is induced during S phase (Shepard et al., 2003).





G

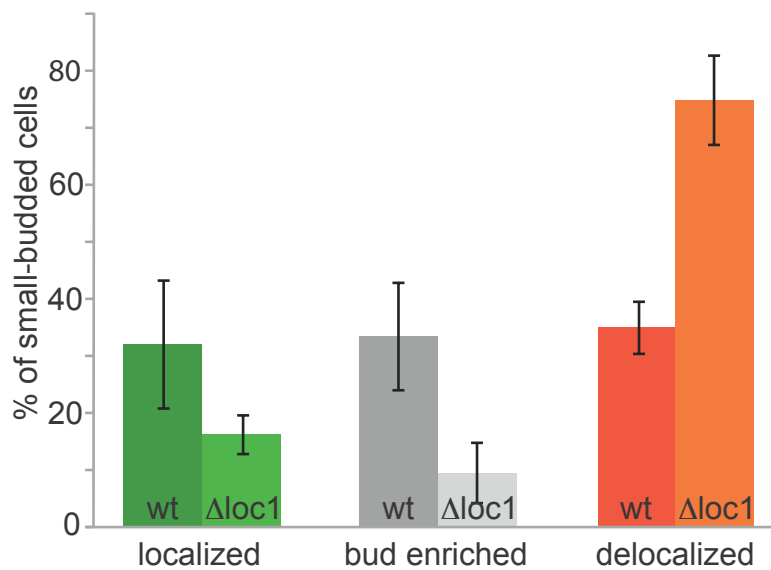


Figure 13 | WSC2 mRNA shows increased delocalization in a $\Delta loc1$ background.

A-F | Fluorescent *in situ* hybridization (FISH) of cells carrying WSC2 on a high-copy number plasmid. The signal strongly accumulated at the bud tip (A), was enriched in the bud (B), or uniformly distributed over mother cell and bud (C). Nuclei were visualized with DAPI (D-F). Only cells with small buds visible in the DAPI filter were counted.

G | Efficiency of WSC2 mRNA localization as determined by FISH in wild type (wt) or *loc1* knockout ($\Delta loc1$) cells. In $\Delta loc1$ cells, the number of cells with a delocalized WSC2 signal is strongly increased ($35 \pm 4.6\%$ in wt versus $75 \pm 7.8\%$ in $\Delta loc1$ cells, $n(\text{wt})=312$, $n(\Delta loc1)=306$, $P < 10^{-5}$).

For analysis, I transformed a wild type and a *LOC1* deletion strain with a high-copy number plasmid expressing WSC2 under its own promoter to facilitate microscopy; WSC2 overexpression did not impair cell growth (data not shown).

FISH with DIG-labeled probes was performed as described in section 5.5.3. Cells showing fluorescent signals were selected, counted and scored analogous to *IST2* mRNA. The results are shown in Figure 13.

As for *IST2* mRNA, considerably fewer wild type cells as compared to FISH analysis of *ASH1* mRNA showed bud-tip localization (see Discussion). Nonetheless, a significantly smaller amount of Δ loc1 cells (approximately 16%) show correct *WSC2* mRNA localization, as compared to wild type cells (approximately 32%). On the other hand, significantly more Δ loc1 cells have a completely delocalized *WSC2* mRNA signal (Figure 13G).

To summarize, I have demonstrated that deletions of *PUF6* and *LOC1*, respectively, lead to reduced localization of *ASH1* mRNA. I have further shown that deletion of the nucleolar factor *MRT4* also has an effect on localization of *ASH1* mRNA, whereas deletion of *NOP16* does not. Finally, I observed that Δ loc1 cells also have significant defects in localization of two other localizing mRNAs, *IST2* and *WSC2*, respectively.

2.5. Loc1 and Puf6 participate in ribosome biogenesis

The main function of the nucleolus is the synthesis of pre-ribosomal subunits (see Introduction). We have already seen that both Puf6 and Loc1 localize predominantly to this nuclear compartment (sections 2.1, 2.2). Data from genome-wide studies indicate that both proteins interact with a variety of ribosomal proteins and non-ribosomal factors involved in ribosome biogenesis (Gavin et al., 2006; Gavin et al., 2002). These data have been confirmed by a number of additional studies, where Puf6, Loc1, or both have been found in purifications of nucleolar ribosome biogenesis factors (Harnpicharnchai et al., 2001; Horsey et al., 2004; Nissan et al., 2002; Saveanu et al., 2003; Saveanu et al., 2007).

2.5.1. Loc1 and Puf6 are large subunit biogenesis factors

A very common method to get insight into the role of a specific protein in ribosome biogenesis described in the literature is the analysis of polysome profiles (Rotenberg et al., 1988). In a study that investigated yeast 66S pre-ribosomal particles by affinity purification of one central component, Nop7, several proteins not previously assigned to have a role in ribosome biogenesis were identified. Their function was assayed by depletion of the proteins and subsequent sucrose

density gradient centrifugation (Harnpicharnchai et al., 2001). In order to use this system, I first performed sucrose density gradient centrifugation of strains with deletions of two of the factors analyzed in this study, *MRT4* and *NOP16*, respectively, as a proof of principle. Subsequently, I subjected Δ puf6 and Δ loc1 cells to this analysis.

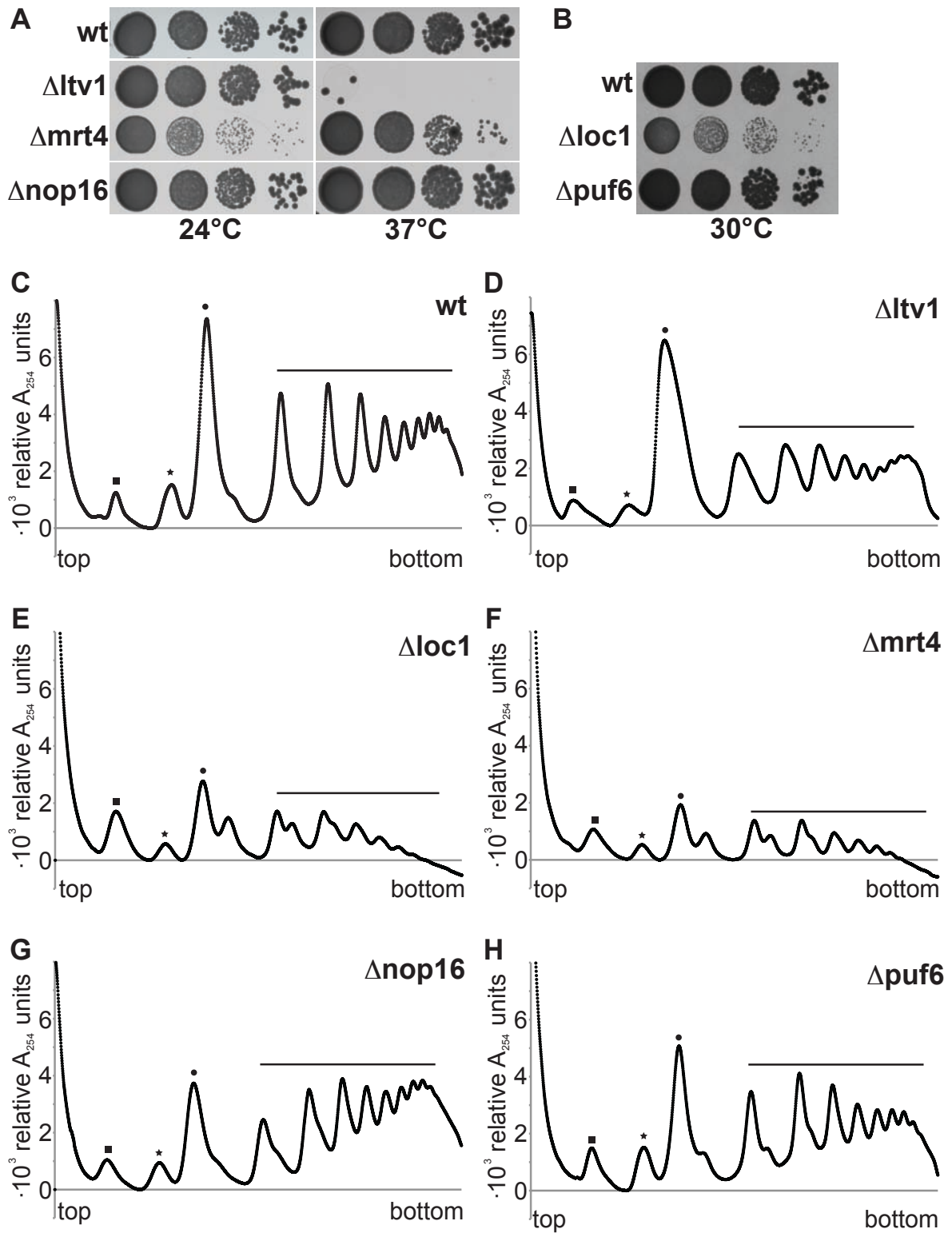
I used the Δ mrt4 and the Δ nop16 strain that had already been analyzed for their phenotype on *ASH1* mRNA localization (section 2.4), but without the *ASH1* plasmid. In addition, I also analyzed a strain lacking a small subunit biogenesis factor, *LTV1* (for low temperature viability; Seiser et al., 2006). The Δ nop16 strain grew normally at all temperatures tested, Δ ltv1 cells grew only at 24°C, and Δ mrt4 cells showed a slow growth phenotype at both 24°C and 37°C (Figure 14A).

Analysis of the polysome profiles confirmed that disruption of the *NOP16* gene does indeed impair, albeit relatively weakly, ribosome biogenesis. While in wild type cells (Figure 14C) the 60S peak was always higher as compared to the 40S peak, peak heights are almost identical in Δ nop16 cells (Figure 14G). Moreover, the Δ nop16 profile shows fewer monosomes relative to free subunits, as compared to wild type, and small so-called half-mer peaks can be observed in mono-, di-, and trisomes (Figure 14G). Polysome profiles of Δ mrt4 cells show a more severe phenotype, consistent with the slow growth of the strain. Here, the 60S peak is much lower in comparison to the 40S peak, the amount of monosomes is greatly reduced as compared to wild type, and prominent half-mers are observed from mono- to tetrasomes (Figure 14F). These half-mers consist of excess small ribosomal subunits, which can form 43S preinitiation complexes and attach to the mRNA, but cannot form complete 80S initiation complexes due to a block in large ribosomal subunit assembly (Rotenberg et al., 1988).

The control profile of Δ ltv1 (Figure 14D) differs from the 60S biogenesis factor deletion profiles (Δ mrt4, Δ nop16) as well as from the wild type profile. The amount of free small subunits is reduced as compared to the other profiles, polysome peak height is reduced, and instead of showing half-mers the peaks appear to lean towards the top of the gradient.

In summary, my results are consistent with the study mentioned above (Harnpicharnchai et al., 2001). The polysome profiles of Δ mrt4 and Δ nop16 strains

show typical properties of 60S biogenesis factors, whereas the control profile of a 40S biogenesis factor is clearly different.



(previous page:)

Figure 14 | Deletion of *LTV1* impairs biogenesis of the small ribosomal subunit, deletion of *LOC1*, *MRT4*, *NOP16* or *PUF6* impairs biogenesis of the large ribosomal subunit to different extents.

A | *MRT4* knockout cells show slow growth at all temperatures tested, whereas deletion of *LTV1* leads to a temperature sensitive phenotype; in contrast, deletion of *NOP16* has no apparent effect on cell growth at all. Cells were spotted in serial dilutions onto YPD and incubated for 3 days at the respective temperature.

B | Deletion of *LOC1* leads to slow growth, whereas deletion of *PUF6* has no effect on growth. Cells were spotted in serial dilutions onto YPD and incubated for 3 days at 30°C.

C-H | Polysome profiles of a wild type (wt) and various ribosome biogenesis factor deletion strains. Deletion of the small subunit biogenesis factor *LTV1* leads to a profile that differs from all other profiles shown. Here, 40S peak size (marked by squares) is slightly reduced as compared to 60S (marked by asterisks), polysome peak sizes (marked by bars) are reduced, and all peaks starting from the 80S peak (marked by circles) seem slightly inclined to the left as compared to wt (D).

Profiles of $\Delta mrt4$ and $\Delta loc1$ are similar to one another (E, F). The respective 60S peaks drop significantly below the 40S peak, 80S peak size is greatly reduced, and polysome peaks are much less prominent as compared to wt. In addition, so-called half-mers appear (see text for details).

Deletion of *NOP16* and *PUF6*, respectively, leads only to a moderate reduction in 60S and 80S peak size, and has nearly no effect on polysome peaks (G, H). Profiles were collected from 300 μ g total RNA loaded onto 7-47% linear sucrose gradients. All profiles were normalized, so that the lowest point in the valley between 40S and 60S corresponds to 0.

Subsequently, I performed sucrose density centrifugation with total RNA (see section 5.2.4). Consistent with the growth phenotype, deletion of *PUF6* leads to a mild defect in 60S subunit biogenesis, similar to deletion of *NOP16*. Peak heights of free large subunits and monosomes, respectively, are diminished, and weak half-mers can be observed (Figure 14H). In contrast, the $\Delta loc1$ profile very much resembles the one obtained for $\Delta mrt4$. It shows a small 60S peak relative to the 40S peak, a strongly reduced number of monosomes, and pronounced half-mers (Figure 14E).

Taken together, my data suggest that deletion of *LOC1* and, to a smaller extent, deletion of *PUF6*, leads to a deficiency in large ribosomal subunits. Further experiments showed that this deficiency, at least in the case of *LOC1*, is indeed caused by depletion of *Loc1* and not by slow growth of the cells (see section 2.8.3)

2.5.2. Deletion of *Loc1* delays large subunit rRNA processing

The nucleolar steps of ribosome biogenesis involve a large number of protein rearrangements and RNA processing steps (see Introduction). After having confirmed that *Puf6* and *Loc1* function in this pathway, I wanted to investigate whether they are required for specific steps in rRNA processing of the pre-60S subunit. Thus, I looked at levels of newly synthesized rRNA intermediates by *in vivo* pulse labeling (Ferreira-Cerca et al., 2005; see section 5.4.4). I pulsed

logarithmically growing yeast cultures for 15 minutes with ^3H -uracil and analyzed RNA levels by Northern Blot (Figure 15).

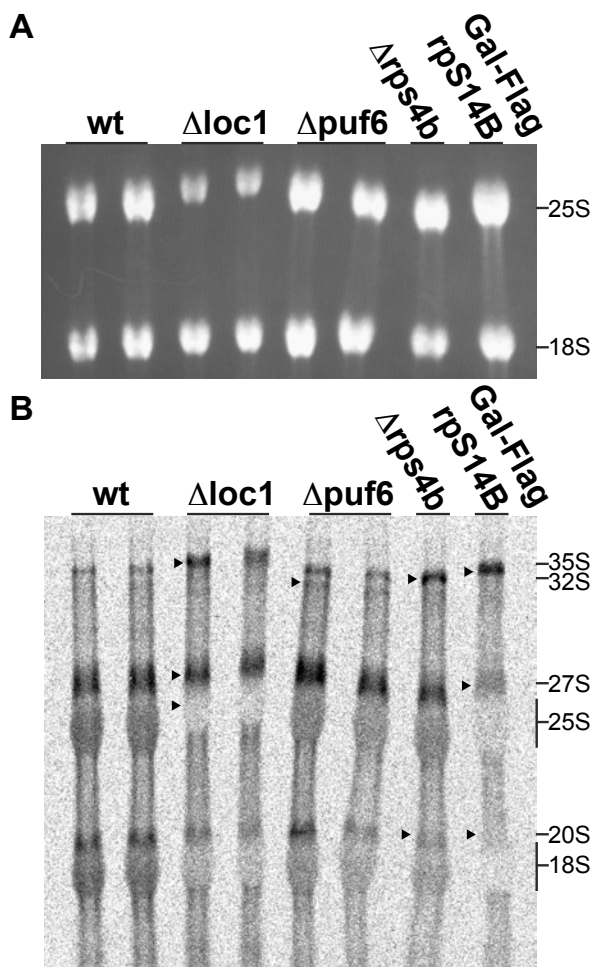


Figure 15 | Relative abundance of some pre-rRNAs changes upon deletion of *LOC1* or *PUF6*.

A | Yeast cells were pulse-labeled with ^3H -uracil for 15 min, and total RNA was extracted. RNA corresponding to 500 cpm was run on a 1% TAE agarose gel to assess RNA quality and control for equal loading. No degradation of the 25S and 18S rRNA band is visible, and loading is equal except for the Δloc1 lanes, where the 25S signal is moderately reduced.

B | Northern Blot of total RNAs tested in (A). For wild type (wt), Δloc1 , and Δpuf6 , strains with two different strain backgrounds have been tested (BY4741 on the left side and BY5563 on the right side), the two control strains Δrps4b and Gal-Flag rps14B are BY4741 derivatives. Arrowheads mark changes in rRNA-precursor signal intensities as compared to wt. Deletion of *LOC1* leads to slightly increased levels of 35S and 27S pre-rRNAs, whereas 25S rRNA levels are reduced (Sébastien Ferreira-Cerca, personal communication). Deletion of *PUF6* leads to a very weak phenotype, showing slightly increased levels of 32S pre-rRNA (Sébastien Ferreira-Cerca, personal communication). In contrast, both control strains show 35S pre-rRNA accumulation, a strong decrease in 20S pre-rRNA levels, and Gal-Flag-rps14B in addition a reduced 27S pre-rRNA levels (Ferreira-Cerca et al., 2005). For the Blot, 10,000 cpm were run on a 1.3% MOPS/formaldehyde agarose gel, transferred onto a positively charged Nylon membrane and exposed to a PhosphorImager screen for 2 days.

Consistent with results in previous sections, deletion of *PUF6* leads only to a weak phenotype that is hard to distinguish from wild type. The only significant change in Δpuf6 cells is an increased level of 32S pre-rRNA, a late 90S intermediate created by cleavage at site A_1 (see Figure 2). On the other hand, deletion of *LOC1* causes a more pronounced phenotype; of course, this phenotype is still weak as compared to essential components of ribosome assembly such as rps14B. In Δloc1 cells, I observe slightly increased levels of 35S pre-rRNA, contained in the initial 90S pre-

ribosomal particle, and of a 27S pre-rRNA species. Levels of mature 25S rRNA are reduced, indicating a delay in large subunit rRNA processing.

In summary, *in vivo* pulse labeling confirms participation of Loc1 in 60S subunit biogenesis and suggests that it is required at the stage of 27S rRNA processing, i.e. at late nucleolar steps of pre-60S maturation.

2.5.3. Total amount of ribosomes is reduced in $\Delta loc1$ cells

The results described in this study so far have confirmed a role for Loc1 in the maturation of pre-60S ribosomal particles. Since deletion of *LOC1* leads to a delay in processing of rRNAs of the large subunit, fewer mature large ribosomal subunits are available at a given time point. In order to counteract this deficit and not to synthesize excess amounts of small subunits that are not needed, one would expect that cells reduce small subunit synthesis as well. To test this hypothesis, I compared the amounts of large and small ribosomal subunits in wild type and $\Delta loc1$ cells. I performed sucrose density gradient centrifugation as described in section 5.2.4, but omitting magnesium and cycloheximide from all buffers, thus disrupting ribosomes into their subunits.

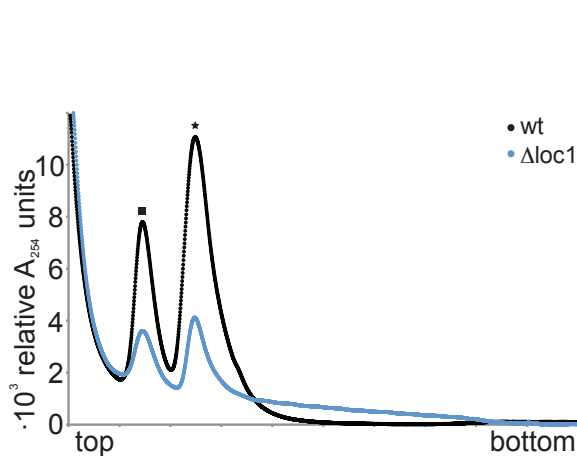


Figure 16 | Cells without Loc1 contain less ribosomal subunits than wild type cells.

Polysome profiles of a wild type (wt) and a *loc1* deletion ($\Delta loc1$) strain. Magnesium was omitted from lysis and gradient buffers to disrupt mono- and polysomes into individual subunits. Height of both the 40S peak (square) and the 60S peak (asterisk) is at least two-fold reduced in $\Delta loc1$ cells. In addition, the ratio of the 60S to the 40S peak decreases from about 1.4 (wt) to about 1.1 ($\Delta loc1$). Profiles were collected from 500 μ g total RNA loaded onto 7-47% linear sucrose gradients without magnesium (see section 5.2.4) and have been arranged in a way that the $\Delta loc1$ 40S peak maximum has the same x-value as the wt 40S peak maximum.

Figure 16 shows that indeed the total amount of ribosomal subunits contained in an equal amount of total RNA is reduced in $\Delta loc1$ cells. However, the decrease in 60S subunits seems to be more severe than the reduction of 40S subunits, because the ratio of the peaks (60S to 40S) decreases by a factor of roughly 1.3. That means that at a given time point there are excess 40S subunits relative to 60S subunits in

a Δ loc1 strain, as indicated by the presence of half-mers in Δ loc1 polysome profiles.

To summarize, my results indicate that Δ loc1 cells contain excess small relative to large ribosomal subunits, and the total number of ribosomes appears to be reduced.

2.6. *ASH1* mRNA is translationally silenced in the nucleolus

2.6.1. She2 and *ASH1* mRNA can be trapped in the nucleolus

In the previous sections I have demonstrated, consistent with published results, that the two proteins Loc1 and Puf6 are located predominantly in the nucleolus and that they are indeed *trans*-acting factors of *ASH1* mRNA localization. An essential prerequisite for an influence of nucleolar proteins on a process that happens in the cytoplasm is that the RNP of interest – in this case the *ASH1* mRNP – enters the nucleolus at some point of its assembly. This would allow interaction of Loc1 and Puf6 with the mRNP.

In his Ph.D. thesis, Tung-Gia Du, a former co-worker, showed that both the RNA-binding protein She2 and at least one localized mRNA, *ASH1*, can be found in the nucleolus under certain conditions (Du, 2007). His results are summarized in Figure 17. With the help of the temperature sensitive (ts) mutant *mex67-5* (Segref et al., 1997) of the mRNA export factor Mex67 (Tap/NXF1 in higher eukaryotes), mRNA export could be blocked by shifting yeast cultures from permissive temperature (26°C) to non-permissive temperature (37°C). Cells had been transformed with a plasmid where *ASH1* was placed under control of a galactose-inducible promoter (*GAL1*). Upon shift to the restrictive temperature, *ASH1* was overexpressed.

In shifted *mex67-5* cells, She2 did not localize to the bud tip as in *MEX67* wild type cells (Figure 17A, D), but rather accumulated in the nucleolus, as shown by indirect immunofluorescence (Figure 17E, H). In contrast, Khd1, a *trans*-acting mRNA localization factor (see introduction), and Npl3, a shuttling mRNA export factor, accumulated in the nucleoplasm, but not in the nucleolus (Du et al., 2008).

In order to detect *ASH1* mRNA in the strains described, double fluorescent *in situ* hybridization was used. Similar to She2, *ASH1* mRNA localized to the bud tip in *MEX67* wild type cells (Figure 17I, K).

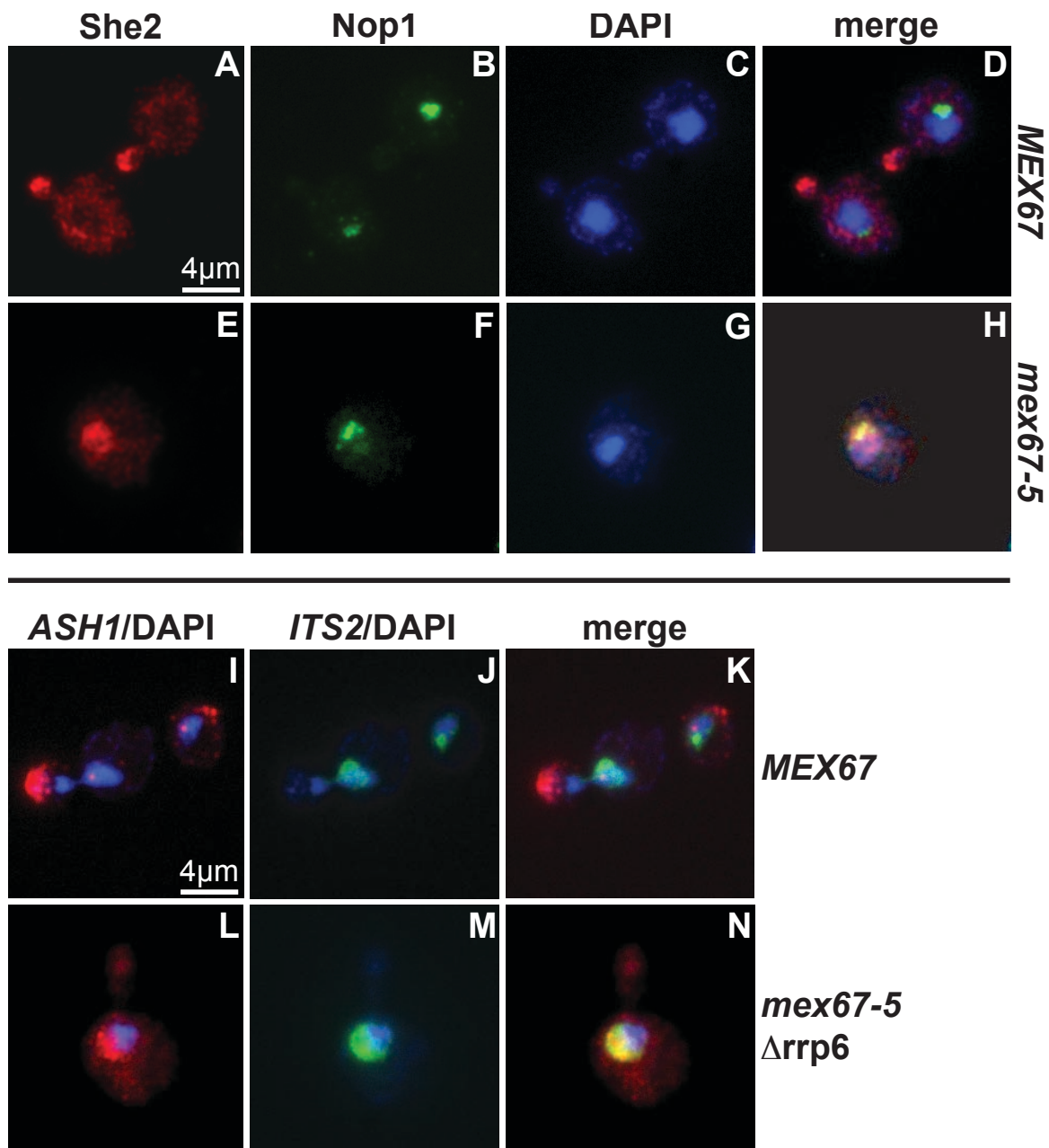


Figure 17 | She2 and ASH1 mRNA accumulate in the nucleolus when mRNA export is blocked.

A-H | She2 accumulates in nucleoli upon mRNA export block. Cells expressing the wild type (wt) allele of the mRNA export factor Mex67 (*MEX67*, A-D) or a temperature-sensitive (ts) mutant allele (*mex67-5*, E-H) were stained by indirect immunofluorescence with antibodies directed against She2 (A, E) and the nucleolar marker Nop1 (B, F). Nuclei were visualized with DAPI (C, G). Both cultures were shifted to the restrictive temperature (37°C) for one hour, and *ASH1* mRNA was overexpressed by galactose induction. She2 localizes to the bud-tip in *MEX67* cells (A, D). However, in *mex67-5* cells, She2 and Nop1 signals overlap in a region of the nucleus, indicating nucleolar accumulation of She2.

I-N | *ASH1* mRNA accumulates in nucleoli upon mRNA export block, if the nuclear exosome is inhibited. Cells expressed either wt *MEX67* (I-K) or the ts-allele *mex67-5* with an additional deletion of *RRP6* (L-N). They were stained by double FISH after shift to 37°C and *ASH1* overexpression by galactose induction for one hour. ITS2 serves as a marker for the nucleolus (see text for details). Nuclei were visualized with DAPI.

Again, in *MEX67* cells *ASH1* mRNA localizes to the bud tip, whereas in *mex67-5/Δrrp6* cells, the signals of *ASH1* and *ITS2* RNAs largely overlap, indicating nucleolar accumulation of *ASH1* mRNA.

All data shown in this figure from Du, 2007 and Du et al., 2008, respectively.

In addition, a nuclear spot, possibly indicating the *ASH1* transcription site, was observed (Du et al., 2008). The rRNA sequence ITS2, which is present only in nucleoli (see section 1.2), was used as a marker for the nucleolus (Figure 17M).

Upon block of mRNA export and additional deletion of *RRP6* (for ribosomal RNA processing; Briggs et al., 1998), a gene encoding a subunit of the nuclear exosome (Hilleren et al., 2001), the signal for *ASH1* mRNA largely overlapped with the ITS2 signal, indicating nucleolar localization (Figure 17L, N; see Discussion).

2.6.2. Cytoplasmic retention of She2 influences Ash1 distribution

With the proof that She2 and *ASH1* mRNA can enter the nucleolus and the assumption that this represents an intermediate step in the maturation of localizing mRNPs under physiological conditions, we wanted to elucidate the functional relevance of nucleolar passage of She2.

Tung-Gia Du started to tackle this question and created a fusion protein that trapped She2 in the cytoplasm. The obvious candidate for the cytoplasmic anchor was the N-terminal part of She3 (She3N), which binds strongly to the motor protein Myo4 (Heuck et al., 2007). The resulting fusion protein She3N-She2 does not enter the nucleus (Du et al., 2008). Quite contrary to the hypothesis that this nuclear exclusion would perturb *ASH1* mRNA localization, he observed correct *ASH1* localization almost at wild type levels in a She3N-She2 strain (Du et al., 2008). However, when we analyzed distribution of Ash1 protein by immunofluorescence, we found that the amount of cells that correctly localized Ash1 protein was significantly reduced (Figure 18H, grey and orange columns). Immunofluorescence was performed as described in section 5.5.2, with a strain that had nine myc-epitopes inserted just 5' of the Stop codon of the *ASH1* ORF. We counted post-anaphase cells, where nuclei of mother and daughter cell have separated, and clustered them into three groups: cells where the Ash1 signal could be observed only in the daughter cell nucleus (asymmetric), preferentially in the daughter cell nucleus (partial asymmetric), and uniformly distributed over mother and daughter cell nuclei (symmetric) (Figure 18B-G).

To summarize, we have demonstrated that a fusion of She2 to the N-terminal part of She3 influences distribution of Ash1, but leaves *ASH1* mRNA localization unchanged.

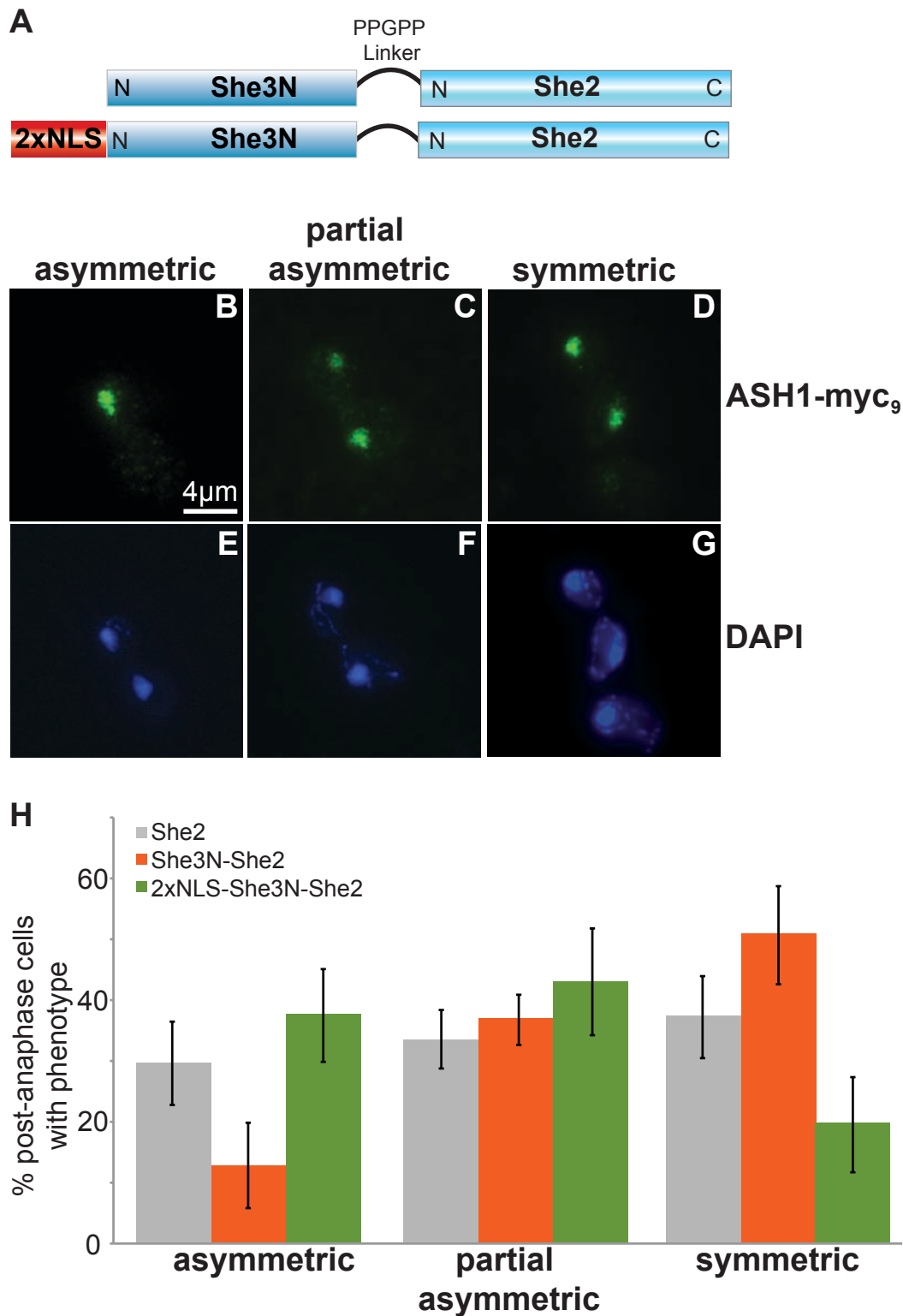


Figure 18 | Loss of asymmetric Ash1 distribution in She3N-She2 cells can be rescued by addition of a nuclear localization sequence.

A | Schematic representation of She2 protein fusions. The N-terminal 200 amino acids, which bind to Myo4, have been fused via a five amino acid linker (Pro-Pro-Gly-Pro-Pro, PPGPP) to the N-terminus of She2 (upper panel) on a plasmid. For some experiments, a double nuclear localization sequence (2xNLS) has been added to the N-terminus of the fusion protein (lower panel).

B-G | Indirect immunofluorescence (IF) of cells expressing a myc₉-tagged version of Ash1. Cells were stained with an antibody directed against the myc-tag (B, C, D). Nuclei were visualized with DAPI (E, F, G). Ash1 strongly accumulated in daughter cell nuclei (asymmetric, B), was enriched in daughter cell nuclei (partial asymmetric, C), or uniformly distributed between mother and daughter

(continued: Figure 18)

cell nuclei (symmetric, D). Only post-anaphase cells, i.e. cells with large buds, where nuclei have already separated, were counted.

H | Ash1-myc₉ distribution as determined by IF in Δ she2. Cells were transformed with a plasmid carrying ORFs coding for either *SHE2*, the *SHE3N-SHE2* fusion protein, or the fusion protein preceded by a double nuclear localization sequence ($2\times$ NLS-*SHE3N-SHE2*). While in wt (She2) cells Ash1 distribution is about one third for each category, roughly half of the She3N-She2 cells ($51\pm 8.1\%$) have a symmetrically distributed Ash1 signal. Addition of a double NLS to the N-terminus of the fusion results in wt-like distribution. The collected data are statistically significant, as determined by a χ^2 test ($n(\text{SHE2})=310$; $n(\text{SHE3N-SHE2})=363$; $n(2\times\text{NLS-SHE3N-SHE2})=361$; She2 vs. fusion: $P<10^{-7}$; She2 vs. $2\times$ NLS fusion: $P<10^{-4}$; fusion vs. $2\times$ NLS fusion: $P<10^{-18}$).

In order to prove that the reason for the altered Ash1 distribution in She3N-She2 cells is in fact cytoplasmic retention of She2, I pursued three strategies.

First, I tried to find a She2 mutant that would show the desired phenotype, i.e. exclusive cytoplasmic localization. I had indications that the extreme C-terminal part of She2 is important for nuclear localization (Böhl, 2001). Thus, I created C-terminal truncations of wild type She2 and the RNA-binding mutant of She2 (N36S-R63K; Du et al., 2008). I used a plasmid expressing the respective version of GFP-She2 under its endogenous promoter and monitored localization of the fusion protein by live imaging (Figure 19).

Full-length wild type She2 was detected at the bud-tip, with some additional signal in the nucleus, while the RNA-binding mutant of She2 was observed only in the nucleus (Figure 19A-D). Removal of ten amino acids from the C-terminus caused a relocation of wild type She2 to the nucleus, the mutant remained unaffected (Figure 19E-H). When I truncated the protein further, I could not detect any fluorescence signal (Figure 19I-L).

I conclude that nuclear exclusion cannot be achieved by a simple C-terminal truncation of She2.

As a second approach, I tried to create fusion proteins independent of the described She3N-She2. Therefore, I fused She2 to other protein domains that are sequestered to the cytoplasm. All fusions were created on plasmids and transformed into a strain with a deletion of *SHE2* but otherwise wild type. Under these conditions, She2 fusions suitable for further experiments should localize to the bud tip, as does the control plasmid expressing She2 alone (Figure 20A, B). Localization was assessed by indirect immunofluorescence with an antibody directed against She2 (Du et al., 2008).

WHI3 (for Whiskey, Nash et al., 2001) encodes a RNA-binding protein, which has been described to sequester *CLN3* mRNA to distinct regions in the cytoplasm. I tried to fuse full-length Whi3 to both ends of She2, but never succeeded in expressing a fusion protein.

MOD5 (for tRNA modification) codes for two isoforms – the shorter one lacking twelve amino acids from the N-terminus – of a transferase implicated in isopentenylolation of tRNAs (Dihanich et al., 1987; Tolerico et al., 1999). After removal of a nuclear localization sequence (NLS) from the extreme C-terminus, the shorter second isoform Mod5-II localizes to the cytoplasm, even when fused to a reporter construct consisting of β -galactosidase and a part of histone H2B (so-called karyophilic β -galactosidase, Tolerico et al., 1999). Thus, I created a plasmid expressing a fusion of Mod5-II lacking the NLS to the C-terminus of She2 (She2-Mod5) and performed immunofluorescence. In contrast to She2, She2-Mod5 is ubiquitously distributed throughout mother and daughter cell; hence it is not suited for further experiments (Figure 20E, F).

STP1 (for species-specific tRNA processing; Wang & Hopper, 1988) encodes a transcription factor that is synthesized as a latent cytoplasmic protein (Andreasson & Ljungdahl, 2004). After proteolytic cleavage at a conserved region (region II) of the N-terminal domain, which removes the apparent cytoplasmic anchor (region I) from the protein, Stp1 enters the nucleus (Andreasson & Ljungdahl, 2004). I fused region I with a few additional amino acids (amino acids 1 to 42) of the *STP1* ORF to the N-terminus of She2 (She2-Stp1_I). Fusion with one copy of Stp1_I was not expressed and consistently led to a Δ she2-phenotype (Figure 20G, H and data not shown). However, when I analyzed She2 distribution of a strain where 3 copies of Stp1_I were fused to She2 (3 \times Stp1_I-She2, Figure 20I, J), I observed large particles. These particles do not localize to the bud tip, instead they accumulate at the bud neck; they were therefore not suited for further experiments.

After these unsuccessful trials with different fusion proteins I decided to follow a third approach to demonstrate that the altered Ash1 distribution in She3N-She2 cells is in fact due to cytoplasmic retention of She2.

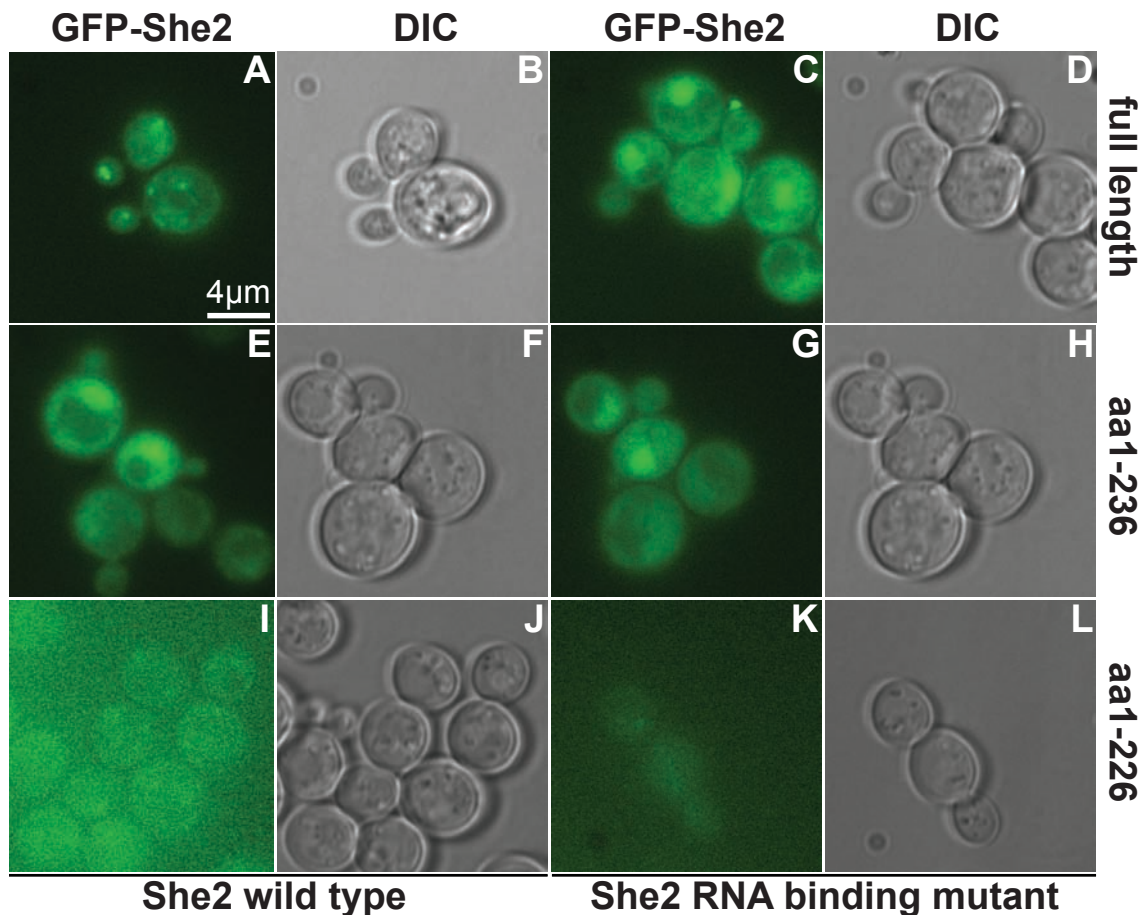


Figure 19 | C-terminal truncations of She2 interfere with its localization.

A-D | Live imaging of full length GFP-She2 in wild type (wt; A, B) or N36S-R63K double point mutant cells (C, D), which cannot bind RNA (Du et al., 2008). While GFP-She2 localizes to the bud tip in wt cells (A), it is trapped in the nucleus in the RNA-binding mutant (C).

E-H | Deletion of 10 amino acids (aa) from the C-terminus leads to relocation of GFP-She2 to the nucleus in wt cells (E, F), but has no effect on localization of GFP-She2 in the RNA-binding mutant (G, H).

I-L | Deletion of 20 amino acids from the C-terminus abolishes localization and/or expression of GFP-She2 in all strains tested.

I thought that I might rescue the impaired Ash1p distribution in She3N-She2 cells if I allowed the protein to enter the nucleus again, for example by adding a nuclear localization sequence (NLS). Insertion of a tandem simian virus 40 (SV40) NLS (2×NLS; Kalderon et al., 1984) between She3N and She2 had no effect on Ash1 protein distribution (Tung-Gia Du, personal communication). Therefore, I added the 2×NLS to the 5'-end of the *SHE3N-SHE2* fusion construct. Subsequently I analyzed localization of She2 and found that it is not altered by this additional fusion (Figure 20C, D). When I looked at Ash1 in a strain transformed with this new construct, I saw that loss of asymmetric distribution is in fact reversed by the addition of a 2×NLS (Figure 18H).

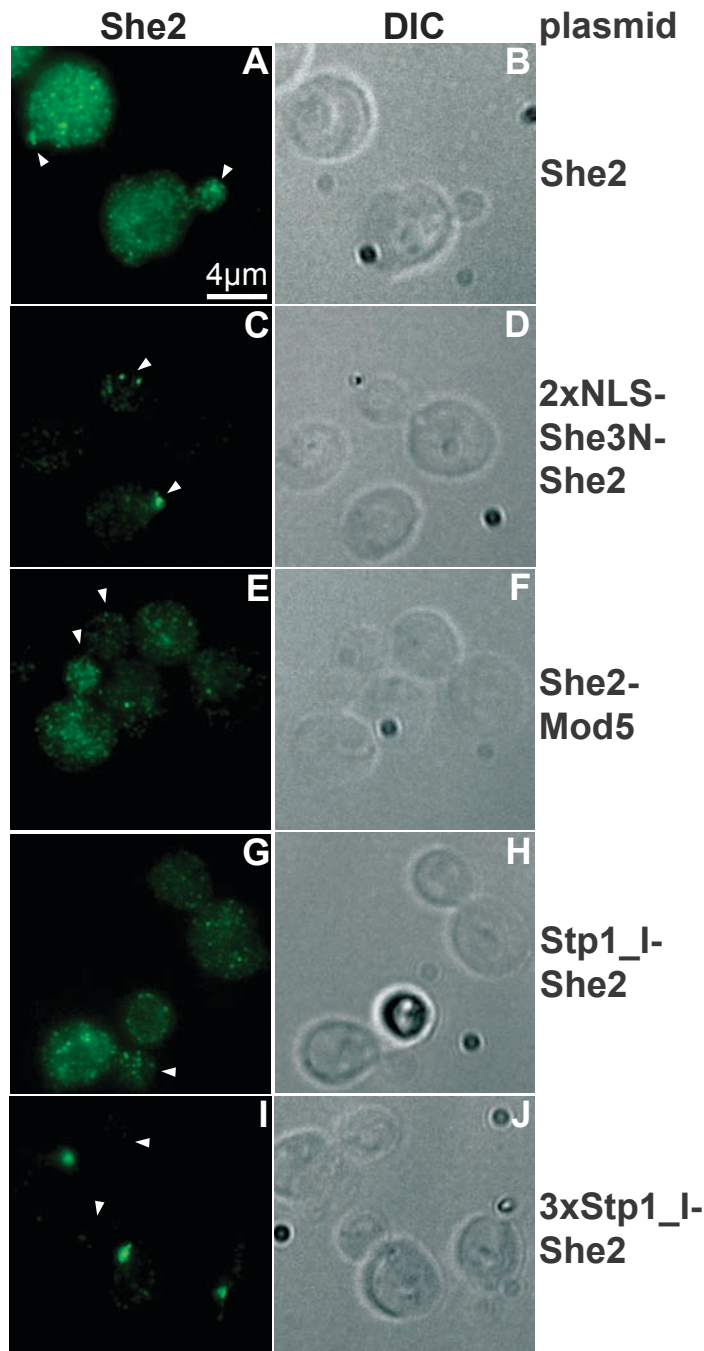


Figure 20 | Fusion of 2xNLS-She3N to She2 does not affect protein localization.

She2 has been fused with different protein domains in order to trap it in the cytoplasm.

Cells expressing the respective fusion proteins from a centromeric plasmid were stained by indirect immunofluorescence with an antibody directed against She2 (A, C, E, G, I). Only cells with small to medium sized buds, as judged by differential interference contrast (DIC; B, D, F, H, J), were analyzed.

Addition of a double nuclear localization sequence and the N-terminal part of She3 (2xNLS-She3N) to the N-terminus of She2 enhances its localization to the bud tip (C, D) as compared to the wild type protein (A, B). Fusion of the short isoform of Mod5 lacking the C-terminal NLS to the C-terminus of She2 leads to ubiquitous cytoplasmic distribution of She2 (E, F). A fusion of the cytoplasmic anchor domain of Stp1 (Stp1_I) to the She2 N-terminus is not expressed and therefore leads to a Δ she2 phenotype (G, H). However, if three copies of this domain are fused to the N-terminus of She2, particles seem to form but get stuck at the bud neck (I, J). Arrowheads mark buds.

Here, about 38% of post-anaphase cells show asymmetric Ash1-myc₉ distribution, compared to only about 13% in the She3N-She2 expressing strain (wild type: 30±6.9%).

Taken together, I could demonstrate that a fusion of She2 to the N-terminal part of She3 influences distribution of Ash1 due to nuclear exclusion of the fusion protein.

2.6.3. Cytoplasmic retention of She2 causes premature translation of *ASH1* mRNA

The observation that *ASH1* mRNA localization remains unchanged in cells where She2 is excluded from the nucleus while Ash1 protein asymmetry is lost could be explained with premature translation of *ASH1* mRNA. In this case, nucleolar passage of the *ASH1* mRNP would account for translational silencing. If translational silencing is lost, e.g. by cytoplasmic retention of She2, the RNA can still localize to the bud tip, but translation will start during the transport, leading to presence of Ash1 protein in mother cells and therefore loss in asymmetric distribution.

To test this hypothesis, we examined kinetics of Ash1 synthesis. We used strains with respective knockouts that allowed induction of *ASH1* expression by addition of galactose to the medium (Figure 21A; Long et al., 1997). In addition to a wild-type control and a strain expressing She3N-She2, we investigated strains disrupted for *SHE2*, *LOC1*, and *PUF6*, respectively. RNA levels were quantified by Northern Blot (Figure 21B), protein levels by Western Blot with an antibody directed against the myc-epitope (Figure 21C).

Although induction kinetics differs in individual experiments, tendencies are comparable. *ASH1* mRNA levels are lowest in wt and She3N-She2 cells and highest in Δ she2 cells (Figure 21G-H). On the contrary, Δ she2 cells generally show low Ash1 levels at later time points of induction, only wt cells range below (Figure 21D-F). When comparing signals of individual Westerns with signals of individual Northern (Figure 21J-L), i.e. adjusting for mRNA levels, expression levels of wt and Δ she2 cells are almost identical. In Δ loc1 and Δ puf6 cells Ash1 protein synthesis is slightly accelerated, consistent with ascribed roles in translational regulation (Gu et al., 2004; Komili et al., 2007; see discussion). Strikingly, in She3N-She2 cells almost three times as much Ash1 is present as compared to wild type cells.

In summary, we have shown that deletion of *LOC1* and *PUF6*, and even more cytoplasmic retention of She2, leads to increased levels of Ash1 protein following galactose induction, suggesting reduced translational inhibition of *ASH1* mRNA.

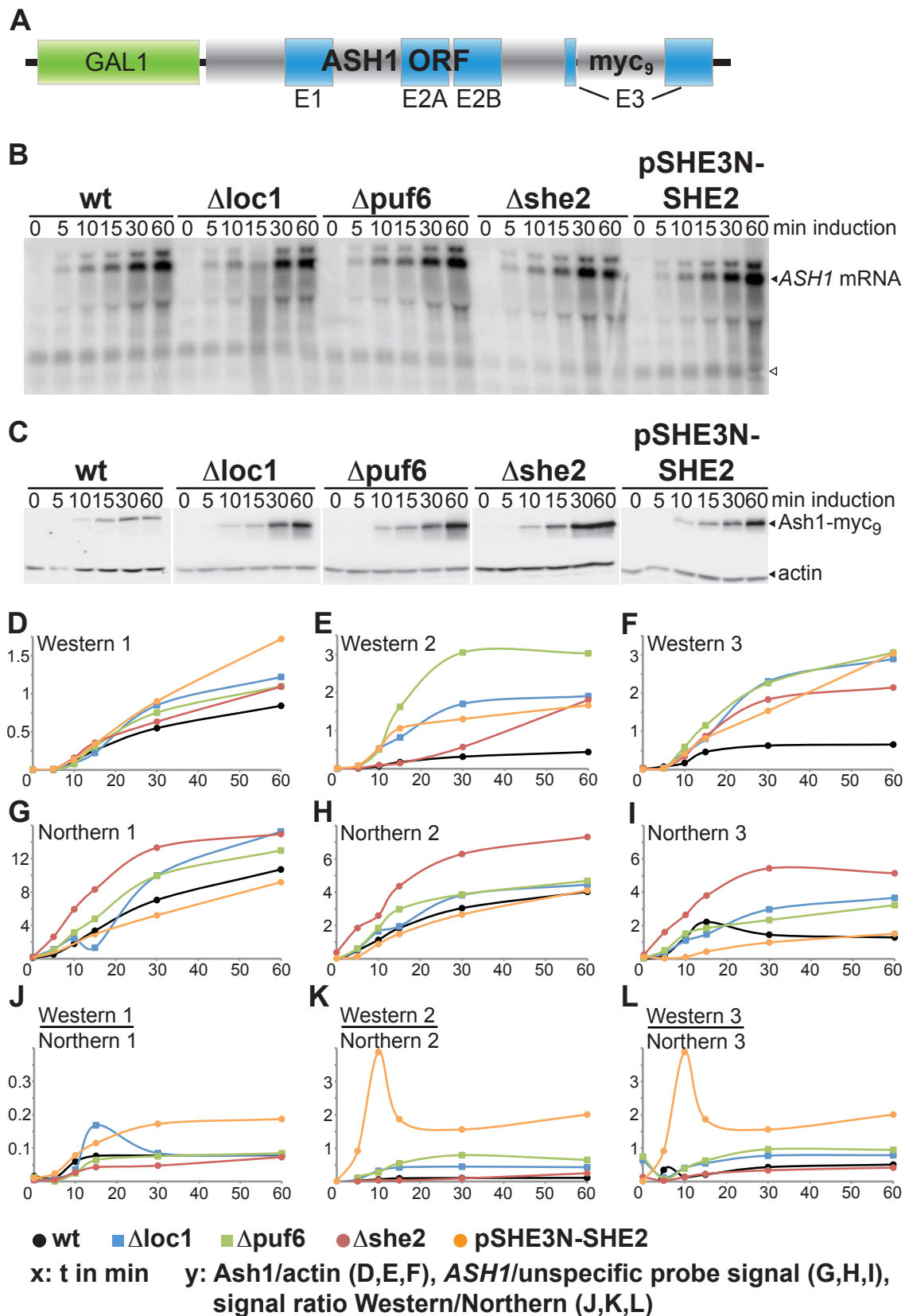


Figure 21 | Ash1 synthesis is accelerated in cells expressing the She3N-She2 fusion protein.

A | Schematic view of the induction construct. The *ASH1* ORF with the four zip-code elements E1, E2A, E2B, and E3 (shown in blue) is placed under control of the *GAL1* promoter (green); for detection by Western Blot, 9 myc-epitopes have been inserted in frame directly before the Stop codon (Long et al., 1997).

(continued: Figure 21)

B | *ASH1* mRNA levels are induced by addition of galactose. Cells of the indicated strains were grown to log-phase in raffinose-containing medium, then *ASH1* expression was induced by addition of 4% (v/v) galactose. Samples of the cultures were taken at 0, 5, 10, 15, 30, and 60 min after shift and processed for Northern and Western Blotting, respectively. The depicted Northern Blot shows a roughly similar induction in all strains (for quantification see below). *ASH1* mRNA signals could be detected from time point 5 min onwards. *ASH1* mRNA signals were normalized to a cross-reacting unspecific band (triangle).

C | All mutants tested show an accelerated Ash1 synthesis as compared to wild type (wt). For all mutant strains the Ash1-myc₉ signal at 60 min after shift is much stronger than in wt cells, as detected by Western Blot analysis. Signals were normalized to actin levels.

D - F | Quantification of Western Blots. Normalized Ash1 signals were plotted against time. The charts show that although induction is comparable to some extent - wt (black circles) induction is the weakest, Δ she2 (red circles) induction the second weakest - levels of induction for the remaining mutants differ, and induction kinetics are different between single experiments (y-axis range 0-1.75 in D, 0-3.5 in E and F).

G - I | Quantification of Northern Blots. Like Ash1 protein, also *ASH1* mRNA kinetics can differ in overall signal intensity, as shown by Northern Blot (y-axis range 0-16 in G, 0-8 in H and I). However, similarities are also obvious: Δ she2 cells show the strongest induction, wt cells and cells expressing the She3N-She2 fusion (orange circles) the weakest. Normalized *ASH1* mRNA signals were plotted against time.

J - L | Signal ratio of single Western Blots to Northern Blots. The charts clearly show that cells expressing the She3N-She2 fusion protein have synthesized approximately twice as much Ash1 protein after 60 min induction than all other strains tested. In Δ puf6 (green squares) and Δ loc1 cells (blue squares), Ash1 synthesis is accelerated as well. By contrast, Ash1 synthesis in Δ she2 cells is almost identical to wt. The outlying values for pSHE3N-SHE2 at 15 minutes in K and L derive from the relatively low Northern signal for this strain at this time point (H, I). Note that the y-axis range of chart J is only 10% of the range of charts K and L.

2.7. *Loc1* does not inhibit *ASH1* mRNA translation directly

Our data on a possible role of *Loc1* in translational regulation of the *ASH1* mRNP are corroborated by a recent study (Komili et al., 2007). One question that has not been answered so far is whether this role is direct or indirect. A direct role in translational regulation of *ASH1* mRNA has been demonstrated for the two other accessory localization factors *Khd1* and *Puf6* (Deng et al., 2008; Paquin et al., 2007). Both proteins bind to the mRNA and inhibit translation during transport through interaction with translation initiation factors. In principle, this is also imaginable for *Loc1*; on the other hand, it has been convincingly shown that *Loc1* is a strictly nuclear protein (Long et al., 2001).

My working hypothesis to resolve this problem was the following: if deletion of *Loc1* leads to increased Ash1 synthesis and *Loc1* exerts a direct role in translational silencing, then overexpression of *Loc1* should lead to decreased Ash1 synthesis. Hence, I created strains where tagged versions of either the known direct translational inhibitor *Khd1* or *Loc1* were overexpressed from a galactose-inducible promoter on a plasmid; the empty plasmid served as a negative control.

Expression levels of both proteins were comparable, as judged by Western Blot (data not shown).

I followed Ash1 protein levels over time by Western Blot (Figure 22). Overexpression of Khd1 strongly reduces Ash1 protein levels. In contrast, overexpression of Loc1 does not seem to have any effect on Ash1 levels at all.

Taken together, these data indicate that Loc1 does not have a direct role in translational silencing of the *ASH1* mRNP, consistent with an exclusive nucle(ol)ar localization.

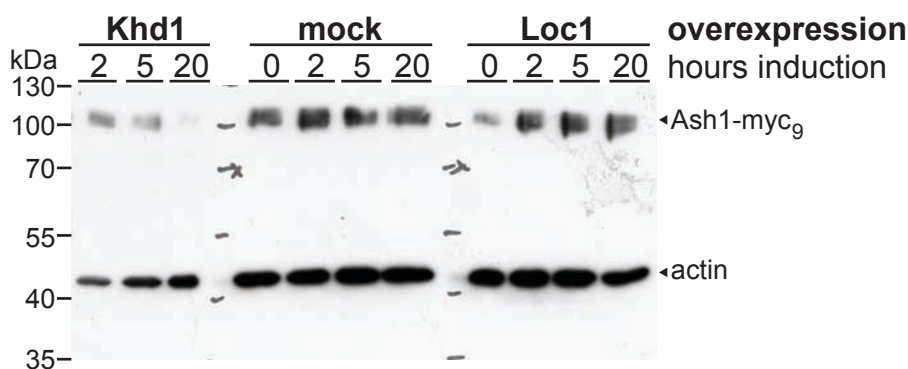


Figure 22 | Overexpression of Loc1 does not influence Ash1 levels.

A plasmid with a galactose-inducible promoter (*GAL1*) carrying either no insert (mock overexpression, Loc1-HA₆ (Loc1 overexpression), or Khd1-HA₆ (Khd1 overexpression) was transformed into a strain where 9 myc-epitopes have been inserted into the *ASH1* ORF to allow detection by Western Blot. All strains were grown in raffinose-containing medium to early log phase and then shifted to medium containing galactose. Aliquots were removed at indicated time points and processed for Western Blot analysis. Ash1 protein levels are strongly reduced after 20 hours overexpression of Khd1, a translational repressor of Ash1. In contrast, Ash1 levels remain unaffected by overexpression of Loc1 as well as by a mock overexpression.

2.8. Function of Loc1 in mRNA localization and ribosome biogenesis seems to be coupled

2.8.1. Loc1 truncation analysis does not identify separable functional domains

In previous sections of the present thesis I have demonstrated that a deletion of *LOC1* has little effect on translational silencing of Ash1, but impairs mRNA localization and ribosome biogenesis significantly. However, most studies that cover Loc1 concentrate on just one of the processes. Only recently there has been a study that tried to integrate functions of Loc1 in ribosome assembly and translational regulation (Komili et al., 2007). Since ribosome biogenesis is one of the most fundamental processes in a cell (Warner, 1999), it is well possible that a

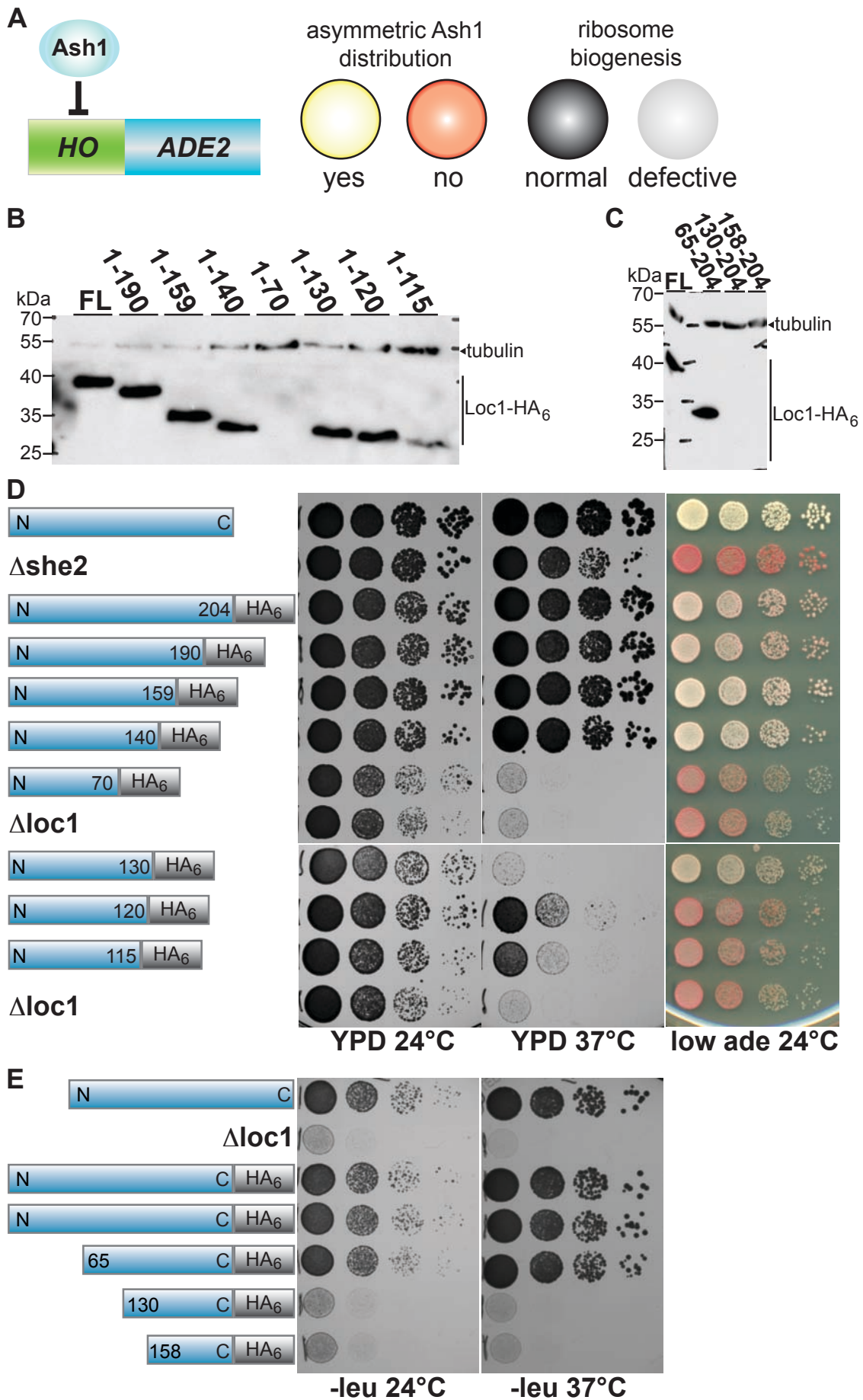
deletion of *LOC1* affects primarily ribosome biogenesis, whereas the described impact on localization of mRNAs is a secondary effect.

In order to address this question, I first wanted to investigate whether functions of Loc1 in RNA localization and ribosome biogenesis are confined to distinct regions of the protein. As shown above, secondary structure prediction does not point to the existence of any known domains (Figure 7); therefore, I decided to analyze the protein by truncation. For a first approximation, I needed a system that allowed easy and fast readout.

Most of the proteins implicated in *ASH1* mRNA localization are non-essential, hence, knockouts do not or only slightly impair cell growth (Jansen et al., 1996; see below). However, $\Delta loc1$ cells grow slowly at 30°C and die at 37°C (Figure 14B). I concluded that this temperature sensitivity is linked to Loc1's role in ribosome biogenesis and that I could therefore use it to assess whether this process is affected by specific truncations (Figure 23A). Impairment of *ASH1* mRNA localization and consecutive defective Ash1 protein distribution could be monitored with a system originally used to identify the She proteins (Jansen et al., 1996). There, the *ADE2* gene is placed under control of the *HO* promoter, which is regulated by the transcription repressor Ash1. If Ash1 is distributed symmetrically between mother and daughter cell, *ADE2* is completely repressed and cells accumulate a red pigment, the polymerized form of an intermediate in adenine biosynthesis (Smirnov et al., 1967; Figure 23A).

Before the respective strains were spotted onto selection plates, I checked expression levels of Loc1 truncations by Western Blot. Deletion of up to 84 amino acids from the C-terminus did not significantly alter protein expression (Figure 23B). However, already a truncation where only the first 130 amino acids remain (1-130) appears slightly reddish and hardly grows at 37°C. It is unclear why the subsequent truncation 1-120 grows better at 37°C. From truncation 1-120 to 1-115, temperature sensitivity increases, and colonies are red (Figure 23D).

Out of three plasmid-borne N-terminal truncations only one was expressed (Figure 23C). This N-terminal truncation (65-204) displayed no growth phenotype; for technical reasons (cell growth even of wild type was strongly impaired on plates lacking leucine and containing low adenine), red/white screening was not possible here.



(preceding page)

Figure 23 | The extreme N- and C-terminal parts of *Loc1* seem to be dispensable for *Loc1* function.

A | Schematic representation of a plate assay to determine in a first approximation correct Ash1 protein distribution (red/white screening) and ribosome biogenesis (growth at 37°C). In the strain background used, the *ADE2* gene is placed under control of the *HO* promoter, which is transcriptionally repressed by Ash1. In budding cells where Ash1 is symmetrically distributed between mother and daughter cell nuclei, *ADE2* is repressed and colonies turn red (Jansen et al., 1996).

B | C-terminal truncations of *Loc1*. Western Blot analysis shows that expression levels are comparable for full-length protein (FL) and truncations up to 84 amino acids (lane 1-120). Further truncation reduces *Loc1* expression (1-115). The largest truncation (1-70), where 134 amino acids have been removed from the C-terminus, is not expressed. Truncations were created by homologous recombination of PCR products as described in section 5.4.3.

C | N-terminal truncations of *Loc1*. Plasmids carrying N-terminal truncations of *LOC1* were transformed into a $\Delta loc1$ strain grown in full medium and analyzed by Western Blot. Only the first truncation, where the N-terminal 64 amino acids have been removed (65-204), is expressed.

D | Removal of up to 64 amino acids from the C-terminus seems not to affect growth or Ash1 distribution. The plate assay shows that removal of 10 additional amino acids affects growth at 37°C, but seems to have little effect on Ash1 distribution, as spotted colonies remain white (see Discussion). Further truncation of the C-terminus affects both growth and Ash1 distribution. A wild type (wt) strain has been used as negative control, a *she2* deletion strain ($\Delta she2$) as positive control for the red/white selection.

E | Removal of up to 64 amino acids from the N-terminus does not inhibit growth. With the minimal plates used, which lack leucine to select for the plasmid and low adenine, all colonies were reddish and grew slowly, thus Ash1 distribution could not be tested.

From the data presented above, one could suspect that temperature sensitivity and red pigmentation are coupled. Therefore, I tested deletions of other mRNA localization factors as well as deletions of non-essential ribosome biogenesis factors, thereby extending the analysis from section 2.4. Deletion of *SHE2* served as control for loss of asymmetric Ash1 protein distribution; $\Delta she2$ cells show the most intense red pigmentation of colonies of all factors tested, while growth at 37°C is barely inhibited (Figure 24A). Disruption of *PUF6* does not inhibit growth significantly, but cells are reddish; $\Delta khd1$ behaves as wild type in this assay. Interestingly, some deletions of ribosome biogenesis factors seem to affect Ash1 distribution (Figure 24B). A strain with a deletion in *NOP16* (see section 2.4) shows slightly reddish color, but grows like wild type; the phenotype of $\Delta ssf1$ (for suppressor of swi4, an early 60S biogenesis factor; Fatica et al., 2002) in the plate assay resembles that of $\Delta puf6$. Knockout of the late 60S biogenesis factor *ARX1* (for associated with ribosomal export complex; Nissan et al., 2002) and the putative 90S biogenesis factor *NOP6* (Fromont-Racine et al., 2003), respectively, cause temperature sensitivity, but do not impair growth at 24°C or Ash1 distribution at all (Figure 24B). Cells carrying a deletion in *RRP8* (for ribosomal RNA processing), a factor required for cleavage of pre-rRNA at site A₂ (see Figure 2; Bousquet-

Antonelli et al., 2000) have a mild growth defect and slight reddish color. Deletion of the 40S biogenesis factor *LTV1* (see section 2.5.1) leads to temperature sensitivity and red colonies on plates containing low adenine, and an even more intense color can be observed in $\Delta mrt4$ cells, which show a growth defect already at 24°C as well. The defective Ash1 distribution indicated by the red $\Delta mrt4$ colonies is consistent with the impaired *ASH1* mRNA localization described above (Figure 11).

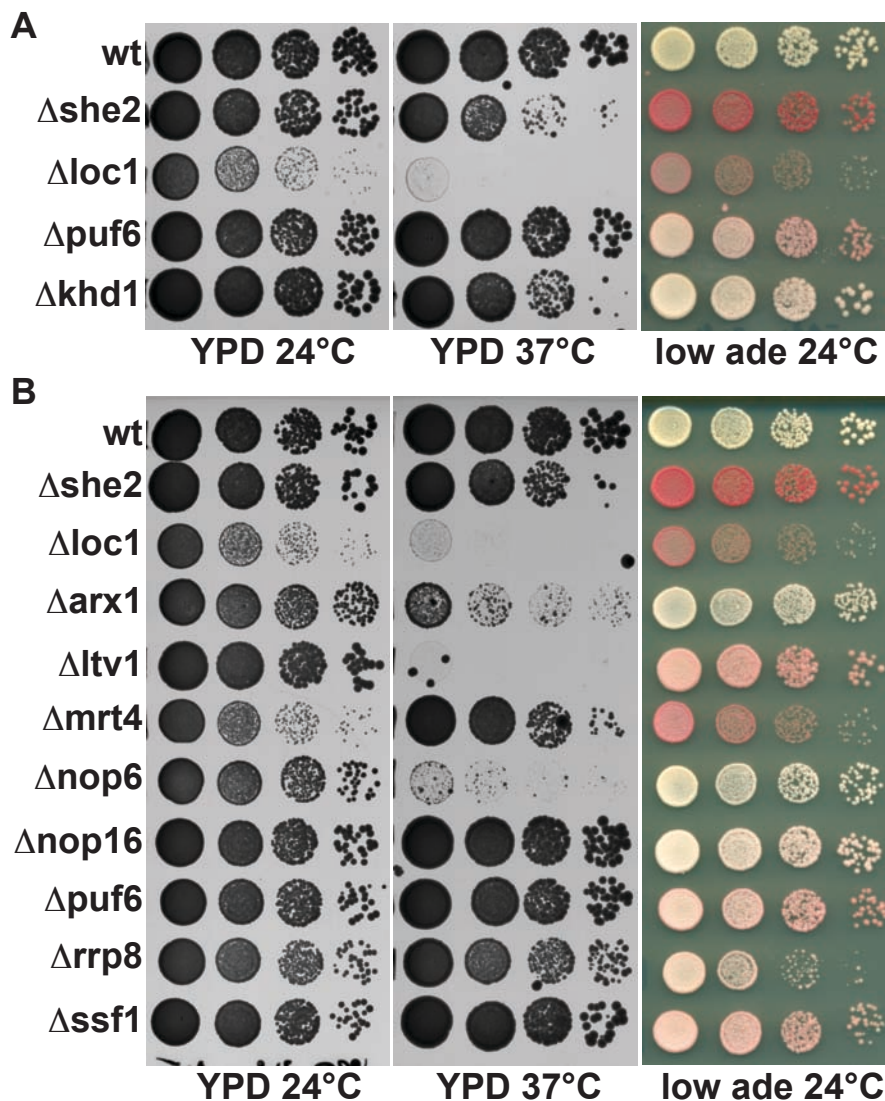


Figure 24 | Several ribosome biogenesis mutants show defective Ash1 distribution, whereas not all *trans*-acting RNA-localization factors do so.

A | The plate assay (see Figure 23A) shows that from the three *trans*-acting *ASH1* mRNA localization factors *Loc1*, *Puf6*, and *Khd1*, $\Delta loc1$ strongly impairs growth at 37°C as well as Ash1 distribution. $\Delta khd1$ has no growth defect and only a moderate effect on Ash1 distribution (only slightly reddish colonies). $\Delta puf6$ shows no slow growth phenotype.

B | Several non-essential ribosome biogenesis factors also affect Ash1 distribution. The plate assay shows that slow growth and red color (indicating symmetric Ash1 distribution) are not necessarily coupled (e.g. $\Delta arx1$, $\Delta nop6$). Interestingly, defective Ash1 distribution is not restricted to known *ASH1* mRNA localization factor deletions.

Taken together, the data presented indicates that the extreme C- and N-terminal parts of Loc1 seem to be dispensable for Loc1 function, and no functional protein domains could be identified. Furthermore, temperature sensitivity does not necessarily cause red-colored colonies in the plate assay.

2.8.2. Rapid and efficient depletion of Loc1 from yeast cultures is possible with glucose shut-off

Truncation analysis of Loc1 showed that there are no distinct protein domains with separate function in ribosome biogenesis and mRNA localization, respectively. Still, it is imaginable that depletion of Loc1 would first result in defective ribosome biogenesis before impairing *ASH1* mRNA localization. To test this hypothesis of a “first response”, I needed a system that allows rapid and efficient depletion of Loc1, preferably within one cell division cycle.

A number of ways to deplete proteins from cells have been described in the literature. Probably the easiest is addition of a drug to the growing culture, which induces depletion of the desired protein. Thus, I decided to test a doxycycline-regulatable promoter system first (Garí et al., 1997). Here, a tagged version of the *LOC1* ORF is inserted into a plasmid in order to place it under the control of two tetracycline operator ($tetO_2$) boxes. A Cytomegalovirus (CMV) promoter-controlled transcriptional transactivator (tTA) contains a tetracycline-inducible repressor (tetR), which allows expression of $tetO$ -regulated genes only in the absence of tetracycline (Figure 25A; Garí et al., 1997).

Western Blot analysis showed that Loc1-HA₆ is indeed expressed in the absence of doxycycline (dox), though at a slightly lower apparent molecular weight as compared to genomically tagged Loc1. In addition, several less intense cross-reacting bands were always detected (Figure 25B). Addition of doxycycline to growing cultures depleted Loc1 quite efficiently, but not completely, since it was still detectable four hours after dox had been added (Figure 25B). After two hours, roughly one generation time, the protein level was just reduced to about 50%. I considered this not fast enough and therefore decided that the Tet_{off} system was not suited for my experiments.

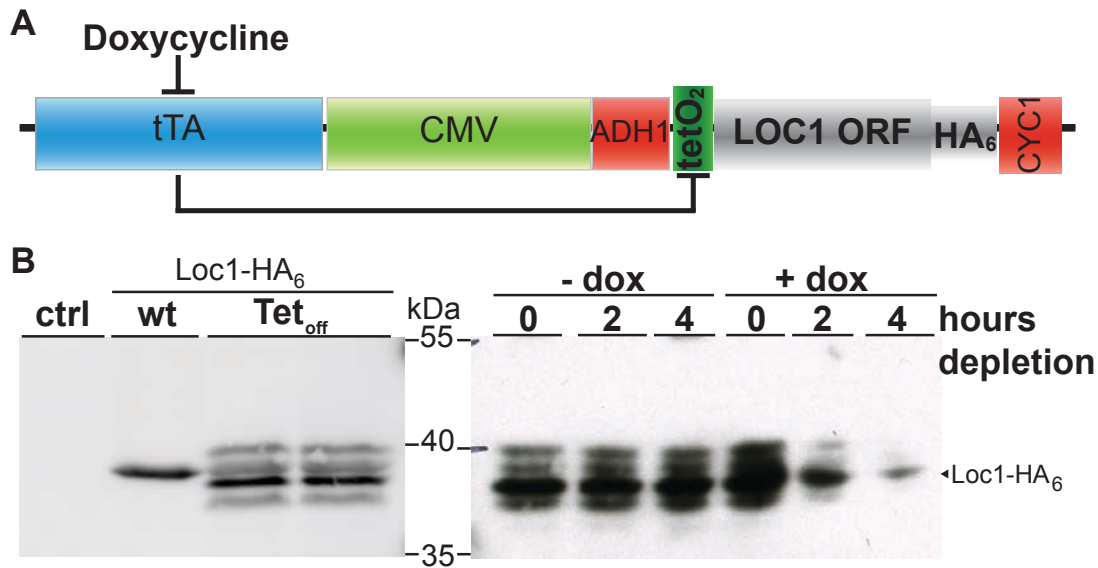


Figure 25 | Control of *Loc1* expression with a doxycycline-regulatable promoter is not sufficient for rapid, complete depletion.

A | Schematic view of the tetracycline-regulatable promoter construct (Garí et al., 1997). The *LOC1* ORF is inserted into the MCS of a plasmid between a double tandem repeat of the tetracycline operator ($tetO_2$), and a *CYC1* terminator sequence. The transcriptional transactivator (tTA) is controlled by a Cytomegalovirus (CMV) promoter. Both parts are separated by the *ADH1* terminator sequence. For all experiments doxycycline (dox) was used, a member of the tetracycline antibiotics.

B | (left panel) Western Blot to control for expression. *Loc1*-HA₆ has a slightly lower apparent molecular weight when expressed from the *Tet_{off}*-plasmid (*Tet_{off}*), as compared to a genomic HA₆-tag (wt). The empty plasmid is not detected by the HA-antibody (ctrl). (right panel) Western Blot of a *Loc1* depletion time course. After 4 h in medium containing 2 μ g/ml doxycycline, the signal corresponding to *Loc1*-HA₆ is greatly reduced as compared to the signal from cells grown without doxycycline. However, depletion is not complete.

Next, I tried depletion of *Loc1* by a heat-inducible degron, which has been described to allow very rapid depletion (Sanchez-Diaz et al., 2004). Here, genomic *LOC1* is N-terminally tagged with a so-called degron cassette under control of a copper-inducible promoter (*CUP1*; Figure 26A). The single myc-epitope in the degron cassette proved to be insufficient for detection by Western Blot, therefore a C-terminal tag had to be added to *Loc1*. After shift of the temperature to 37°C, an exposed arginine residue in the mutant mouse dihydrofolate reductase (DHFR^{ts}) is bound by Ubr1 (for ubiquitin protein ligase E3 component n-recogin; Bartel et al., 1990). Ubr1 is associated with the ubiquitin-conjugating enzyme Rad6 (for radiation sensitive; Jentsch et al., 1987), binding of Ubr1 therefore induces ubiquitylation of exposed lysines and subsequent proteasomal degradation (Figure 26B; Sanchez-Diaz et al., 2004).

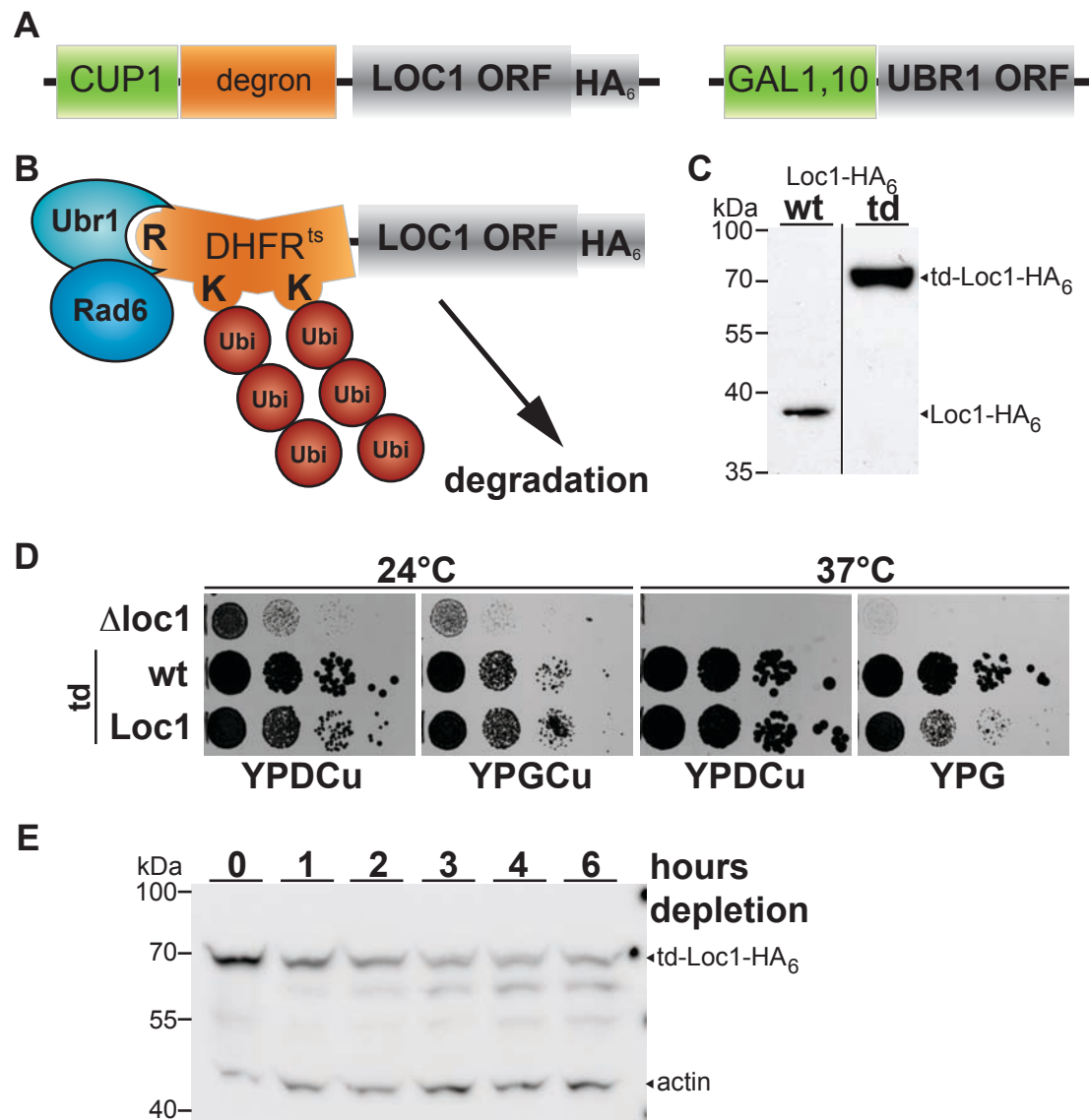


Figure 26 | Fusion of *Loc1* to a heat-inducible degron is not suited for rapid, complete depletion of *Loc1*.

A | Components of the heat-inducible degron system (Sanchez-Diaz et al., 2004). The *LOC1* ORF is fused with the degron cassette at the N-terminus. Besides a selection marker (kanMX, not shown), the degron cassette consists of a copper-inducible promoter (*CUP1*), followed by the degron, which contains a mutant, temperature-sensitive version of murine dihydrofolate reductase (*DHFR^{ts}*) and a single myc epitope. In addition, the ts-degron (td) strain background has *UBR1* placed under the control of a galactose-inducible promoter (*GAL1,10*).

B | Principle of the heat induction to destabilize td-fused *Loc1*. The N-terminal arginine residue (R) is bound by Ubr1/Rad6: This induces ubiquitylation of exposed lysine (K) residues, which favors degradation of the fusion protein at 37°C (Sanchez-Diaz et al., 2004).

C | Western Blot to verify an additional C-terminal HA₆-tag. *Loc1*-HA₆ has an apparent molecular weight of approximately 38 kDa in a wild type background (wt), and of approximately 70 kDa, when fused to the N-terminal ts-degron (td).

D | Depletion of td-*Loc1*. Serial dilutions of a *loc1* deletion strain ($\Delta loc1$), the degron strain (wt), and the td-strain of *Loc1* were spotted onto plates and incubated at the respective temperature for 3 days. In the presence of high levels of Ubr1 at 37°C, td-*Loc1* cells grow slightly worse as compared to 24°C, suggesting that *Loc1* is indeed depleted to a certain extent. Ubr1 expression is very low on plates containing glucose (YPDCu), but high on plates containing galactose (YPG(Cu)). Copper is included in some plates to maintain expression levels of the td-fusion.

E | Western Blot of a td-*Loc1* depletion time course. After 6 h at 37°C in YPG, the td-*Loc1*-HA₆ signal is reduced and degradation bands are visible. However, depletion is not complete.

I controlled for expression of the ts-degron-Loc1 (td-Loc1) fusion protein by Western Blot (Figure 26C). Then, I analyzed depletion with dot tests on different plates. If *UBR1* expression is repressed (glucose plates) and td-Loc1 expression induced, cells grow like wild type. Contemporaneous repression of td-Loc1 expression and induction of *UBR1* at 37°C leads to smaller colonies as compared to wild type (Figure 26D). However, the observed phenotype is rather mild. A depletion time-course and subsequent Western Blot analysis reveals that even six hours after shift to galactose and restrictive temperature, td-Loc1-HA₆ is not efficiently depleted, consistent with the mild growth defect (Figure 26E). It is therefore unusable for the analysis of a first response.

One of the oldest systems used to deplete proteins in yeast is glucose shut-off. It is easily applicable but requires a shift of the carbon source. Since neither the Tet_{off} nor the td system worked, I tried to deplete Loc1 by glucose shut-off with two constructs (Figure 27A). In the first construct, a shortened *GAL1* promoter (*GALS*, Mumberg et al., 1994) controls expression of N-terminally HA₃-tagged Loc1; the shortening serves to keep galactose induction relatively low, but still enables full repression (Janke et al., 2004; Mumberg et al., 1994), and I speculated that depletion might be faster when starting from a lower protein level. Besides, Loc1 is expressed at low levels in wild type (Ghaemmaghami et al., 2003). The second construct regulates HA₃-Loc1 expression from a standard *GAL1* promoter, but with a shortened spacer between tag and protein, resulting in a shorter fusion protein (Figure 27B; Longtine et al., 1998).

Western Blot analysis of a depletion time course shows that both constructs are expressed at similar levels in galactose-containing medium (Figure 27B). Upon shift to glucose, the *GALS*-promoter construct (Knop-cassette) requires more than five hours until the HA-signal disappears completely. In contrast, HA₃-Loc1 under control of the *GAL1* promoter (Longtine-cassette) is undetectable already three hours after promoter shut-off. Growth of the Loc1-depleted cells remains unaffected for the first two hours after shift to glucose, then cells grow significantly slower (Figure 27D).

To summarize, glucose shut-off is an excellent means to completely deplete Loc1 from a logarithmically growing yeast culture within three hours, in contrast to systems using tetracycline repression and a heat-inducible degron, respectively.

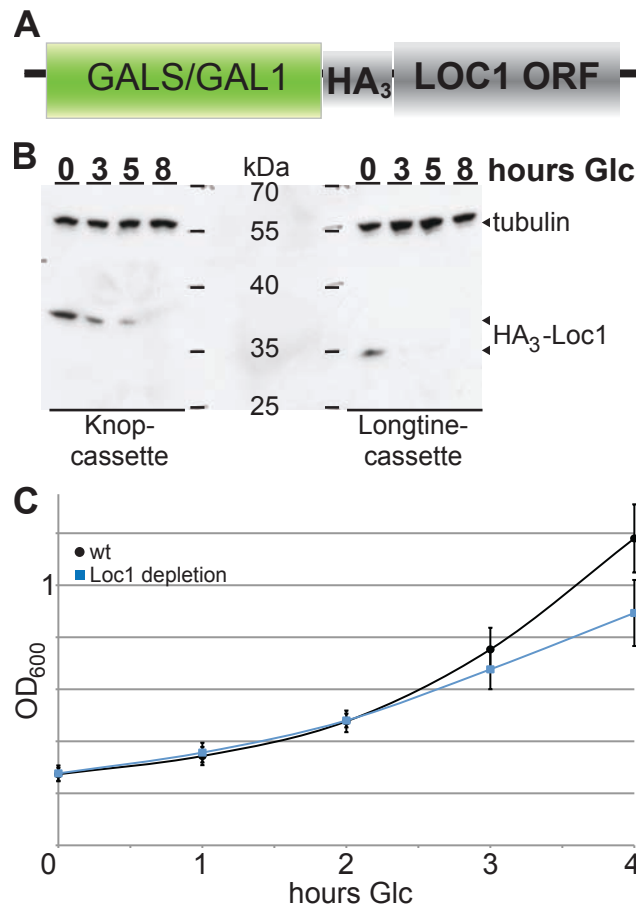


Figure 27 | Regulation of *LOC1* expression by a specific Galactose promoter can be used to completely deplete *Loc1* in less than three hours.

A | Schematic view of the Glucose shut-off construct. The *LOC1* ORF is tagged at the N-terminus with 3 copies of the HA epitope for detection by Western Blot, and placed under control of either a shortened version of the *GAL1* promoter (*GALS*, Janke et al., 2004) or the full length *GAL1* promoter (*GAL1*, Longtine et al., 1998).

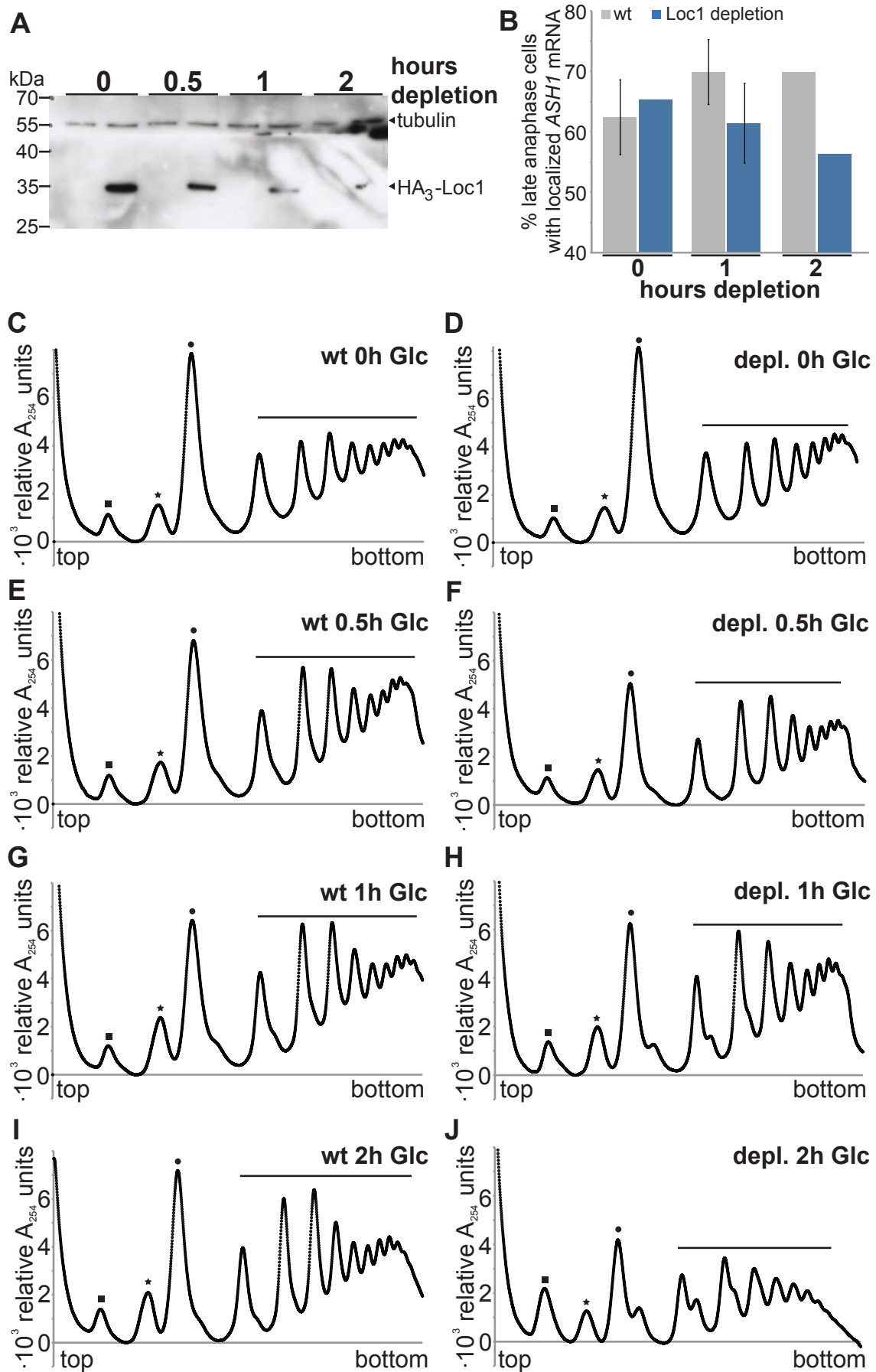
B | *GAL1* promoter-driven *HA₃-LOC1* can be rapidly depleted in glucose-containing medium. Western Blot analysis shows that the *GALS* promoter-driven *Loc1* is depleted completely only after 8 hours promoter shut-off (left panel). In contrast, *Loc1* is not detectable by Western Blot after 3 hours promoter shut-off using the *GAL1* promoter construct. Cells were grown overnight in galactose-containing medium (YPG), diluted and grown for another generation in fresh YPG, before being washed and released into complete medium containing glucose (YPD). Aliquots were removed from the culture at indicated time points and subjected to Western Blot analysis. An antibody directed against tubulin has been used to control equal loading.

C | Growth analysis of a wild type (wt, black) and *Loc1* depletion strain (Longtine-cassette; blue). During the first two hours after the shift to YPD, both strains grow equally well. Subsequently, growth of the *Loc1* depleted cells slows down. Data comes from three independent experiments.

2.8.3. Depletion of *Loc1* affects *ASH1* mRNA localization and ribosome biogenesis simultaneously

With a powerful tool for *Loc1* depletion at hand, I was able to examine whether the function of *Loc1* in ribosome biogenesis and *ASH1* mRNA localization is kinetically distinguishable or not.

I performed a time course and removed aliquots for FISH and sucrose density gradient centrifugation from logarithmically growing cultures of a wild type and a *Loc1* depletion strain, respectively.



(preceding page)

Figure 28 | Effects of *Loc1* depletion on localization of *ASH1* mRNA and biogenesis of ribosomes seem to be coupled and can be detected after one hour depletion.

A | *Loc1* is almost completely depleted after 2 hours shift to glucose-containing medium. Aliquots from cultures of a wt and a *Loc1* depletion strain shifted to YPD were taken at indicated time points and subjected to Western Blot analysis. An antibody directed against tubulin was used to control loading. After two hours, the HA₃-*Loc1* signal is reduced to roughly 10% of time point 0.

B | One hour depletion of *Loc1* causes significantly reduced *ASH1* mRNA localization. *ASH1* localization of late anaphase cells from a culture immediately (0 h depletion) and one hour (1 h depletion) after shift to YPD was determined by fluorescent *in situ* hybridization (FISH; see Figure 10). Whereas 70±5.4% of wild type (wt) cells localize *ASH1* mRNA correctly after one hour, only 61±6.6% of *Loc1*-depleted cells do so (n(wt)=144, n(*Loc1* depl.)=113, $P<0.03$). The phenotype increases with time, after two hours depletion only about 55% of cells still localize *ASH1* mRNA correctly. Error bars indicate standard deviation from three experiments, single experiments without error bars.

C-H | One hour depletion of *Loc1* mildly impairs large ribosomal subunit biogenesis. In wild type (wt) cells, profiles of time points 0, 0.5, 1 and 2 hours after shift to glucose are comparable except for a small shoulder in the 80S peak (marked by a circle), which may be caused from the shift itself (C, E, G, I). In *Loc1*-depleted cells, the shoulder at 1 hour after shift (H) is much more prominent and can be seen in the disome and trisome peak as well. It corresponds to the half-mer peak also seen in $\Delta loc1$ cells (see Figure 14). After two hours *Loc1* depletion, the 40S peak (square) is already higher than the 60S peak (asterisk), the 80S and polysome peaks are diminished, and the half-mer peaks further increase (J). Profiles were collected from 300 μ g total RNA loaded onto 7-47% linear sucrose gradients. All profiles were normalized, so that the lowest point in the valley between 40S and 60S corresponds to 0.

Both strains had been transformed with a high-copy *ASH1* plasmid to facilitate FISH (see section 2.4). A control Western Blot showed that about two thirds of the protein are depleted after one hour in YPD (Figure 28A). At this time point, both 60S biogenesis and RNA localization are significantly impaired as compared to wild type. Correct *ASH1* mRNA localization is observed in about 70% of wild type cells one hour post-shift, but in only 60% of *Loc1*-depleted cells (Figure 28B). Concomitantly, distinct half-mer peaks appear at mono-, di-, and trisomes (Figure 28H). Further depletion worsens the phenotype, two hours after shift the 60S peak is lower than the 40S peak, the amount of monosomes is significantly reduced as compared to wild type, and prominent half-mers are observed from mono- to trisomes; percentage of cells localizing *ASH1* mRNA correctly decreases as well (Figure 28B, J). Apart from a slightly lower monosome peak, I did not detect any differences between wild type and *Loc1*-depleted cells 30 minutes after shift, neither in FISH nor in polysome gradients (Figure 28E, F and data not shown).

Taken together, these results suggest that the functions of *Loc1* in large ribosomal subunit biogenesis and mRNA localization are not separable in terms of time or protein domains.

2.9. Future directions

2.9.1. Translational regulation of *ASH1* mRNA might be tightened by modifications

The results shown above suggest that nucleolar transit of *ASH1* mRNA is required to ensure translational silencing. The nucleolus might not only be the site where Puf6 is loaded onto the *ASH1* mRNP (Deng et al., 2008). It is possible that certain mRNAs traveling through this nuclear compartment might also be modified (Decatur & Fournier, 2003; see also Discussion), since one important function of the nucleolus is the post-transcriptional modification of RNAs (Gerbi et al., 2003). The most frequent modifications are the small nucleolar RNA (snoRNA) guided conversion of uridine to pseudouridine (Ψ) and methylation of 2'-hydroxyl groups in ribose (Kiss, 2002; Figure 29A).

In order to test the hypothetical presence of modified nucleotides in *ASH1* mRNA, I tried to set up a published experimental system, but with the use of fluorescent instead of radioactively labeled probes, as described in section 5.1.10 (Ganot et al., 1999).

The experimental setup is based on primer extension. Ψ residues are covalently coupled to the compound CMC (see section 5.1.10.1; Figure 29C); the resulting adduct poses an obstacle to reverse transcriptase, causing stuttering of the transcribing enzyme (Denman et al., 1988). Similarly, in the presence of very low nucleotide concentrations, 2'-O-methylations constitute a conformational barrier to the passage of reverse transcriptase (Maden et al., 1995; Figure 29B). Pausing of the enzyme can be seen as distinct bands on a sequencing gel. As a proof of principle, I tried to map two known 2'-O-methylation sites in yeast 25S rRNA (Figure 29D) and known Ψ sites yeast U2 snRNA (Massenet et al., 1999). Subsequently, I wanted to extend the analysis to the E3 element of *ASH1* mRNA, where both Puf6 and Loc1 have been shown to bind (Figure 4; Figure 29E).

Preliminary results are shown in Figure 30. While the visualization of Ψ residues did not work (data not shown), probably due to the low abundance of U2 snRNA in the total RNA preparation, the two 2'-O-methylated cytosines at positions 1437 and 1451 of the 25S rRNA region were clearly identified (Figure 30A). However, mapping of putative 2'-O-methylated ribose molecules or pseudouridines was not

possible for the examined region of *ASH1*, though the ORF had been highly overexpressed by a two-hour galactose induction (Figure 30B).

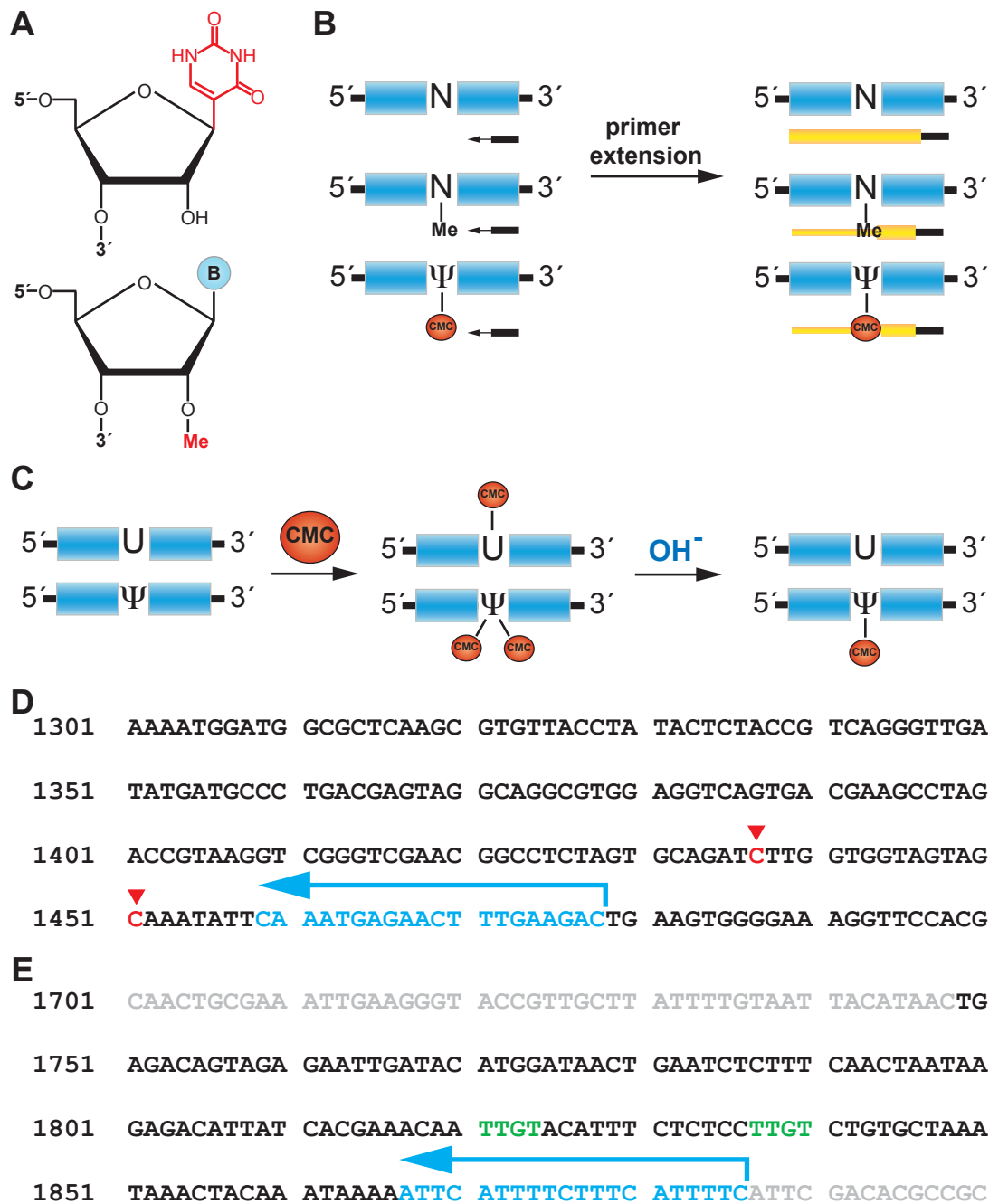


Figure 29 | Nucleotide modifications can be detected by primer extension.

A | Structures representing pseudouridine (Ψ ; top) and 2'-O-methylated ribonucleotides (Me; bottom). Pseudouridine differs from uridine in the connection of the base to the sugar.

B | Principle of primer extension experiments to detect 2'-O-methylation and pseudouridylation. Unmodified nucleotides (N) allow reverse transcriptase to pass at normal speed and to synthesize read-through transcripts (top panel). In contrast, 2'-O-methylated nucleotides (at very low free nucleotide concentrations, middle panel) or pseudouridines treated with CMC (bottom panel) represent obstacles for the passage of the enzyme and cause pausing or termination of reverse transcription, resulting in bands visible in sequencing gels (Bakin & Ofengand, 1993; Maden et al., 1995).

(continued: Figure 29)

C | Schematic view of CMC treatment to detect pseudouridines. Purified RNA is incubated with CMC, which binds to the imino-groups of e.g. uracil (U) and pseudouridine (Ψ), respectively. While the CMC-U intermediate and one of the CMCs bound to Ψ are cleaved under alkaline conditions, the second CMC bound to Ψ is stable (Bakin & Ofengand, 1993). B and C adapted from Bakin & Ofengand, 1993.

D | Genomic DNA sequence (nucleotides 1301 to 1500) of *RDN25-1* encoding 25S rRNA (Johnston et al., 1997). The oligonucleotide used for primer extension is indicated in cyan (reverse complement), 2'-O-methylated nucleotides in red (Ganot et al., 1999).

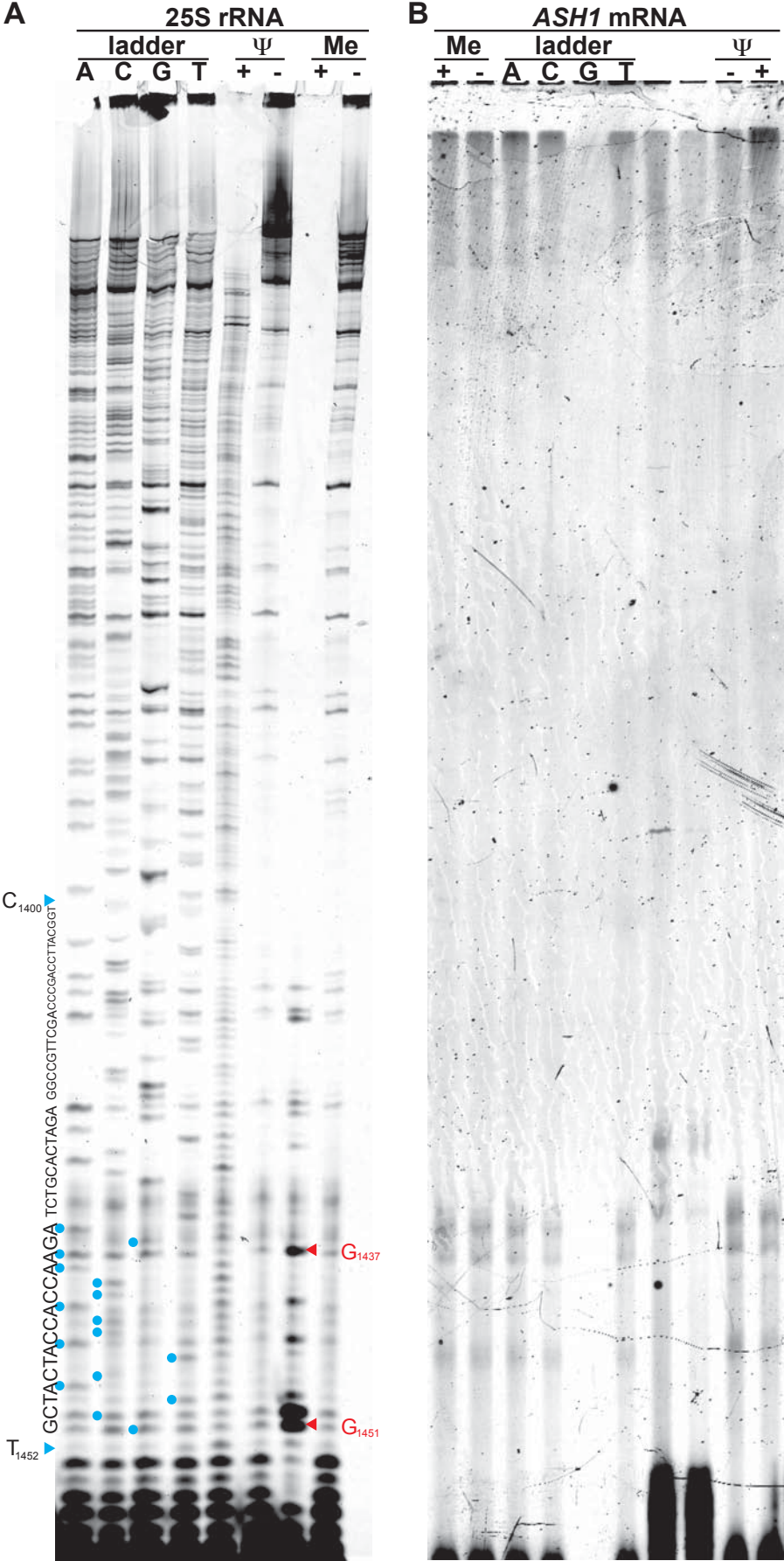
E | Genomic DNA sequence of a part of the *ASH1* ORF (nucleotides 1701 to 1767) and 133 nt of the 3'-UTR (Dujon et al., 1994). The E3 localization element is shown in black, flanking sequences in grey, the oligonucleotide used for primer extension in cyan (reverse complement), and possible Puf6 binding sites (see Gu et al., 2004) in green.

To summarize, an experimental setup based on primer extension with fluorescently labeled primers to map post-transcriptional modifications of RNAs works in principle, but there are some technical problems to overcome before it can be applied on *ASH1* mRNA.

2.9.2. Loc1 might act as a chaperone for RNA folding

In addition to the precise rationale behind nucleolar passage of localizing mRNPs, the molecular mechanism of Loc1 function remains to be elucidated. I have demonstrated that it exerts an indirect role in translational regulation of *ASH1* mRNA, and that it participates both in the localization of mRNAs and in early large ribosomal subunit biogenesis. Since these functions could not be separated spatially or temporally with the experiments performed, I speculated on a mechanism that could integrate all functions. One scenario that would explain an effect on mRNA localization, a delay in large subunit biogenesis and reduced translational regulation is that Loc1 assists both mRNAs and rRNAs to fold. To test for a possible RNA chaperone activity of a protein of interest, there are several assays available (Rajkowitzsch et al., 2005).

In yeast, a very easy assay, although of limited significance, is genetic interaction with Lhp1 (for La homologous protein), a protein implicated in RNA folding (Wolin & Wurtmann, 2006; Yoo & Wolin, 1994). I created deletion strains for both *LOC1* and *LHP1*, mated and sporulated them, and dissected tetrads. Though a double deletion is not synthetic lethal, it does grow slightly worse than a $\Delta loc1$ strain; $\Delta lhp1$ cells show no growth phenotype at all (Figure 31A). Similarly, I detected a



(previous page:)

Figure 30 | Primer extension experiments allow detection of 2'-O-methylated nucleotides in 25S rRNA, but not in *ASH1* mRNA.

A | Primer extension experiment to detect 2'-O-Me and Ψ modifications in a region of 25S rRNA. The sequence is assigned from nucleotides C₁₄₀₀ to T₁₄₅₂; in the lower part of the gel, blue circles indicate individual base signals. While no pseudouridylations are detectable, the two known 2'-O-methylations C₁₄₃₇ and C₁₄₅₁ (red triangles) can be detected (see Ganot et al., 1999). Primer extension sequences are reverse complement, therefore Cs appear as Gs and are indicated accordingly in the figure (see Figure 29).

B | Primer extension experiment of a region of *ASH1* mRNA containing the E3 element. Although *ASH1* has been highly overexpressed by galactose induction, no signals are detectable.

synthetic sick phenotype in a double deletion of *LOC1* and *LSM7*, a member of the like Sm protein family also suggested to have RNA chaperone-like functions (data not shown; for a review of Lsm protein functions see Beggs, 2005). These observations do at least not contradict putative involvement in RNA folding, but a genetic interaction *per se* does not allow to draw meaningful conclusions.

A more generally applicable and significant assay to test RNA chaperone activity involves a ribozyme folding trap (Prenninger et al., 2006). This *in vivo* system only requires expression of the folding trap and the protein to be tested for chaperone activity in *E. coli*, and subsequent total RNA extraction and primer extension with a “poisoned” primer mix that contains ddTTP (Figure 31B). Incorporation of ddTTP into the RNA causes termination of reverse transcription; length of the extension products allows judging whether or not splicing has occurred. However, several attempts to perform the assay failed, most likely because the test proteins were not expressed, as verified by SDS-PAGE. Thus, I subcloned the gene encoding the control RNA chaperone, *stpA* (Zhang et al., 1995), into the same expression vector as *LOC1*, where the respective proteins had a N-terminal His₆-tag and it was possible to purify them with Nickel-NTA agarose. A test expression showed that *Loc1* is highly expressed, whereas *StpA* is barely detectable on Coomassie level (Figure 31C). However, without a positive control, it was pointless to pursue the assay.

In summary, a strain deleted for both *LHP1* and *LOC1* shows a mild synthetic growth defect, which might point at a function of *Loc1* as RNA chaperone. After the problem of the low control chaperone expression will have been solved, an *in vivo* RNA chaperone assay can be used to prove this hypothesis.

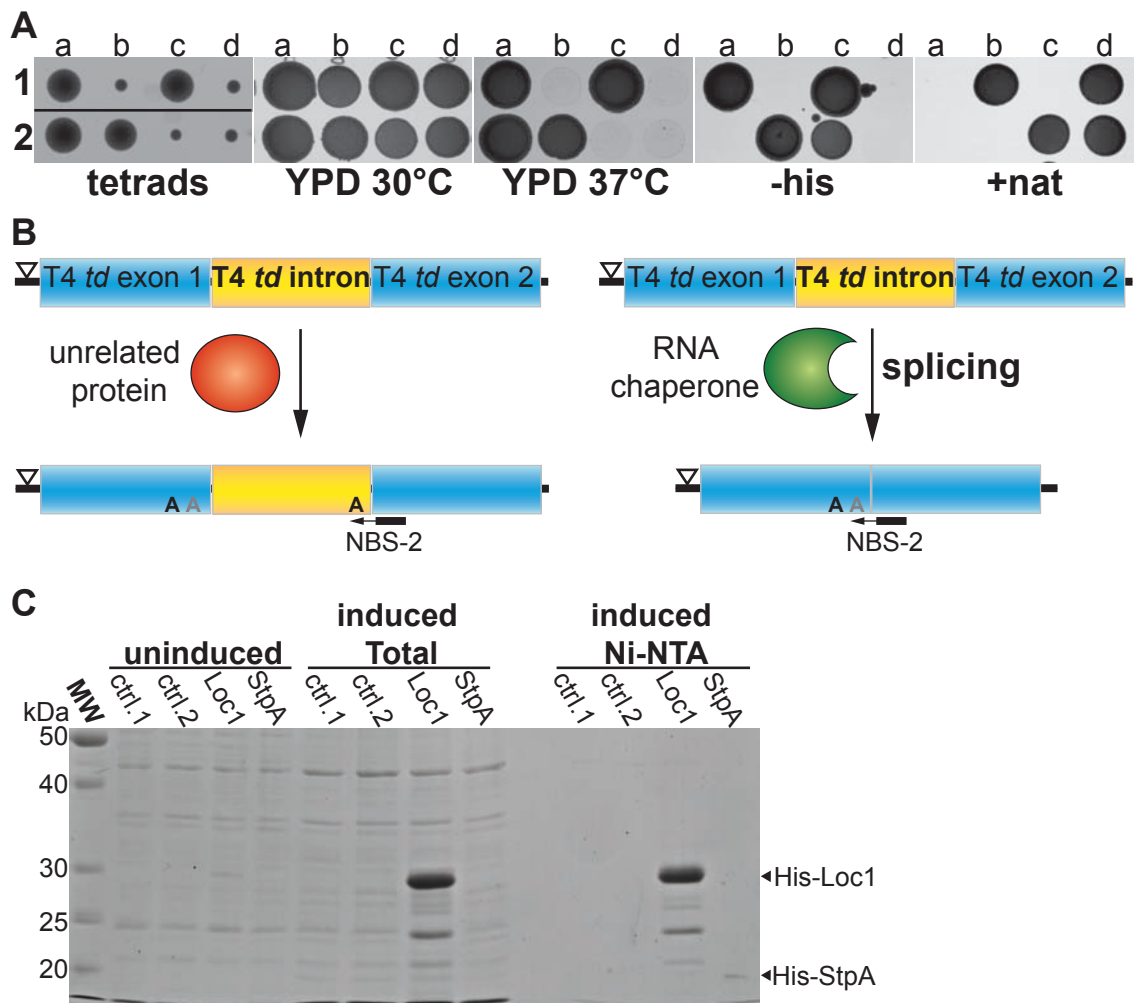


Figure 31 | Could *Loc1* be a RNA chaperone?

A | Double deletion of *LOC1* and *LHP1* does not result in synthetic lethality. Tetrad analysis of two sample tetrads generated from a diploid strain carrying a deletion in one allele of *LOC1* and *LHP1*, respectively. Spores that are $\Delta loc1$ can grow on plates containing clonNAT (nat), while spores that are $\Delta lhp1$ can grow on plates lacking histidine. All spores carry at least one gene knockout. $\Delta lhp1$ cells show no growth phenotype at all, whereas $\Delta loc1$ cells grow slower at 30°C and not at all at 37°C. Spore 2c, which carries both knockouts, shows a slightly worse growth phenotype than $\Delta loc1$ alone. Cells were spotted onto plates indicated, which were incubated either at 30°C or 37°C for 3 days.

B | Principle of an *in vivo* RNA chaperone assay using a RNA folding trap (Prenninger et al., 2006). A mutant version of the T4 phage thymidylate synthase gene (*T4 td*) has a stop codon (∇) placed in front of the first exon, which reduces self-splicing. The intron folds into a stable so-called RNA folding trap, which cannot be resolved by unrelated proteins (red; left panel). Splicing only occurs if a RNA chaperone (green) allows the intron to refold into its native structure. The efficiency of splicing can be monitored by primer extension with a poisoned nucleotide mix containing ddTTP. From the primer NBS-2, a reverse transcript is elongated until it reaches an A. The first A is located at position +5 for unspliced templates, and at position +16 for most spliced templates. In some cases, splicing occurs via a cryptic splice site, which causes the first A to be located at position +8.

C | Test expression of a candidate and a control RNA chaperone. *Escherichia coli* BL21 cells were transformed with 4 vector sets (see below). Cells were grown in TBYE medium and induced with IPTG for 3 hours. Cell pellets were then purified over Ni-NTA (see section 5.3.3) and aliquots analyzed by SDS-PAGE. Significant expression is detectable only for *Loc1*. (vector sets: **ctrl. 1** – *T4 td* wild type, empty expression vector; **ctrl. 2** – *T4 td* mutant, empty expression vector; **Loc1** – *T4 td* mutant, His₆/thrombin/T7-*Loc1*, **StpA** – *T4 td* mutant, His₆/thrombin/T7-*StpA*).

3. Discussion

3.1. The nucleolar protein Loc1 influences mRNA localization

Since the initial description of the She proteins and their function in localization of *ASH1* mRNA (Jansen et al., 1996; Long et al., 1997), further *trans*-acting factors have been characterized, among them Loc1 and Puf6. Both proteins have been shown to be mainly present in the nucleus, in contrast to other localization factors (Gu et al., 2004; Long et al., 2001). Microscopic data in the present study indicate that Loc1 and Puf6 are predominantly confined to a subnuclear compartment, the nucleolus. This result is in agreement with a genome-wide analysis of protein localization using GFP-fusions (Huh et al., 2003), and with data from an independent study focusing on Loc1 (Urbinati et al., 2006).

To date, more than 30 mRNAs in yeast have been shown to localize at least partially to the bud tip in a She-dependent manner (see Table 1). However, most of our knowledge on the function of *trans*-acting factors other than She proteins, such as Khd1, Loc1, or Puf6, derives from analysis of only one localizing mRNA, *ASH1* (Gu et al., 2004; Irie et al., 2002; Long et al., 2001). In part, this can be explained by historical reasons, since *ASH1* was the first localized mRNA identified in yeast and consequently is also characterized best. Correct delivery of *ASH1* mRNA and tight translational regulation are indispensable to achieve mating type switching and thus formation of diploid **a**/ α cells. In contrast, RNA asymmetry seems to be less important for other targeted transcripts (Shepard et al., 2003) and invokes the question whether they require regulation to a similar extent as *ASH1*. In a comparative analysis of deletions of four predominantly nucleolar proteins (Mrt4, Nop16, Loc1, and Puf6, the latter two being established *ASH1* mRNA localization factors) I found that Loc1 has by far the greatest impact on *ASH1* targeting. Therefore, I used a complete deletion of *LOC1* to analyze the effect on localization of two more mRNAs, *IST2* and *WSC2*, which differ from *ASH1* in their cell cycle regulation. Furthermore, the respective proteins Ist2 and Wsc2 are integral membrane proteins, and Ist2 distribution is not restricted to buds (Jüscke et al., 2004).

Due to experimental limitations it was more difficult to detect bud tip localization of these mRNAs even in wild type cells despite the use of strains carrying a high copy number plasmid with the ORF of interest. This is a result of the different probes that were used for FISH of *IST2* and *WSC2* mRNA: While the directly labeled oligonucleotides used for *ASH1* visualization contain an exactly defined number of fluorescent labels per probe and display a high signal/noise ratio, digoxigenin-labeling by *in vitro* transcription is never complete, and the relative number of labels per probe is lower.

Despite this experimental limitation, I detected a strong increase of small-budded cells with delocalized *WSC2* mRNA from $\approx 35\%$ to $\approx 75\%$ upon deletion of *LOC1*. For *IST2* mRNA, the effect was much less prominent, but still statistically significant.

Recent work has proven that Khd1 and Puf6 participate in localization of more than one mRNA. Similar to $\Delta loc1$ cells, *IST2* mRNA delocalizes in $\Delta puf6$ cells (Deng et al., 2008). For Khd1, on the other hand, binding sites in the coding regions of bud-tip localized mRNAs like *MID2*, *MTL1* (for Mid2-like; Rajavel et al., 1999), and *WSC2* mRNA have been mapped. *MTL1* mRNA and Mtl1 protein levels have been shown to increase upon overexpression of Khd1 (Hasegawa et al., 2008).

In conclusion, *ASH1* mRNA localization factors Khd1, Puf6, and now also Loc1 are involved in targeting of additional mRNAs, arguing against the notion that *ASH1* mRNA localization is an exception in terms of regulation and number of *trans*-acting factors. Whether the involvement of the mentioned factors applies to all localized mRNAs or only to a specific subset remains to be determined.

3.2. The nucleolus is a site of ribonucleoprotein maturation

The so-called nuclear history is essential for correct assembly and transport of RNPs in a variety of eukaryotic cells. Examples comprise *Vg1* and *VegT* in *Xenopus* oocytes, *oskar* in *Drosophila* oocytes and β -actin in vertebrate cells (see section 1.5). In addition, Fragile X mental retardation protein (FMRP), a RNA-binding protein suggested to participate in localization of mRNAs to dendrites, has been shown to accumulate in nuclei or subnuclear structures if nuclear RNA export is blocked by siRNA-knockdown of Tap/NXF1, the mammalian homolog of Mex67 (Kim et al., 2009). FMRP is encoded by the *FMR1* gene, whose mutation is the cause for fragile X mental retardation syndrome, an inherited disease associated with defective mRNA transport (for review, see Dahm & Macchi, 2007 and references

therein). Whether the observed subnuclear structures correspond to nucleoli remains to be determined. Interestingly, nucleolar accumulation upon block of nuclear export has already been shown for another mammalian RNA-binding protein, Staufen2 (Macchi et al., 2004; see section 3.2.3).

The finding that two predominantly nucleolar proteins affect mRNA targeting, together with other results of this thesis and several previously published studies, suggests that the nucleolus is involved in translational regulation and localization of mRNAs. For a long time, the nucleolus has been seen mainly as a ribosome factory (Olson et al., 2000). However, it is now well established that the nucleolus contributes to various cellular processes, including cell cycle regulation, stress responses and formation of multiple RNPs in addition to ribosome formation (for review, see Boisvert et al., 2007). First indications for a role of the nucleolus for the export of RNAs to the cytoplasm came from irradiation experiments with heterokarya (Sidebottom & Harris, 1969). The following examples shall provide a basis for the model of nucleolar function in yeast mRNA localization presented below.

3.2.1. Signal recognition particle (SRP)

The signal recognition particle (SRP), a complex of six proteins and one RNA (7S SRP-RNA; scR1 in yeast) that binds to ribosomes translating secretory proteins and accompanies them to the endoplasmic reticulum (Halic & Beckmann, 2005), is assembled inside the nucleolus. For yeast it has been demonstrated that the four core SRP proteins (Srp14, Srp21, Srp68, and Srp72) enter the nucleolus independently from one another via a Ran-dependent ribosomal protein transport route. Subsequent assembly with scR1 yields a pre-SRP, which leaves the nucleolus and, after addition of a further protein component (Sec65), the nucleus (Grosshans et al., 2001). If scR1 is processed aberrantly at the 3'-end or cells lack any of the core proteins, the RNA is trapped inside the nucleolus, indicating that incorrectly assembled pre-SRP are not export-competent (Grosshans et al., 2001). Intriguingly, mammalian SRP-RNA accumulates in intranucleolar regions where protein and RNA markers for ribosome biogenesis are less concentrated (Politz et al., 2002). This ultimately led to the proposal of a nonribosomal landscape in the nucleolus with functions distinct from ribosome biogenesis (Politz et al., 2005).

3.2.2. The nucleolus and viral infection

Nucleolar targeting is also a common phenomenon observed for a variety of viral proteins (see Hiscox, 2007 for review). For example, the herpesvirus saimiri (HVS) RNA-binding ORF57 protein, which is important for cytoplasmic accumulation of virus mRNA, localizes to the nucleolus of infected cells, where it colocalizes with components of the mRNA export machinery that are redistributed to the nucleolus during infection. If nucleolar entry of the ORF57 protein is impeded by deletion of its nucleolar localization sequence (NoLS), the intronless viral mRNA cannot be exported from the nucleus, though it still can interact with both mRNA and RNA export factors (Boyne & Whitehouse, 2006). Similarly, nucleolar exclusion of the groundnut rosette virus (GRV; a plant RNA virus) ORF3 protein abolishes formation of cytoplasmic RNPs and long distance movement through the phloem, which is a prerequisite for systemic infection (Kim et al., 2007). Interestingly, ORF3 protein is probably redistributed to the cytoplasm along with a subpopulation of the predominantly nucleolar protein fibrillarin, which also seems to be involved in viral RNP formation (Kim et al., 2007). Finally, correct function of human immunodeficiency virus type 1 (HIV-1) proteins Tat and Rev requires nucleolar localization, and since the HIV-1 RNA could also traverse the nucleolus as part of an export strategy, it has been speculated that assembly of an RNP containing HIV-1 RNA might at least start there (Hiscox, 2007; Michienzi et al., 2000).

3.2.3. The nucleolus and cytoplasmic mRNA localization

In addition to viral RNPs and non-mRNA-containing RNPs, there is data pointing towards a functional relevance of nucleolar transit for some mRNPs as well. In a seminal study with different cell lines, the transcripts of *c-myc*, *N-myc* and *myoD1* were found to be enriched in nucleoli, while γ -actin mRNA was not (Bond & Wold, 1993). More recently, the mammalian brain-specific 62 kDa isoform of Stauf2 (Stau2⁶²), a double-stranded RNA (dsRNA) binding protein, has been shown to accumulate in nucleoli in certain conditions (Macchi et al., 2004). Stauf2 has first been discovered as a localization factor for the maternal mRNAs *oskar* and *bicoid* in *Drosophila*, but meanwhile two mammalian homologs have been identified (for review, see Miki et al., 2005). Both homologs are nucleocytoplasmic shuttling proteins. They associate with distinct but overlapping subsets of mRNAs and

participate in mRNA transport along microtubules in neurons (Furic et al., 2008). Prevalent nucleolar localization of Stau2⁶² fused to YFP was observed if the third RNA-binding domain (RBD3) was mutated so that the protein failed to bind RNA or if exportin-5 (Exp-5), which is involved in dsRNA export, was downregulated (Macchi et al., 2004). Yet, direct binding of Stau2 to a specific mRNA as well as nucleolar transit of any putatively bound mRNA has not been proven so far. Therefore, a physiological significance of Stau2 nucleolar enrichment is elusive to date (Jellbauer & Jansen, 2008; Kiebler et al., 2005).

In yeast, several findings suggest a participation of the nucleolus in mRNA export. Experiments with temperature-sensitive conditional mutants of genes involved in RNA metabolism, such as *RPA190* (for RNA polymerase A, the largest subunit of Pol I) and the *MTR* genes (for mRNA transport defective), revealed nucleolar accumulation of poly(A)⁺ RNA upon heat shock (Kadowaki et al., 1994; Kadowaki et al., 1995; Schneiter et al., 1995). A caveat in these studies is that the nucleolus disassembles during the long heat shock conditions used (≥ 2 h at 37°C or 42°C), making it difficult to monitor nucleolar accumulation of proteins (Liu et al., 1996). Furthermore, poly(A)⁺ RNA is very heterogeneous, and recent findings suggest that a nucleolar poly(A) domain in Δ rrp6 cells contains snoRNAs and not mRNAs. Thus, it seems that the results mentioned above and of a similar study in *Schizosaccharomyces pombe* (Ideue et al., 2004) are inconclusive.

First data on nucleolar accumulation specific transcripts in yeast were obtained by a live imaging approach using the U1A-GFP system (Brodsky & Silver, 2000). When the 3'-UTR of *ASH1* was fused to the 3'-end of a construct containing 16 U1A hairpin loops and the *PGK1* ORF (for 3-phosphoglycerate kinase; Lam & Marmur, 1977), the GFP signal accumulated in nucleoli at nonpermissive temperature in three conditional mRNA export factor mutants, including *mex67-5*. A similar accumulation was observed if *PGK1* was replaced by another ORF, *SSA4* (for stress 70 subfamily A, a gene encoding a heat shock protein; Werner-Washburne et al., 1987), but not if the *ASH1* 3'-UTR was exchanged for the endogenous 3'-UTRs (Brodsky & Silver, 2000).

Work on mRNAs encoding heat shock genes *SSA4* and *HSP104* (for heat shock protein) revealed that these transcripts accumulate at the site of transcription upon block of nuclear mRNA export (Jensen et al., 2001). Interestingly, they localize to the nucleolus analogous to *ASH1* mRNA if the experiment is performed

in cells lacking the nuclear exosome component *RRP6* (Thomsen et al., 2003; Figure 17L-N). Two hypotheses have been formulated to explain these observations.

First, the nucleolus with its high local concentration of RNA-binding proteins might simply be a reservoir for surplus RNAs. To date, it remains an unresolved issue why heat shock mRNAs accumulate in the nucleolus under the conditions described and there is no evidence indicating a precise function for this accumulation (Torben Heick Jensen, personal communication). On the other hand, poly(A)⁺ RNA localizes to the nuclear periphery and not to the nucleolus when RNA export is blocked and *RRP6* is deleted (Thomsen et al., 2003), suggesting some discrimination between different RNA populations.

Second, it is conceivable that heat shock mRNAs and possibly other specific transcripts require nucleolar transit as part of their default exit route (Thomsen et al., 2003). Our observations with *ASH1* mRNA argue in favor of this hypothesis. Not only does the RNA accumulate in the nucleolus in a *mex67-5 Δrrp6* strain at nonpermissive temperature, but also one of its main binding partners, She2. We could even show that *ASH1* FISH signals are not detectable in the nucleolus when She2 is deleted in a *Δrrp6* strain, suggesting that the protein is required for nucleolar accumulation of *ASH1* (Du et al., 2008). Moreover, She2 is trapped in the nucleolus similar to Stau2-RBD3 point mutants if it cannot bind to RNA, which is the case for the RNA-binding mutant She2(N36S, R63K) (Du et al., 2008; Gonsalvez et al., 2003). This, together with the finding that for instance Khd1 does not accumulate in nucleoli in *mex67-5* cells at 37°C implies that nucleolar shuttling of She2 is specific and not a mere consequence of high RNA-binding affinity, which would lead the protein to a compartment with elevated RNA concentrations (Du et al., 2008). The nucleolus also accommodates the localization factors Loc1 and Puf6, which have recently been shown to interact *in vivo* with She2 and *ASH1* mRNA (Shen et al., 2009).

3.2.4. A model of nucleolar function in mRNA localization

At present, it cannot be completely ruled out that nucleolar localization of She2 and *ASH1* does not occur under physiological conditions, because we have no tool in hand to monitor their probably very fast transit. However, with the identification of a NLS in She2 and the finding that She2 is actively imported into

the nucleus depending on the importin α Srp1 (for suppressor of rpb1; SGDproject, March 2009), it is beyond doubt that at least the nucleus plays a role in *ASH1* mRNP formation (Du et al., 2008; Shen et al., 2009). Most likely, this role involves proper translational silencing, since exclusion of She2 from the nucleus, either by fusing it to She3N or by mutating the NLS causes defective distribution of Ash1 protein, but has little effect on *ASH1* mRNA localization (Figure 18; Figure 21; Shen et al., 2009). *ASH1* mRNA distribution is not affected at all in the She3N-She2 mutant (Du et al., 2008), while point mutations in the NLS (mutant She2-M5A, Shen et al., 2009) apparently led to diminished anchoring of the mRNA. Still, about 90% of *ASH1* mRNA in She2-M5A localizes to the bud. Ash1 protein distribution has not been quantified in this mutant, but assuming a rate similar to She3N-She2 (Figure 18), the 10% delocalized transcript can hardly explain symmetric Ash1 distribution in 50% of cells.

The specification that the nucleolus has a significant share in nuclear steps of mRNP formation seems probable if we take the following results into account. First, She2 co-immunoprecipitates with both Loc1 and Puf6, suggesting an *in vivo* interaction (Gu et al., 2004; Shen et al., 2009). Second, *ASH1* mRNA interacts with Loc1 and Puf6 *in vivo*, and this interaction depends on nuclear She2 (Shen et al., 2009). This has been a longstanding question I had tried to tackle unsuccessfully with immunoprecipitation experiments followed by reverse transcription PCR (IP-RT, data not shown). I speculated that the time-frame is too narrow to detect the interaction, and consistently successful detection required cross-linking RNPs before immunoprecipitation (Shen et al., 2009). Third, She2 accumulates in the nucleolus if it cannot bind RNA (Du et al., 2008). It is currently unknown how She2 is involved in recruitment of Loc1 and Puf6 to *ASH1*, but since it does not leave the nucleolus without the RNA, it seems more likely that it brings the RNA to the nucleolus than that it brings the protein factors to the RNA in the nucleoplasm.

Taken together, the data presented above allow drawing a first model for a nucleolar step in the formation of localizing mRNPs with the example of *ASH1* mRNP, but the model might be applicable to other targeted mRNPs as well (Figure 32). Pol II transcription provides primary transcripts in the nucleoplasm, which can in principle freely diffuse through the entire nucleus including proteinaceous subnuclear compartments (Gorski et al., 2006). She2 is actively imported into the

nucleus and binds to the transcript. Whether this binding occurs already in the nucleoplasm or in the nucleolus is unclear at the moment, since RNA binding is not a prerequisite for nucleolar entry of She2 (Du et al., 2008). Inside the nucleolus, the translational repressor Puf6 is loaded onto the pre-mRNP. This step might require a loading helper to displace She2 from the blocked Puf6 binding site (see Figure 4) or to change the conformation of the mRNA to increase affinity for Puf6.

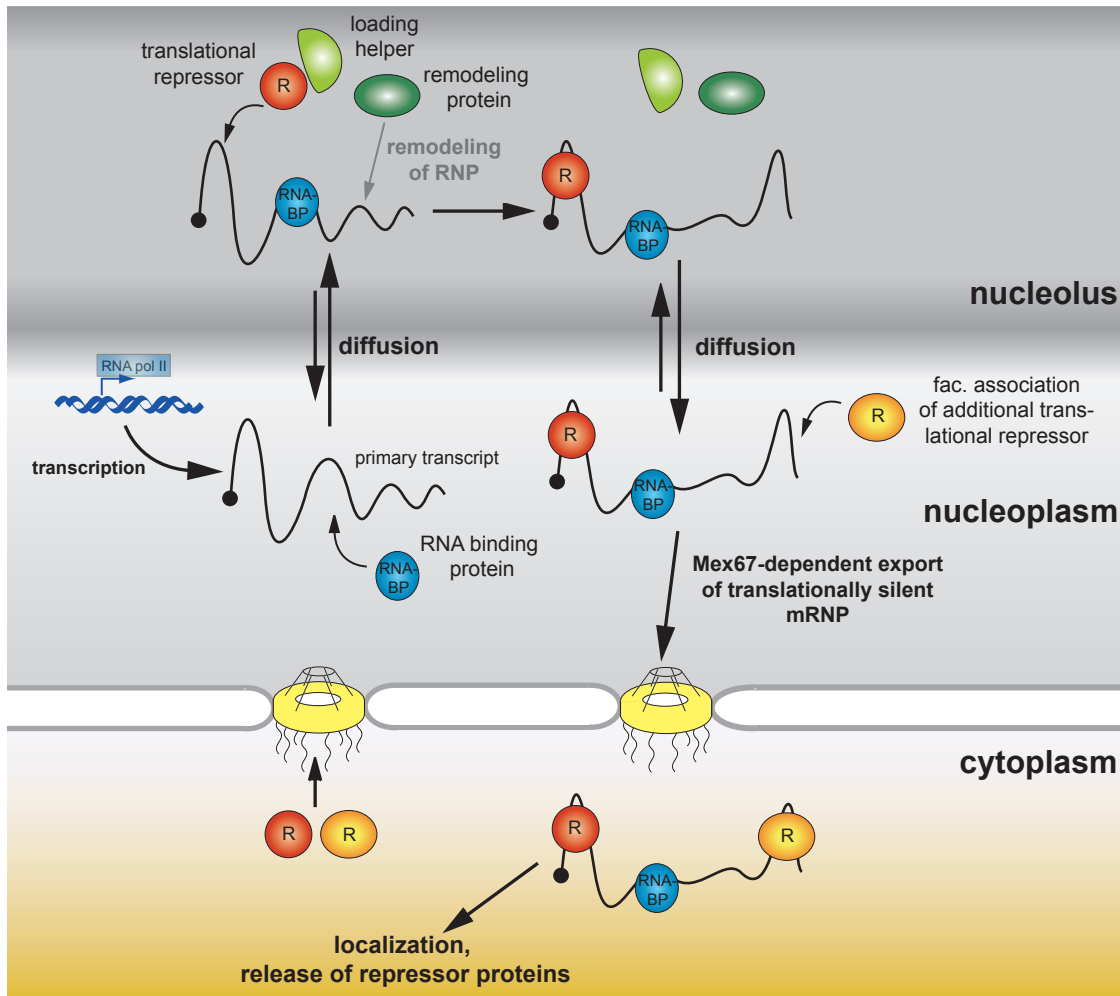


Figure 32 | Hypothetical model of nucleolar function in cytoplasmic mRNA localization.

In yeast, the RNA-binding protein She2 (blue) binds transcripts in the nucleoplasm and the complex diffuses into the nucleolus. Alternatively, binding could occur directly in the nucleolus. There, Puf6 (red) is loaded onto the complex, possibly involving a loading helper and/or remodeling of the complex (dark and light green); Loc1 could participate in these processes. Back in the nucleoplasm, recruiting Khd1 (yellow) to the mRNP tightens translational silencing. The mRNP is subsequently exported to the cytoplasm and transported to the bud tip. See text for details. (Figure adapted from Jellbauer & Jansen, 2008).

A candidate protein to accomplish one or both of these tasks is Loc1 (see below). In addition, residential nucleolar proteins may further remodel the mRNP, so that for example signals for nucleolar retention might be masked and the complex can

diffuse back to the nucleoplasm. There, additional translational control is obtained by recruitment of Khd1, and the mRNP is exported from the nucleus. Once in the cytoplasm, She2 binds to She3, and the complex is transported to the bud tip in a myosin-dependent fashion along actin cables. At the destination, translational repressors Puf6 and Khd1 are phosphorylated, and translation of the mRNA can start.

3.2.5. Implications of a nucleolar role in mRNP formation

Could the presented model be valid for other localizing RNPs as well? It has been demonstrated that another cellular RNA-binding protein, Stau2⁶², can accumulate in nucleoli as well (Macchi et al., 2004). Similarly, several viral RNA-binding proteins such as HIV-1 Rev, HVS ORF57 protein, and GRV ORF3 protein require transient nucleolar localization for proper function in viral RNA export or RNP assembly (Boyne & Whitehouse, 2006; Dundr et al., 1995; Kim et al., 2007). Furthermore, GRV ORF3 even helps to integrate the mainly nucleolar fibrillarin into functional RNPs (Kim et al., 2007), a finding reminiscent of the incorporation of Puf6 into the *ASH1* mRNP. Thus, occurrence of functional nucleolar transit in RNP biogenesis aside from the *ASH1* mRNP appears conceivable.

A second question that arises from the model presented is what possible advantage cells might gain from a nucleolar step in mRNP assembly. One obvious explanation is certainly economic use of resources. If a subset of mRNPs needs to be remodeled, they could simply be directed to the site where a large number of enzymes required to process and remodel precursors of ribosomes, the most abundant cellular RNPs, resides anyway (see section 1.2). The fact that for instance snRNP and SRP assembly steps occur in the nucleolus corroborates this view (see section 3.2.1; Gerbi et al., 2003).

Moreover, there are initial results that not only ribosomal RNAs, but also snRNAs and even mRNAs may be modified through 2'-O-ribose-methylation and pseudouridylation (reviewed in Decatur & Fournier, 2003). When the technical problems described (section 2.9.1) will be solved, also *ASH1* mRNA can be tested for the presence of such modifications. In general, modification of mRNAs may represent a possibility to distinguish between different sets of RNPs, for example localizing and non-localizing mRNPs. Besides, methylation or pseudouridylation of nucleotides might contribute to translational control, acting as molecular speed

bumps to slow down scanning ribosomes. Consequently, modifications are likely to be found in the non-translated regions of mRNAs, for example the 5'-UTR or the 3'-UTR; in trypanosomes, a Ψ residue has indeed been identified in the spliced leader (SL), a small RNA transferred to the 5'-end of pre-mRNAs 30 – 100 nt upstream of the Start codon (Jäger et al., 2007; Liang et al., 2002).

Finally, transit of mRNPs through the nucleolus could furnish a quality control step. For instance, it has been speculated that so-called specialized ribosomes containing a specific subset of ribosomal proteins, are necessary for controlled translation of *ASH1* mRNA, and that *Loc1* is involved in their biogenesis (Komili et al., 2007). Although it remains completely obscure how these specialized ribosomes can be assembled, their precursors might somehow prime localizing mRNPs. On the other hand, lack of any translational activity renders the nucleolus a well-suited environment to initiate translational silencing. mRNPs that fail to be regulated could be immediately marked for degradation, e.g. by the nuclear exosome and would not even leave the nucleus. Interestingly, such a process has already been shown for defective, nuclear-restricted pre-60S subunits: rRNA precursors are polyadenylated, and the pre-ribosomes, together with the nuclear exosome and the TRAMP complex (for *Trf4/Air/Mtr4* polyadenylation), accumulate in a subnucleolar region termed the No-body (Dez et al., 2006).

3.3. *Loc1* and *Puf6* contribute to biogenesis of 60S ribosomal subunits

Characterization of *Loc1* and *Puf6* in the course of this study and by others has revealed a role for both proteins in ribosome biogenesis (Figure 14; Figure 15; Figure 16; Harnpicharnchai et al., 2001; Urbinati et al., 2006). Both *Loc1* and *Puf6* co-purify with a large complex that only disassembles at high salt concentrations (Figure 9). With the help of mass spectrometry I was able to identify two known interactors of *Puf6* (Table 2). The overall band pattern is consistent with other purifications of 60S subunit biogenesis factors such as *Cic1*, *Nog1*, *Nop7* and *Rlp24* (Harnpicharnchai et al., 2001; Nissan et al., 2002; Saveanu et al., 2003). Indeed, purifications with the mentioned proteins as bait – either in studies focused on individual proteins (see above) or in a systematic analysis (Gavin et al., 2006) – identified *Loc1* and *Puf6* as members of the respective complexes. I concluded that the large number of bands with an apparent molecular weight below 50 kDa corresponded to ribosomal proteins of the large subunit, as identified in the *Loc1*

and Puf6 purifications of the high throughput study (Gavin et al., 2006). A control purification of Hpr1, a nuclear protein implicated in mRNA export, did not show this band pattern after the second purification step (Figure 9B). At standard purification conditions, it was very difficult to see the band corresponding to Loc1, possibly due to the low concentration of just 3650 molecules per cell (Puf6: 21500 molecules/cell; Ghaemmaghami et al., 2003). Purification under high salt conditions showed a distinct band below 30 kDa that corresponded to Loc1, and this band is also visible in standard purifications (Figure 9B).

In contrast to immunoprecipitations from other groups, I have never identified an interaction between She2 and Puf6 or Loc1 in TAP (Figure 9C and data not shown). I speculated that the pre-60S particle I purified when using Puf6 or Loc1 as bait is rather stable, while interaction of nucleolar She2 with Puf6 and Loc1 would be only transient. Consequently, use of She2 as bait purifies mainly cytoplasmic interactors such as Myo4 (Gavin et al., 2006).

A more direct assay to investigate the role of Loc1 and Puf6 in ribosome biogenesis is sucrose density gradient centrifugation of total RNA from strains carrying knockouts of *LOC1* and *PUF6*, respectively (Rotenberg et al., 1988). Consistent with the TAP results, polysome profiles of $\Delta loc1$ and, to a smaller extent, $\Delta puf6$ cells, were characteristic for defective large subunit (LSU) biogenesis and greatly differed from profiles of cells where a 40S factor had been deleted (Figure 14; Adams et al., 2002 and references therein). The observed halfmers result most likely from defective LSU biogenesis and not from a block in translation initiation (Rotenberg et al., 1988), since the 60S peak is also reduced. The effects on 60S subunit maturation are a direct consequence of protein depletion and not caused indirectly by slow growth, since a $\Delta puf6$ strain grows at wild-type levels even at 37°C (Figure 24), and Loc1 depletion leads to the described defects in ribosome biogenesis long before cell growth is affected (Figure 28). For Loc1, polysome profiles at conditions that disrupt ribosomes into subunits confirmed that the total number of ribosomal subunits is reduced in $\Delta loc1$ cells, and that the amount of large subunits decreases disproportionately to small subunits (Figure 16).

Finally, detailed analysis of newly synthesized rRNA intermediates by *in vivo* pulse labeling (Ferreira-Cerca et al., 2005) further clarified where in large subunit assembly Loc1 and Puf6 possibly act. Again, only a weak phenotype was detected

for Δ puf6 cells, which showed slightly increased levels of 32S pre-rRNA (Figure 15). This hints at a minor role in early nucleolar steps of ribosome biogenesis, consistent with the observation that Puf6 was found to be associated only with early pre-ribosomal particles in tandem affinity purifications (Nissan et al., 2002). Cells carrying a *LOC1* deletion, on the other hand, showed increased levels of 35S and 27S pre-rRNA, and reduced levels of mature 25S rRNA (Figure 15), similar to other 60S biogenesis factors, albeit much weaker. Data from pulse-chase experiments of Δ loc1 cells substantiated these observations (Urbinati et al., 2006). The reason for the increase of 35S pre-rRNA, which is generally observed upon mutation of almost any 60S factor, is not entirely clear. Discussed hypotheses include the interaction of 40S and 60S biogenesis pathways, the possibility of generating only large subunits from 35S pre-rRNA by alternative cleavages, and a control mechanism the early processing machinery uses to ensure correct assembly of factors needed in subsequent steps (Adams et al., 2002; Fromont-Racine et al., 2003; Venema & Tollervey, 1999).

An increase in 27S pre-rRNA indicates that processing of RNA species of this size is slowed down in Δ loc1 cells, consistent with defects in other 60S biogenesis factors. It remains unclear which 27S species are enriched, since results are inconsistent with all other data presented in the respective study (Urbinati et al., 2006). Most likely *Loc1* is not directly involved in rRNA processing, because this would cause a much stronger block and have deleterious effects on cells. However, *Loc1* is not an essential protein. From the data presented in this thesis, I assume that absence of *Loc1* delays processing of 27S rRNA, decreasing 25S rRNA levels as a consequence. I further speculate that in wild type cells, *Loc1* may contribute to refolding of pre-rRNA to enable fast access of nucleases (see below). Alternatively, it might recruit enzymes to processing sites.

In conclusion, *Loc1* is implicated in early steps of large ribosomal subunit biogenesis. Data suggest that it associates with pre-60S particles after cleavage at site A₂, probably immediately prior to cleavage at site C₂ and dissociates before the pre-60S particles leave the nucleolus (Figure 2), a view consistent with previous assignments (Dez & Tollervey, 2004; Fatica & Tollervey, 2002). *Loc1* likely participates in processing steps during this time-frame, but its exact function

remains to be proven. Puf6 association with pre-60S particles temporally overlaps with Loc1 association; however, the role of Puf6 in ribosome biogenesis is unclear.

3.4. Loc1 might contribute to remodeling of mRNAs in the nucleolus

Besides affecting biogenesis of the large ribosomal subunit, disruption of *LOC1* compromises localization of *ASH1* mRNA and asymmetric distribution of Ash1 protein. In the present thesis, I provide evidence that Loc1 function in these pathways may be coupled. First, truncation analysis of the protein did not show that different parts of the protein are specifically required for one process (Figure 23). Second, rapid depletion of Loc1 by glucose shut-off led to concomitant impairment of both processes already at one hour post-shift, arguing against a first response in ribosome biogenesis with a subsequent indirect effect on RNA localization due to reduced levels in 60S subunits (Figure 28).

Functional coupling in the present context signifies that Loc1 is involved in analogous reactions relevant for mRNA localization as well as for ribosomal subunit maturation. The main question arising from this definition is how these reactions look like on a molecular level or, in simple words, what the molecular function of Loc1 could be.

So far, technical problems have prevented my analysis of modifications in RNAs other than rRNAs (see section 2.9.1). Since cells survive without Loc1, a direct involvement in methylation or pseudouridylation of RNAs does not seem very likely. However, physical interaction with Gar1 (for glycine and arginine rich domain protein; Bousquet-Antonelli et al., 1997), a core protein of H/ACA snoRNPs responsible for Ψ formation, has recently been reported (Tarassov et al., 2008). Puf6 also interacts physically with core components of H/ACA snoRNPs (Cbf5, Gar1) as well as with C/D snoRNPs (Nop1) (Collins et al., 2007; Gavin et al., 2006; Gavin et al., 2002; Krogan et al., 2006). It is therefore possible that Loc1 and Puf6 help to recruit RNA modifying complexes to pre-ribosomal particles and perhaps also pre-mRNPs, though it cannot be excluded that physical interaction in this case just implies to belong to the same huge complex, the pre-60S particle.

The second hypothesis on the molecular function of Loc1 is, as mentioned above, that it might act in folding of RNAs. Interestingly, most proteins with assigned RNA chaperone activity are multifunctional and cause pleiotropic effects when mutated (Schroeder et al., 2004). Moreover, nucleic acid chaperone function has already

been reported for a protein implicated in mRNA localization, FMRP (Gabus et al., 2004). Lack of a positive control has so far impeded to test Loc1 in an *in vivo* RNA chaperone assay, but this difficulty should be resolvable in the near future. Despite a missing direct proof, some findings suggest that the presented hypothesis is reasonable. First of all, I have found a synthetic sickness phenotype in a double deletion of *LOC1* and *LHP1* (section 2.9.2), the yeast homolog of La, as well as in a double deletion of *LOC1* and *LSM7* (data not shown). Both genetic interactions have meanwhile been confirmed by high-throughput analysis (Wilmes et al., 2008). La and Sm-like proteins stabilize noncoding RNAs and supposedly modulate RNA structure (Wolin & Wurtmann, 2006). Genetic interaction of Loc1 with La and a nuclear Lsm protein may be plausibly explained with a redundant function in the same pathway, in this case RNA folding.

The amino acid sequence and predicted secondary structure of Loc1 (Figure 7) hint to a function in RNA folding as well. Loc1 shows several properties of a natively disordered protein (Fink, 2005), e.g. a high level of disorganized structure, especially in the central third, as indicated by prediction of secondary structure and intrinsic protein disorder (DisEMBL™; Linding et al., 2003). In addition, Loc1 has a high net charge (isoelectric point pI=11.1; SGDproject, March 2009), and a high level of disorder-promoting amino acids such as glutamic acid (E), lysine (K), and arginine (R), which alone account for almost 40% of Loc1 primary sequence (Figure 7). Despite widespread occurrence of natively disordered regions in cellular proteins, especially in the nucleolus, it is interesting to note that the highest frequency of disorganized structure of all protein classes is found in RNA chaperones, and it appears that these unstructured regions are critical for function (Fink, 2005). Disordered segments allow keeping the protein surface small, while allowing a substantially larger interface for interaction with substrates as compared to ordered segments. Importantly, disordered segments also furnish structural plasticity, permitting recognition of different targets with contemporaneous maintenance of specificity (Emmott & Hiscox, 2009; Gunasekaran et al., 2003).

If we apply these general findings to the particular case of Loc1, it is evident that the most probably natively unfolded central region allows binding to multiple target RNAs, comprising localizing mRNAs as well as pre-rRNA. On the other hand, the N- and C-terminal parts of the protein, which show a higher degree of

predicted secondary structure, might be dispensable for function. Consistently, I find that truncation of these parts does not significantly impair Loc1 function (Figure 23).

In conclusion, a model for the molecular function of Loc1 could be formulated as follows (Figure 33). Loc1 binds to double-stranded RNAs in the nucleolus. Specificity for localizing mRNAs like *ASH1*, *IST2*, and *WSC2* and ribosomal RNAs may be conferred by proteins interacting with the RNAs *in vivo*, such as She2, since Loc1 does not show specific binding to dsRNAs *in vitro* (Long et al., 2001). Binding to substrates triggers partial un- and refolding, favoring loading of additional factors to distinct motifs. Even displacement of previously bound factors is conceivable. For example, Loc1 might displace She2 from the E3 LE of *ASH1* mRNA; subsequent refolding might promote binding of Puf6 to E3 perhaps as part of a nucleolar “handover” process, similar to the nuclear handover proposed for of β -actin mRNA from ZBP2 to ZBP1 (Pan et al., 2007). Finally, Loc1 releases the refolded RNAs.

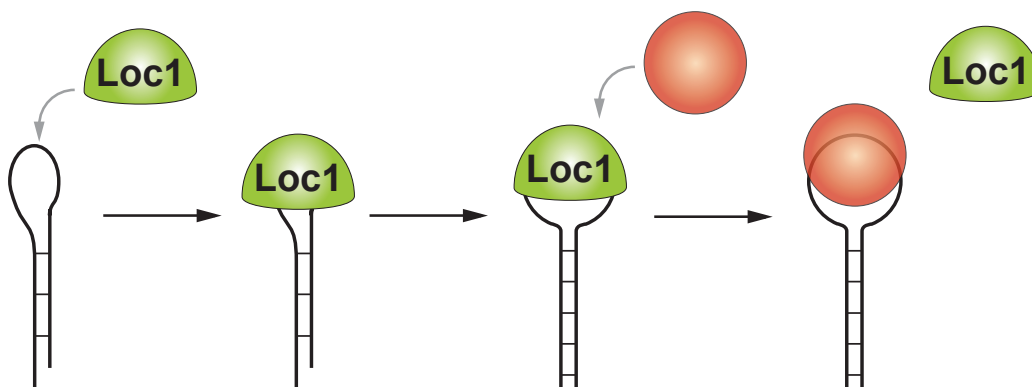


Figure 33 | Putative Loc1 function in RNA folding.

Loc1 binds to dsRNAs in the nucleolus. Partial unfolding and refolding, probably involving the natively disordered central domain of Loc1, allows recruiting of protein factors to the remodeled RNA, e.g. Puf6 to *ASH1* mRNA.

Experiments are in progress to validate this currently hypothetical model. Chances are that they will help to unravel the detailed molecular mechanism of Loc1 function, integrating its action in such diverse processes as ribosome biogenesis and mRNA localization. In addition, they might as well bring forward the search for functional homologs of Loc1 in higher eukaryotes.

4. Materials

4.1. Chemicals – Enzymes – Antibodies

4.1.1. Enzymes & Proteins

Name	Supplier
Avian Myeloblastosis Virus (AMV) Reverse Transcriptase	Promega
Calf Intestine Alkaline Phosphatase (CIAP)	Fermentas
DNase-free RNase	Roche
DNA Polymerase I, Large (Klenow) Fragment	New England BioLabs
Herculase® II Fusion Enzyme	Stratagene
Lysozyme	Sigma-Aldrich
Moloney Murine Leukemia Virus (M-MuLV) Reverse Transcriptase	Fermentas
Proteinase K	Roche Applied Science
Restriction Endonucleases	Fermentas, New England BioLabs
RNasin® Plus RNase Inhibitor	Promega
RQ1 RNase-free DNase	Promega
SUPERase-In™	Ambion
T4 DNA Ligase	Fermentas
T4 DNA polymerase	New England BioLabs
T7 RNA Polymerase	Promega
Taq Polymerase	Axon
Vent _R ® DNA Polymerase	New England BioLabs
Zymolyase 20T	Seikagaku Corporation
Zymolyase 100T	Seikagaku Corporation

4.1.2. Antibiotics & Drugs

Name	Supplier
Ampicillin (Amp)	Roth
Chloramphenicol (Cla)	Sigma-Aldrich
Cycloheximide (CHX)	Sigma-Aldrich
Doxycycline (dox)	Sigma-Aldrich
Geneticin (G418)	Gentaur

Kanamycin (Kan)	Sigma-Aldrich
Nourseothricin (clonNAT, nat)	Werner BioAgents
Tetracycline (Tet)	Sigma-Aldrich

4.1.3. Special chemicals

All standard laboratory chemicals were purchased from the centralized purchasing of the Gene Center. Special chemicals are listed below.

Name	Supplier
40% Acrylamide/Bisacrylamide (19:1) (fluorescence-free)	Roth
<i>N</i> -cyclohexyl- <i>N'</i> - β -(4-methylmorpholinium)-ethylcarbodiimide <i>p</i> -tosylate (CMC)	Fluka
4',6-Diamidino-2-phenylindole dihydrochloride (DAPI); in this study substituted by Hoechst Stain solution	Sigma-Aldrich
Diethylpyrocarbonate (DEPC)	Roth
Isopropyl- β -D-1-thiogalactopyranoside (IPTG)	
Urea (fluorescence-free)	Roth

4.1.4. DNA, RNA & Size Standards

Name	Supplier
Herring Sperm DNA	Sigma-Aldrich
Salmon sperm DNA, 10 mg/ml	Invitrogen
Yeast genomic DNA, 10 mg/ml	Invitrogen
O'GeneRuler™ DNA ladder mix	Fermentas
RNA markers	Promega

4.1.5. Antibodies

Name	Source
Mouse monoclonal anti-Actin (clone C4)	Millipore
Mouse monoclonal anti-Fibrillarin (clone 28F2)	abcam
Mouse monoclonal anti-HA HA.11 (clone 16B12)	Covance
Mouse monoclonal anti-myc (clone 9E10)	IMP, Vienna
Mouse monoclonal anti-myc (clone 9E11)	IMP, Vienna
Rat monoclonal anti-Tubulin (clone 3H3087)	Santa Cruz
Rat monoclonal anti-HA high affinity (clone 3F10)	Roche Applied Science
Rabbit polyclonal anti-She2 (323/4, E12, #7)	Tung-Gia Du
AlexaFluor® 488 goat anti-mouse IgG (H+L)	Molecular Probes

AlexaFluor® 488 goat anti-rabbit IgG (H+L)	Molecular Probes
AlexaFluor® 488 goat anti-rat IgG (H+L)	Molecular Probes
AlexaFluor® 488 rabbit anti-mouse IgG (H+L)	Molecular Probes
AlexaFluor® 594 rabbit anti-mouse IgG (H+L)	Molecular Probes
polyclonal sheep anti-Digoxigenin-AP Fab fragments (anti-DIG)	Roche Applied Science
Peroxidase-conjugated AffiniPure goat anti-mouse IgG (H+L)	Jackson ImmunoResearch
Peroxidase-conjugated AffiniPure goat anti-rat IgG (H+L)	Jackson ImmunoResearch
Peroxidase-conjugated AffiniPure goat anti-rabbit IgG (H+L)	Jackson ImmunoResearch

4.2. Strains

4.2.1. Yeast strains

Name	Essential Genotype	Origin
RJY5	<i>MATα, ade2-1, can1-100, his3-11,15, leu2-3,112, trp1-1, ura3, HO-ADE2, HO-CAN1</i>	Jansen et al., 1996 (K4452)
RJY137	<i>MATα, ade2-1, can1-100, his3-11,15, leu2-3,112, trp1-1, ura3, ASH1-myc9</i>	Bobola et al., 1996 (K5863)
RJY280	<i>MATα, ade2-1, can1-100, his3-11,15, leu2-3,112, trp1-1, ura3, ash1::URA3, (2\times) TRP1::GAL-ASH1-myc</i>	I. Gonzalez
RJY358	<i>MATα, ade2-1, can1-100, his3-11,15, leu2-3,112, trp1-1, ura3, GAL, psi+</i>	n/a
RJY359	<i>MATα, ade2-1, can1-100, his3-11,15, leu2-3,112, trp1-1, ura3, GAL, psi+</i>	n/a
RJY1149	<i>MATα, ade2-1, can1-100, his3-11,15, leu2-3,112, trp1-1, ura3-52, GAL+, mex67::HIS3, pUN100-LEU2-mex67-5</i>	Segref et al., 1997 (mex67-5)
RJY1357	<i>MATα, ade2-1, can1-100, his3-11,15, leu2-3,112, trp1-1, ura3, pRS426-IST2</i>	D. Ferring
RJY1462	<i>MATα, ade2-1, can1-100, his3-11,15, leu2-3,112, trp1-1, ura3, ASH1-myc9, she2::URA3</i>	n/a
RJY2017	<i>MATα, his3Δ1, leu2Δ0, met15Δ0, ura3Δ0, puf6::kanMX4</i>	EUROSCARF (Y04330)
RJY2049	<i>MATα, his3Δ1, leu2Δ0, met15Δ0, ura3Δ0</i>	EUROSCARF (BY4741)
RJY2050	<i>MATα, his3Δ1, leu2Δ0, lys2Δ0, ura3Δ0</i>	EUROSCARF (BY4742)
RJY2124	<i>Mata, ade2-1, can1-100, his3-11,15, leu2-3,112, trp1-1, ura3, UBR1::GAL-HA-UBR1 (HIS3)</i>	EUROSCARF (YKL200)
RJY2182	<i>MATα, ade2-1, can1-100, his3-11,15, leu2-3,112, trp1-1, ura3, she2::URA3, p413-GAL1-ASH1, YCplac111-GFP-SHE2</i>	T.-G. Du
RJY2415	<i>MATα, ade2-1, can1-100, his3-11,15, leu2-3,112, trp1-1, ura3-52, GAL+, mex67::HIS3, pUN100-LEU2-mex67-5, pGAL1-10-ASH1::URA3, she2::kanMX4</i>	T.-G. Du
RJY2786	<i>MATα, his3Δ1, leu2Δ0, met15Δ0, ura3Δ0, she2::kanMX4, YCplac111-GFP-SHE2(N36S, R63K)</i>	T.-G. Du
RJY2799	<i>MATα, can1Δ, his3Δ1, leu2Δ0, lys2Δ0, ura3Δ0, lypΔ, mfa1::MFA1pr-HIS3, cir+, gal2</i>	Tong et al., 2001 (BY5563)
RJY2810	<i>MATα, can1Δ, his3Δ1, leu2Δ0, lys2Δ0, ura3Δ0, lypΔ, mfa1::MFA1pr-HIS3, cir+, gal2, puf6::natNT2</i>	this study
RJY2811	<i>MATα, his3Δ1, leu2Δ0, lys2Δ0, ura3Δ0, loc1::HIS3MX6</i>	this study
RJY2819	<i>MATα, ade2-1, can1-100, his3-11,15, leu2-3,112, trp1-1, ura3, LOC1-CBP-TEV-ProtA::K.I.TRP1</i>	this study
RJY2820	<i>MATα, ade2-1, can1-100, his3-11,15, leu2-3,112, trp1-1, ura3, PUF6-CBP-TEV-ProtA::K.I.TRP1</i>	this study
RJY2833	<i>MATα, ade2-1, can1-100, his3-11,15, leu2-3,112, trp1-1, ura3, HO-ADE2, HO-CAN1, she2::URA3, loc1::natNT2</i>	T.-G. Du

Materials

RJY2845	<i>MATa, can1Δ, his3Δ1, leu2Δ0, lys2Δ0, ura3Δ0, lypΔ, mfa1::MFA1pr-HIS3, cir+, gal2, loc1::natNT2</i>	this study
RJY2881	<i>MATa, ade2-1, can1-100, his3-11,15, leu2-3,112, trp1-1, ura3, GAL, psi+, puf6::natNT2</i>	this study
RJY2882	<i>MATα, ade2-1, can1-100, his3-11,15, leu2-3,112, trp1-1, ura3, GAL, psi+, puf6::natNT2</i>	this study
RJY2894	<i>MATa, ade2-1, can1-100, his3-11,15, leu2-3,112, trp1-1, ura3, loxP-ProtA-TEV-CBP-LOC1</i>	this study
RJY2930	<i>MATa, ade2-1, can1-100, his3-11,15, leu2-3,112, trp1-1, ura3, GAL, psi+, loc1::natNT2</i>	this study
RJY2931	<i>MATα, ade2-1, can1-100, his3-11,15, leu2-3,112, trp1-1, ura3, GAL, psi+, loc1::natNT2</i>	this study
RJY2932	<i>MATa, ade2-1, can1-100, his3-11,15, leu2-3,112, trp1-1, ura3 PUF6-CBP-TEV-ProtA::K.l.TRP1, she2::HIS3MX6</i>	this study
RJY2934	<i>MATa, ade2-1, can1-100, his3-11,15, leu2-3,112, trp1-1, ura3 PUF6-CBP-TEV-ProtA::K.l.TRP1, SHE2-myc9::HIS3MX6</i>	this study
RJY2935	<i>MATa, ade2-1, can1-100, his3-11,15, leu2-3,112, trp1-1, ura3, mrt4::HIS3MX6</i>	this study
RJY2937	<i>MATa, ade2-1, can1-100, his3-11,15, leu2-3,112, trp1-1, ura3, lsm7::HIS3MX6</i>	this study
RJY2943	<i>MAT ? ade2-1, can1-100, his3-11,15, leu2-3,112, trp1-1, ura3-52, HPR1-CBP-TEV-ProtA::K.l.TRP1</i>	Sträßer et al., 2002
RJY2964	<i>MATa, ade2-1, can1-100, his3-11,15, leu2-3,112, trp1-1, ura3 PUF6-CBP-TEV-ProtA::K.l.TRP1, loc1::HIS3MX6</i>	this study
RJY2965	<i>MATa, ade2-1, can1-100, his3-11,15, leu2-3,112, trp1-1, ura3 PUF6-CBP-TEV-ProtA::K.l.TRP1, LOC1-HA3::HIS3MX6</i>	this study
RJY2997	<i>MATα, his3Δ1, leu2Δ0, lys2Δ0, ura3Δ0, YEplac195-ASH1</i>	this study
RJY3133	<i>Mata, ade2-1, can1-100, his3-11,15, leu2-3,112, trp1-1, ura3, UBR1::GAL-HA-UBR1 (HIS3), LOC1::kanMX4-pCUP1-myc-td</i>	this study
RJY3147	<i>MATa, ade2-1, can1-100, his3-11,15, leu2-3,112, trp1-1, ura3, nop16::HIS3MX6</i>	this study
RJY3148	<i>MATa, his3Δ1, leu2Δ0, met15Δ0, ura3Δ0, nop16::HIS3MX6</i>	this study
RJY3150	<i>Mata, ade2-1, can1-100, his3-11,15, leu2-3,112, trp1-1, ura3, UBR1::GAL-HA-UBR1 (HIS3), LOC1::kanMX4-pCUP1-myc-td, LOC1-HA6::natNT2</i>	this study
RJY3153	<i>MATa, ade2-1, can1-100, his3-11,15, leu2-3,112, trp1-1, ura3, LOC1-HA6::natNT2</i>	this study
RJY3162	<i>MATa, ade2-1, can1-100, his3-11,15, leu2-3,112, trp1-1, ura3, ash1::URA3, (2×) TRP1::GAL-ASH1-myc loc1::HIS3MX6</i>	this study
RJY3163	<i>MATa, ade2-1, can1-100, his3-11,15, leu2-3,112, trp1-1, ura3, ash1::URA3, (2×) TRP1::GAL-ASH1-myc puf6::HIS3MX6</i>	this study
RJY3164	<i>MATa, ade2-1, can1-100, his3-11,15, leu2-3,112, trp1-1, ura3, ash1::URA3, (2×) TRP1::GAL-ASH1-myc she2::HIS3MX6</i>	this study
RJY3188	<i>MATα, ade2-1, can1-100, his3-11,15, leu2-3,112, trp1-1, ura3, HO-ADE2, HO-CAN1, LOC1-HA6::natNT2</i>	this study
RJY3189	<i>MATα, ade2-1, can1-100, his3-11,15, leu2-3,112, trp1-1, ura3, HO-ADE2, HO-CAN1, LOC1(aa1-190)-HA6::natNT2</i>	this study
RJY3190	<i>MATα, ade2-1, can1-100, his3-11,15, leu2-3,112, trp1-1, ura3, HO-ADE2, HO-CAN1, LOC1(aa1-159)-HA6::natNT2</i>	this study

Materials

RJY3191	<i>MATα</i> , <i>ade2-1</i> , <i>can1-100</i> , <i>his3-11,15</i> , <i>leu2-3,112</i> , <i>trp1-1</i> , <i>ura3</i> , <i>HO-ADE2</i> , <i>HO-CAN1</i> , <i>LOC1(aa1-140)-HA6::natNT2</i>	this study
RJY3192	<i>MATα</i> , <i>ade2-1</i> , <i>can1-100</i> , <i>his3-11,15</i> , <i>leu2-3,112</i> , <i>trp1-1</i> , <i>ura3</i> , <i>HO-ADE2</i> , <i>HO-CAN1</i> , <i>LOC1(aa1-72)-HA6::natNT2</i>	this study
RJY3200	<i>MATα</i> , <i>ade2-1</i> , <i>can1-100</i> , <i>his3-11,15</i> , <i>leu2-3,112</i> , <i>trp1-1</i> , <i>ura3</i> , <i>HO-ADE2</i> , <i>HO-CAN1</i> , <i>loc1::natNT2</i>	this study
RJY3211	<i>MATα</i> , <i>ade2-1</i> , <i>can1-100</i> , <i>his3-11,15</i> , <i>leu2-3,112</i> , <i>trp1-1</i> , <i>ura3</i> , <i>HO-ADE2</i> , <i>HO-CAN1</i> , <i>LOC1(aa1-115)-HA6::natNT2</i>	this study
RJY3221	<i>MATα</i> , <i>ade2-1</i> , <i>can1-100</i> , <i>his3-11,15</i> , <i>leu2-3,112</i> , <i>trp1-1</i> , <i>ura3</i> , <i>HO-ADE2</i> , <i>HO-CAN1</i> , <i>LOC1(aa1-130)-HA6::natNT2</i>	this study
RJY3222	<i>MATα</i> , <i>ade2-1</i> , <i>can1-100</i> , <i>his3-11,15</i> , <i>leu2-3,112</i> , <i>trp1-1</i> , <i>ura3</i> , <i>HO-ADE2</i> , <i>HO-CAN1</i> , <i>LOC1(aa1-120)-HA6::natNT2</i>	this study
RJY3223	<i>MATα</i> , <i>ade2-1</i> , <i>can1-100</i> , <i>his3-11,15</i> , <i>leu2-3,112</i> , <i>trp1-1</i> , <i>ura3</i> , <i>ASH1-myc9</i> , <i>p416-GALS-KHD1-HA6</i>	this study
RJY3237	<i>MATα</i> , <i>ade2-1</i> , <i>can1-100</i> , <i>his3-11,15</i> , <i>leu2-3,112</i> , <i>trp1-1</i> , <i>ura3</i> , <i>ASH1-myc9</i> , <i>p416-GALS</i>	this study
RJY3238	<i>MATα</i> , <i>ade2-1</i> , <i>can1-100</i> , <i>his3-11,15</i> , <i>leu2-3,112</i> , <i>trp1-1</i> , <i>ura3</i> , <i>ASH1-myc9</i> , <i>p416-GALS-LOC1-HA6</i>	this study
RJY3260	<i>MATα</i> , <i>ade2-1</i> , <i>can1-100</i> , <i>his3-11,15</i> , <i>leu2-3,112</i> , <i>trp1-1</i> , <i>ura3</i> , <i>HO-ADE2</i> , <i>HO-CAN1</i> , <i>mrt4::HIS3MX6</i>	this study
RJY3261	<i>MATα</i> , <i>ade2-1</i> , <i>can1-100</i> , <i>his3-11,15</i> , <i>leu2-3,112</i> , <i>trp1-1</i> , <i>ura3</i> , <i>HO-ADE2</i> , <i>HO-CAN1</i> , <i>puf6::HIS3MX6</i>	this study
RJY3262	<i>MATα</i> , <i>ade2-1</i> , <i>can1-100</i> , <i>his3-11,15</i> , <i>leu2-3,112</i> , <i>trp1-1</i> , <i>ura3</i> , <i>HO-ADE2</i> , <i>HO-CAN1</i> , <i>khd1::HIS3MX6</i>	this study
RJY3264	<i>MATα</i> , <i>ade2-1</i> , <i>can1-100</i> , <i>his3-11,15</i> , <i>leu2-3,112</i> , <i>trp1-1</i> , <i>ura3</i> , <i>HO-ADE2</i> , <i>HO-CAN1</i> , <i>nop16::HIS3MX6</i>	this study
RJY3265	<i>MATα</i> , <i>ade2-1</i> , <i>can1-100</i> , <i>his3-11,15</i> , <i>leu2-3,112</i> , <i>trp1-1</i> , <i>ura3</i> , <i>HO-ADE2</i> , <i>HO-CAN1</i> , <i>she2::natNT2</i>	this study
RJY3269	<i>MATα</i> , <i>ade2-1</i> , <i>can1-100</i> , <i>his3-11,15</i> , <i>leu2-3,112</i> , <i>trp1-1</i> , <i>ura3</i> , <i>ash1::URA3</i> , (2 \times) <i>TRP1::GAL-ASH1-myc</i> , <i>she2::HIS3MX6</i> , <i>YCplac22-SHE3N-SHE2</i>	this study
RJY3272	<i>MATα</i> , <i>ade2-1</i> , <i>can1-100</i> , <i>his3-11,15</i> , <i>leu2-3,112</i> , <i>trp1-1</i> , <i>ura3</i> , <i>HO-ADE2</i> , <i>HO-CAN1</i> , <i>arx1::natNT2</i>	this study
RJY3273	<i>MATα</i> , <i>ade2-1</i> , <i>can1-100</i> , <i>his3-11,15</i> , <i>leu2-3,112</i> , <i>trp1-1</i> , <i>ura3</i> , <i>HO-ADE2</i> , <i>HO-CAN1</i> , <i>ltv1::HIS3MX6</i>	this study
RJY3274	<i>MATα</i> , <i>ade2-1</i> , <i>can1-100</i> , <i>his3-11,15</i> , <i>leu2-3,112</i> , <i>trp1-1</i> , <i>ura3</i> , <i>HO-ADE2</i> , <i>HO-CAN1</i> , <i>nop6::HIS3MX6</i>	this study
RJY3275	<i>MATα</i> , <i>ade2-1</i> , <i>can1-100</i> , <i>his3-11,15</i> , <i>leu2-3,112</i> , <i>trp1-1</i> , <i>ura3</i> , <i>HO-ADE2</i> , <i>HO-CAN1</i> , <i>rrp8::HIS3MX6</i>	this study
RJY3276	<i>MATα</i> , <i>ade2-1</i> , <i>can1-100</i> , <i>his3-11,15</i> , <i>leu2-3,112</i> , <i>trp1-1</i> , <i>ura3</i> , <i>HO-ADE2</i> , <i>HO-CAN1</i> , <i>ssf1::HIS3MX6</i>	this study
RJY3361	<i>MATα</i> , <i>ade2-1</i> , <i>can1-100</i> , <i>his3-11,15</i> , <i>leu2-3,112</i> , <i>trp1-1</i> , <i>ura3</i> , <i>natNT2-pGALS-HA3-LOC1</i>	this study
RJY3362	<i>MATα</i> , <i>ade2-1</i> , <i>can1-100</i> , <i>his3-11,15</i> , <i>leu2-3,112</i> , <i>trp1-1</i> , <i>ura3</i> , <i>HIS3MX6-pGAL1-HA3-LOC1</i>	this study
RJY3419	<i>MATα</i> , <i>ade2-1</i> , <i>can1-100</i> , <i>his3-11,15</i> , <i>leu2-3,112</i> , <i>trp1-1</i> , <i>ura3</i> , <i>mrt4::HIS3MX6</i> , <i>YEplac195-ASH1</i>	this study
RJY3453	<i>MATα</i> , <i>ade2-1</i> , <i>can1-100</i> , <i>his3-11,15</i> , <i>leu2-3,112</i> , <i>trp1-1</i> , <i>ura3</i> , <i>ASH1-myc9</i> , <i>she2::URA3</i> , <i>YCplac22-SHE3N-SHE2</i>	this study
RJY3454	<i>MATα</i> , <i>ade2-1</i> , <i>can1-100</i> , <i>his3-11,15</i> , <i>leu2-3,112</i> , <i>trp1-1</i> , <i>ura3</i> , <i>ASH1-myc9</i> , <i>she2::URA3</i> , <i>YCplac22-SHE2(Kpn I)</i>	this study
RJY3455	<i>MATα</i> , <i>ade2-1</i> , <i>can1-100</i> , <i>his3-11,15</i> , <i>leu2-3,112</i> ,	this study

	<i>trp1-1, ura3, ASH1-myc9, she2::URA3, YCplac22-2xNLS-SHE3N-SHE2</i>	
RJY3463	<i>MATa, his3Δ1, leu2Δ0, met15Δ0, ura3Δ0, YEplac195-ASH1</i>	this study
RJY3469	<i>MATa, ade2-1, can1-100, his3-11,15, leu2-3,112, trp1-1, ura3, lhp1::HIS3MX6</i>	this study
RJY3470	<i>MATa/a, ade2-1, can1-100, his3-11,15, leu2-3,112, trp1-1, ura3, GAL, psi+, LHP1/lhp1::HIS3MX6, LOC1/loc1::natNT2</i>	this study
RJY3478	<i>MATa, ade2-1, can1-100, his3-11,15, leu2-3,112, trp1-1, ura3, lhp1::HIS3MX6, loc1::natNT2</i>	this study
RJY3479	<i>MATa, ade2-1, can1-100, his3-11,15, leu2-3,112, trp1-1, ura3, lhp1::HIS3MX6, loc1::natNT2</i>	this study
RJY3501	<i>MATa, ade2-1, can1-100, his3-11,15, leu2-3,112, trp1-1, ura3, pRS426-WSC2</i>	this study
RJY3502	<i>MATa, ade2-1, can1-100, his3-11,15, leu2-3,112, trp1-1, ura3, GAL, psi+, loc1::natNT2, YEplac195-ASH1</i>	this study
RJY3503	<i>MATa, ade2-1, can1-100, his3-11,15, leu2-3,112, trp1-1, ura3, loc1::natNT2, pRS426-IST2</i>	this study
RJY3504	<i>MATa, ade2-1, can1-100, his3-11,15, leu2-3,112, trp1-1, ura3, loc1::natNT2, pRS426-WSC2</i>	this study
RJY3505	<i>MATa, ade2-1, can1-100, his3-11,15, leu2-3,112, trp1-1, ura3, YEplac195-ASH1</i>	this study
RJY3506	<i>MATa, ade2-1, can1-100, his3-11,15, leu2-3,112, trp1-1, ura3, GAL, psi+, LOC1-yeGFP::HIS3MX6</i>	this study
RJY3507	<i>MATa, ade2-1, can1-100, his3-11,15, leu2-3,112, trp1-1, ura3, GAL, psi+, PUF6-yeGFP::HIS3MX6</i>	this study
RJY3511	<i>MATa, ade2-1, can1-100, his3-11,15, leu2-3,112, trp1-1, ura3, HIS3MX6-pGAL1-HA3-LOC1, YEplac195-ASH1</i>	this study
RJY3514	<i>MATa, ade2-1, can1-100, his3-11,15, leu2-3,112, trp1-1, ura3, HO-ADE2, HO-CAN1, PUF6-HA6::natNT2</i>	this study
RJY3520	<i>MATa, ade2-1, can1-100, his3-11,15, leu2-3,112, trp1-1, ura3, pRS426-pGAL1-ASH1</i>	this study

4.2.2. *Escherichia coli* strains

Name	Origin
XL1-Blue	Stratagene
BL21-CodonPlus®(DE3)-RIL	Stratagene
C600	Stratagene
TOP10	Invitrogen

4.3. Plasmids

Database entry	Name	Reference
RJP88	YEplac181-ASH1 (C3319)	Long et al., 1997
RJP122	p416-GALS	Mumberg et al., 1994
RJP132	YEplac195-ASH1 (C3431)	Long et al., 1997
RJP135	pFA6a-HIS3MX6	Wach et al., 1997
RJP138	YCplac22	Gietz & Sugino, 1988

RJP143	YEplac181	Gietz & Sugino, 1988
RJP145	YCplac111	Gietz & Sugino, 1988
RJP276	pYM2 (HA3, HIS3MX6)	Knop et al., 1999
RJP280	pYM6 (myc9, k.l.TRP1)	Knop et al., 1999
RJP292	pBS1479	Puig et al., 2001
RJP309	pRS426-pGAL1-ASH1	A. Jaedicke
RJP393	pBS1761	Puig et al., 2001
RJP407	pSH47	Güldener et al., 1996
RJP413	YEplac195	Gietz & Sugino, 1988
RJP577	pRS426-IST2 (pCJ15)	Jüschke et al., 2004
RJP673	pRS426-WSC2 (pCJ55)	C. Jüschke
RJP849	pKL187	Sanchez-Diaz et al., 2004
RJP916	YCplac111-SHE2	Du et al., 2008
RJP920	YCplac111-GFP-SHE2	Du et al., 2008
RJP957	pCM182	Garí et al., 1997
RJP1098	YCplac111-SHE3N-SHE2	Du et al., 2008
RJP1100	YCplac22-SHE3N-SHE2	Du et al., 2008
RJP1101	YCplac22-SHE2	Du et al., 2008
RJP1150	pRS313-SHE2(N36S, R63K)	Du et al., 2008
RJP1213	pFA6a-natNT2	Janke et al., 2004
RJP1218	pYM17 (HA6, natNT2)	Janke et al., 2004
RJP1220	pYM19 (myc9, HIS3MX6)	Janke et al., 2004
RJP1243	pYM44 (yeGFP, HIS3MX6)	Janke et al., 2004
RJP1279	pYM-N32 (HA3, pGALS, natNT2)	Janke et al., 2004
RJP1400	YEplac195-LOC1-HA6	this study
RJP1474	pCM182-LOC1-HA6	this study
RJP1382	p416-GALS-LOC1-HA6	this study
RJP1508	YCplac111-LOC1-HA6	this study
RJP1511	YCplac111-LOC1-5'-UTR	this study
RJP1518	p416-GALS-KHD1-HA6	this study
RJP1521	YCplac111-LOC1(aa65-204)-HA6	this study
RJP1522	YCplac111-LOC1(aa130-204)-HA6	this study
RJP1523	YCplac111-LOC1(aa158-204)-HA6	this study
RJP1541	pFA6a-HIS3MX6-pGAL1-HA3	Longtine et al., 1998
RJP1593	YCplac111-GFP-SHE2(aa1-236)	this study
RJP1594	YCplac111-GFP-SHE2(aa1-226)	this study
RJP1595	YCplac111-GFP-SHE2(N36S, R63K; aa1-236)	this study
RJP1595	YCplac111-GFP-SHE2(N36S, R63K; aa1-226)	this study
RJP1597	YCplac22-SHE3N-SHE2	Du et al., 2008

RJP1598	YCplac22-2×NLS-SHE3N-SHE2	Du et al., 2008
RJP1609	YCplac22-SHE2(Xho I)	this study
RJP1610	TOPO-MOD5_II	this study
RJP1611	TOPO-STP1_region_I	this study
RJP1612	YCplac22-SHE2-MOD5_II	this study
RJP1613	YCplac22-1×STP1_I-SHE2	this study
RJP1614	YCplac22-3×STP1_I-SHE2	this study
RJP1622	pTZ18U-tdΔP6-2 wt	Prenninger et al., 2006
RJP1623	pTZ18U-tdΔP6-2 SH1	Prenninger et al., 2006
RJP1624	pSU20	Prenninger et al., 2006
RJP1625	pSU18-stpA	Zhang et al., 1995
RJP1628	pSU18-LOC1	this study
RJP1629	pSU18	this study
RJP1687	pET28a(+)	Novagen
RJP1688	pET28a(+)-LOC1	M. Müller
RJP1689	pET28a(+)-stpA	this study

4.4. Oligonucleotides

All oligonucleotides used in this study were purchased from Thermo Scientific or MWG Biotech (now Eurofins MWG Operon). Oligonucleotides are listed in alphabetical order with database number, name, and sequence.

4.4.1. Directly labeled oligonucleotides

4.4.1.1. Fluorescently labeled oligonucleotides for FISH of *ASH1* mRNA

Sequences of Cy3-labeled oligonucleotides used in this study were described in Long et al., 1997. Asterisks mark amino-modified thymidine residues where the fluorochrome was bound.

5'-GCTT*GCCTTGTGAATT*CTGGTGAATT*GCCTGGTGT* AATGAGGAAATT*GG
5'-GATGCCTT*AGTGATGGT*AGGCTTGTGT*GGGCGCTCCGGT*CTCTTAGAT*A
5'-GGAACTT*GGACGACCTAGT*CGATTCCAATT*CCTTGCCGT*AATTGAACT*AT
5'-AT*GGTTCTATT*GGTTGGTGGACT*CATCGCGGTGT*GACGGGAGGAGTAAT*A
5'-AAGCT*TTGAACTGTT*CGTCTTTTGT*GACTGGCATT*GGCATGGGAAAT*G

4.4.1.2. Fluorescently labeled oligonucleotides for primer extension

For primer extension, all oligonucleotides labeled at the 5'-end with fluorescein (FAM™) were purchased from MWG Biotech.

RJ03185	5'-FAM-ASH1-E3	5'-GAAAATGAAAGAAAATGAAT
RJ03186	5'-FAM-NBS-2	5'-GACGCAATATTAACGGT
RJ02439	5'-FAM-25SrRNA	5'-GTCTTCAAAGTTCTCATTTG
RJ02733	5'-FAM-U2snRNA	5'-TGGGTGCCAAAAAATGTGTATT

4.4.2. Oligonucleotides for generation of labeled probes

4.4.2.1. Oligonucleotides for *ASH1* probe synthesis

RJO176 *ASH1* ORF297 fw 5'-CCAATAGAACCATGGAGCGC
RJO217 *ASH1* 3'-UTR rev 5'-GAAGATGCCGCGGCGTG

4.4.2.2. Oligonucleotides for *IST2* probe synthesis

RJO671 *IST2*_pr1 fw 5'-CTATACTTATTTGCACG
RJO675 *IST2*_pr1 revT7 5'-taatacactcactataggGCCAATATTGAAAAGGC
RJO672 *IST2*_pr2 fw 5'-GGAAAGCTGTGCTTTATAG
RJO676 *IST2*_pr2 revT7 5'-taactataggCCACGAGTGGTTTATTG
RJO673 *IST2*_pr3 fw 5'-CAGCCTGCCTCTTCTGCC
RJO677 *IST2*_pr3 revT7 5'-taatacactcactataggCCGCAACACCATATGAG
RJO674 *IST2*_pr4 fw 5'-CGATGCTGCCACTAAG
RJO678 *IST2*_pr4 revT7 5'-taatacactcactataggGTGATGATGATGGTGGGGC

4.4.2.3. Oligonucleotides for *WSC2* probe synthesis

RJO2894 *WSC2*_pr1 fw 5'-GCACCTAGATCTCATAACAAGTC
RJO2895 *WSC2*_pr1 revT7 5'-cgtaatacactcactataggCCTGCGTCAAAGACTGTAAGTG
RJO2896 *WSC2*_pr2 fw 5'-CTACTGCTACCTCAACATCGAC
RJO2897 *WSC2*_pr2 revT7 5'-cgtaatacactcactataggAGTGCTAGAGGAAGTGGTGG
RJO2898 *WSC2*_pr3 fw 5'-CAGTCCGTGGTTTCTCAAGC
RJO2899 *WSC2*_pr3 revT7 5'-cgtaatacactcactataggCCAGTGAGTACGGCTGGTAC
RJO2900 *WSC2*_pr4 fw 5'-GCCACTTATGATCTGCCGAC
RJO2901 *WSC2*_pr4 revT7 5'-cgtaatacactcactataggGTCAGCGCAAAGAACTATTATT

4.4.3. Oligonucleotides for gene disruption

Δ arx1

fw: RJO2955 5'-ACTTTTAAGAAAAACCCGACCCGACTAATATTGCTAAAACATATCcgtaacgctgcaggtcgac
rev: RJO2956 5'-ATACTTATATTATTTATATACTAGCTTTAGAAATGATGAAGTTTCatcgatgaattcgagctcg

Δ khd1

fw: RJO1292 5'-CGGGTAACTTAGAGACAGCATTAGTATATATACCAGCCcagctgaagcttcgtacgc
rev: RJO1293 5'-GTTTTGTCTGTGTGGGACGTGCGCACGACACGTATATAgcataggccactagtgatctg

Δ lhp1

fw: RJO3179 5'-TCTATTTGGTTCTACTGGAACTAAAGTAGCATCTGCAAAGAAGTAcgtacgctgcaggtcgac
rev: RJO3180 5'-ATATGCTATGATAATGAGATACGAGAACCAGAAGAAACACAAGAAatcgatgaattcgagctcg

Δ loc1

fw: RJO691 5'-GGTTAGATATCTGTAAATCTATACAATTAAGGAAAGATGGCACCcagctgaagcttcgtacgc
rev: RJO692 5'-ATACAACAGACTTATCCGTATTTAGTTTAGTCAATCAAACgcataggccactagtgatctg

fw: RJO2326 5'-TTATAAGGTTAGATATCTGTAATCTATACAATTAAGGAAAGATGcgtacgctgcaggtcgac
rev: RJO2327 5'-ATTATACAACAGACTTATCCGTATTTAGTTTAGTCAATCAAACAACTAatcgatgaattcgagctcg

Δ lsm7

fw: RJO2522 5'-AGCAGCACTTTGTTTACTACACAGAACATTAACCAAAAAAACcgtacgctgcaggtcgac
rev: RJO2523 5'-AACTGTAAGGAAGGGAGTTTATATGAGATTATATTATTAACatcgatgaattcgagctcg

Δ ltv1

fw: RJO2959 5'-GTATAGTATTTCAAAGACTTTAAGGGGAATATAAAAAGCACGAAGcgtacgctgcaggtcgac
rev: RJO2960 5'-CACAGTACTTGTAATGTAGGTGCTTTCTCATCTCATTCTACTCCTatcgatgaattcgagctcg

Δ mrt4

fw: RJO2516 5'-ATCACTGTCTATCGTCCATAAAAAGATTTATATAGTTGAATCcgtaacgctgcaggtcgac
rev: RJO2517 5'-TACAATGGTCTATTAATAAAGGCTTCCAAATAATAGTTCAGCatcgatgaattcgagctcg

Δ nop6

fw: RJO2963 5'-CTAATGTAGAGGACAGGATAGAGATTGAAGACGTCTACAGCTAAAacgtacgctgcaggtcgac
rev: RJO2964 5'-TTTCTTTTGTCTAAGATACATGGCGTATAAAAATTAATTTGTACatcgatgaattcgagctcg

Δ nop16

fw: RJO2757 5'-TTAATATCAAACCTGCAAATACACTAAGTAAAAAAGTTGCATACcgtacgctgcaggtcgac
rev: RJO2758 5'-CATATATAAATATTACGTGGTAATCAATTGGTAGTTGCCATTGGTatcgatgaattcgagctcg

Δ puf6

fw: RJO2328 5'-TACTGAAATAAAGCACAATCAGGAATAACAAATTAAGTACAATGcgtacgctgcaggtcgac
rev: RJO2329 5'-AGATGCTTATATACCAAATATTGTGACTTTATCGTAGAAAAATTAatcgatgaattcgagctcg

Δ rrp8

fw: RJO2971 5'-TATATATATTATATCAAACAAATAAGGACGTTAACGAAATTTTATcgtacgctgcaggtcgac
rev: RJO2972 5'-AAAAGAAAAACAATATTTAAATATGAAAATGACGGATGAAGTCGatcgatgaattcgagctcg

Δ she2

fw: RJO2420 5'-GTAAACCTCCTTAATTTTCCTTTTGCATAATACCAGACACTTAAAAcgtacgctgcaggtcgac
rev: RJO2071 5'-ATTAAGTGTGACTTATTTGCTCTTTTGTGAGCTAAAACTGAAGGCCatcgatgaattcgagctcg

Δ ssf1

fw: RJO2975 5'-AATAAAGAGTATAATCCAGATATAGCAGACAATAAAATTTCAAGcgtacgctgcaggtcgac
rev: RJO2976 5'-GGATAGCCAGCTTAACTAAAAATTTCTTGGTACCGGAGACAATatcgatgaattcgagctcg

4.4.4. Oligonucleotides for epitope tagging

Knop-Loc1

fw: RJO3002 5'-TTATAAGGTTAGATATCTGTAAATCTATACAATTAAGGAAAGATGcgtacgctgcaggtcgac
rev: RJO3003 5'-GACTTCTCTCTCAGATTTTGTCTCTTAGAAGGTTCTTTGGTGcctcgaattcctctgctcg

Loc1 C-terminal truncation (rev primer: RJO2340)

aa1-190

fw: RJO2790 5'-AATAAACGTGATATGTTGAAAAGTGAAGCAAAGCTAGTGAAAGTcgtacgctgcaggtcgac

aa1-159

fw: RJO2789 5'-GAAAGAAAGGAAGCGCTTAAACAAGATAAACTAGAAGAAAAAAAACgtacgctgcaggtcgac

aa1-140

fw: RJO2783 5'-AAGCTTGAAAAGGCTAGAAGATTAGAAGAGATACGAGAATTGAAAACgtacgctgcaggtcgac

aa1-130

fw: RJO2857 5'-GGTGACAAGTACGACGATATAGCTGAGAGTAAGCTTGAAAAGGCTcgtacgctgcaggtcgac

aa1-120

fw: RJO2858 5'-CTGACTTTAAACCGTTTAATAACAACACTATTGGTGACAAGTACGACcgtacgctgcaggtcgac

aa1-115

fw: RJO2835 5'-GCTGATAACGACACTCTGACTTTAAACCGTTTAATAACAACACTATTcgtacgctgcaggtcgac

aa1-70

fw: RJO2782 5'-TTGGCTAGACTTTATGGTGCGAAGAAGGACAAGAAGGGGAAATATcgtacgctgcaggtcgac

Loc1-Knop

fw: RJO2339 5'-TAGTGAAAGTAAAACCTGAAGGAAGGAAGGTAAAAAAGTCTCATTTGCTCAAACgtacgctgcaggtcgac
rev: RJO2340 5'-GTTATATATTATACAACAGACTTATCCGTATTTAGTTTAGTCAATCAAACATatcgatgaattcgagctcg

Longtine-Loc1

fw: RJO3000 5'-TGAAAAAGAAGATCGAATGCAAACCATAAAATTAGAGATCTAATTGgaattcgagctcgtttaaac
rev: RJO3001 5'-TTCTCTCTCAGATTTTGTCTCTTAGAAGGTTTCTTTGGTGCCATgactgagcagcgaattctg

Loc1-TAP

fw: RJO2316 5'-AGTAAACTGAAGGAAGGAAGGTAAAAAAGTCTCATTTGCTCAAatcctggaagagaag
rev: RJO2317 5'-TATATTATACAACAGACTTATCCGTATTTAGTTTAGTCAATCAAAtacgactcactataggg

Loc1-td

fw: RJO2716 5'-TAAACTGAAAAAGAAGATCGAATGCAAACCATAAAATTAGAGATCTAATTGattaaggcgcgagctcg
rev: RJO2717 5'-GCGACTTCTCTTCTCAGATTTTGTCTCTTAGAAGGTTTCTTTGGTGCCATggcaccgctccagcgcctg

TAP-Loc1

fw: RJO2400 5'-AAATTATAAGGTTAGATATCTGTAAATCTATACAATTAAGGAAAAGaacaagaagctggagctcat
rev: RJO2401 5'-TTCTCTCTCAGATTTTGTCTCTTAGAAGGTTTCTTTGGTGCCATcttatcgtcatcatcaagt

Puf6-Knop

fw: RJO2037 5'-GATGAAAGTAACAAAGGCTCTCAGCTTTTGGCTAAATTTGTTAAAAcgtacgctgcaggtcgac
rev: RJO2038 5'-GTACAGATGCTTATATACCAAATATTGTGACTTTATCGTAGAAAAATatcgatgaattcgagctcg

Puf6-TAP

fw: RJ02319 5'-GATGAAAGTAACAAAGGCTCTCAGCTTTTGGCTAAATTGTTAAAAccatgaaaagagaag

rev: RJ02320 5'-TACAGATGCTTATATACCAAATATTGTGACTTTATCGTAGAAAAAtacgactcactataggg

She2-Knop

fw: RJ02070 5'-TGATGTTGTCGCTACTAAATGGCATGACAAATTTGGTAAATTGAAAAACcgtacgctgcaggctgac

rev: RJ02071 5'-ATTAAGTAGTGGTACTTATTTGCTCTTTTGGAGCTAAAACTGAAGGCCatcgatgaattcgagctcg

4.4.5. Oligonucleotides for sequencing or verifying knockouts/taggings

RJ02957	ARX1 5'-UTR fw	5'-GATGAGATGAGCTAAAGCATC
RJ02958	ARX1 3'-UTR rev	5'-CTGAGCAAATGAACCAAGCGG
RJ01763	degron check fw	5'-CTGGTGCAGGCGCTGGAGCG
RJ01764	degron check rev	5'-CGCTCCAGCGCCTGCACCAG
RJ02337	GAL1 prom fw	5'-TAATACTTTCAACATTTTTCGG
RJ02210	HIS3MX6 fw	5'-GCTCCCTTACCTGAAGAGTCG
RJ02633	HIS3MX6 outfw	5'-GTAATGACCATCATCGTGCTG
RJ02632	HIS3MX6 rev	5'-CGACTCTTCAGGTAAGGGAGC
RJ02027	kanMX fw	5'-TGATTTTGGATGACGAGCGTAAT
RJ02495	kanMX outfw	5'-GCAGTTTCATTTGATGCTCGATGAG
RJ02026	kanMX rev	5'-CTGCAGCGAGGAGCCGTAAT
RJ01751	KHD1 5'-UTR fw	5'-CAGTTTGCCAATATAAGCGC
RJ01752	KHD1 3'-UTR rev	5'-AATCTAGAGGAAACGCCAATAGTCTCGA
RJ02020	K.I. TRP1 fw	5'-GAGGTTCCAGTTCCACAGG
RJ02636	K.I. TRP1 outfw	5'-CGGGAACACAAATGATAC
RJ02021	K.I. TRP1 rev	5'-CCTGTGGGAACTGGAACCTC
RJ02637	Knop-tag rev	5'-CGAGGAGCCGTAATTTTTGC
RJ03181	LHP1 5'-UTR fw	5'-CCCTTCACCTTAAACCCTTCC
RJ03182	LHP1 3'-UTR rev	5'-CAAGAGACTCTCTCTGACTGC
RJ02243	LOC1 5'-UTR fw	5'-GAAGTAACGGCGATGAGGTG
RJ02718	LOC1 ORF120 rev	5'-CAAGCTTACTCTCAGCTATATC
RJ02318	LOC1 ORF122 fw	5'-AGCTGAGAGTAAGCTTGAAAA
RJ02244	LOC1 3'-UTR rev	5'-GAACAGAGTAGCATCAGCC
RJ02331	LOC1 3'-UTR rev 2	5'-GAAATCTTCTAGGAAGACGTG
RJ02524	LSM7 5'-UTR fw	5'-GAAAAACAGACAACTGGGAAAC
RJ02525	LSM7 3'-UTR rev	5'-AACTATGTAGCGCATACTATG
RJ02961	LTV1 5'-UTR fw	5'-GTCAAATAAAAAATTTTAAGCG
RJ02962	LTV1 3'-UTR rev	5'-GCCGCGTTTCATAATTATTAC
MWG	M13 uni (-21)	5'-TGTAACACGACGGCCAGT
MWG	M13 rev (-29)	5'-CAGGAAACAGCTATGACC
RJ02514	MRT4 5'-UTR fw	5'-ACCATTAGGACTTTACCCGGC
RJ02515	MRT4 3'-UTR rev	5'-GCTAAAGAGCTGTGAAGATCA
RJ02330	natNT2 fw	5'-AATCGGACGACGAATCGGACG
RJ02496	natNT2 outfw	5'-CGCTCTACATGAGCATGCCCTGCCC

Materials

RJ02965	NOP6 5'-UTR fw	5'-CATTCCTGAAAATTTTCTAAG
RJ02966	NOP6 3'-UTR rev	5'-GGAAGAGTTTACGTATTGGGC
RJ02759	NOP16 5'-UTR fw	5'-AACGTTACCCGAACAGAACAC
RJ02759	NOP16 3'-UTR rev	5'-CTACCTATAGAGCCTTTGTGG
RJ02780	PUF6 5'-UTR fw	5'-GTATTTTCGAAGGTGAAAGCG
RJ02321	PUF6 ORF491 fw	5'-ATTCCAGTATATTGACAGAGA
RJ02332	PUF6 3'-UTR rev	5'-GTGAGGTGAGGATTCGCTATC
RJ02781	PUF6 3'-UTR rev 2	5'-CCTGCACTTTCAATGAGATC
RJ02973	RRP8 5'-UTR fw	5'-CTCGCATCGTCAATAACGGCG
RJ02974	RRP8 3'-UTR rev	5'-GTGGAGTACTTCTTCTAGATG
RJ01813	SHE2 5'-UTR fw	5'-CTTATAGAATGGTTCTTCGTGCATGCC
RJ01816	SHE2 ORF100 rev	5'-CGCAAATGACTGATGAACTTGTTTCAGC
RJ02069	SHE2 ORF262 fw	5'-GAGGCGGATTCGTTTGACAAG
RJ02068	SHE2 ORF486 rev	5'-CAAAGACTCAATCATCCATTGAG
RJ01964	SHE2 3'-UTR rev	5'-CCTAAATTGGGGTCCCTCCCACATCAGAGG
RJ02977	SSF1 5'-UTR fw	5'-CGAAATTGAAATTTTTCCTG
RJ02978	SSF1 3'-UTR rev	5'-GCTATGATTTAAAAGACAAAAG
MWG	T3	5'-AATTAACCCCTCACTAAAGGG
MWG	T7	5'-TAATACGACTCACTATAGGG
MWG	T7 term	5'-CTAGTTATTGCTCAGCGGT
RJ02422	T7 term rev	5'-GCTAGTTATTGCTCAGCGG
RJ0166	YXplac fw	5'-CCCGACTGGAAAGCGGGCAG
RJ0167	YXplac rev	5'-GGAGAAAATACCGCATCAGGC

4.4.6. Oligonucleotides for cloning

RJ02933	KHD1 fw (Spe I)	5'-TTTTTTactagtATGTCACAGTTCTTCGAAGCT
RJ02856	Knop rev pYM3 (Hind III)	5'-TTTTTTTaagcttTATAGTGAATGATCGTTCCAC
RJ02818	Knop-tag rev (Apa I)	5'-TTTTTTTgggcccCGAGGAGCCGTAATTTTTTGC
RJ02635	Knop-tag rev (Kpn I)	5'-TTTTTTTggtaccCGAGGAGCCGTAATTTTTTGC
RJ02580	LOC1 5'-UTR fw (Sph I)	5'-TTTTTTTgcatgcGTTTGGGAAGGAAAGCAG
RJ02929	LOC1 5'-UTR rev (Bam H I)	5'-TTTTTTTggatccCTTTCCTTAATTGTATAGATT
RJ02382	LOC1 fw (Bam H I)	5'-TTTTTTTggatccATGGCACCAAAGAAACCTTCT
RJ02817	LOC1 fw (Cla I)	5'-TTTTTTTatgatATGGCACCAAAGAAACCTTCT
RJ02536	LOC1 fw (Spe I)	5'-TTTTTTTactagtATGGCACCAAAGAAACCTTCT
RJ0562	LOC1 fw (Xho I)	5'-TTTctcgagGTTTGGGAAGGAAAGC
RJ02930	LOC1 ORF65 fw (Bam H I)	5'-TTTTTTTggatccatgAAGGACAAGAAGGGGAAATATTC
RJ02952	LOC1 ORF65 fw (Kpn I)	5'-TTTTTTTggtaccatgAAGGACAAGAAGGGGAAATATTC
RJ02931	LOC1 ORF130 fw (Bam H I)	5'-TTTTTTTggatccatgGCTAGAAGATTAGAAGAGATAC
RJ02953	LOC1 ORF130 fw (Kpn I)	5'-TTTTTTTggtaccatgGCTAGAAGATTAGAAGAGATAC
RJ02932	LOC1 ORF158 fw (Bam H I)	5'-TTTTTTTggatccatgAAAAAAGACGAGATTA AAAA'GAAG
RJ02954	LOC1 ORF158 fw (Kpn I)	5'-TTTTTTTggtaccatgAAAAAAGACGAGATTA AAAAAGAAG

Materials

RJ03187	LOC1 rev (Eco R I)	5'-TTTTTTTgaattcCTATTGAGCAAATGAGACTTTTTTTTAC
RJ02383	LOC1 rev (Xho I)	5'-TTTTTTTctcgagTTGAGCAAATGAGACTTTTTTTTAC
RJ02421	LOC1-tag rev (Pst I/Eco R I)	5'-TTTTTTTgaattcctgcagCGAGGAGCCGTAATTTTTTGC
RJ03162	MOD5_II fw (Xba I)	5'-TTTTTTTtctagaCCCCCGGGCCCCCATGTCTAAAAAAGT TATAGTG
RJ03156	MOD5_II fw (Xho I)	5'-TTTTTTTctcgagATGTCTAAAAAAGTTATAGTG
RJ03163	MOD5_II rev (Xba I)	5'-TTTTTTTtctagaCAAGTTGGATTTATGTCTTCTG
RJ03157	MOD5_II rev (Xho I)	5'-TTTTTTTctcgagGGGGGGCCCCGGGGGAAGTTGGATTTA TGCTTCTG
RJ02518	2×NLS fw (Bam H I)	5'-TTggatccCCCCCGGGCCCCCGGTA
RJ03127	2×NLS fw (Bam H I) 2	5'-TTTTTTTggatccCAAAAAAGAAGAGAAAGGTACC
RJ03160	2×NLS fw (Xba I)	5'-TTTTTTTtctagaCCCCCGGGCCCCCGgtacc
RJ03137	2×NLS fw (Xho I)	5'-TTTTTTTctcgagCCCCCGGGCCCCCGgtacc
RJ03128	2×NLS rev (Bam H I)	5'-TTTTTTTggatccGGGCCCGGTACCTTTCTCTTCTTTTTTG
RJ02498	2×NLS rev (Bgl II)	5'-CGCagatctGGGCCCGGTACCTT
RJ03161	2×NLS rev (Xba I)	5'-TTTTTTTtctagaGGGCCCGGTACCTTTCTCTT
RJ03138	2×NLS rev (Xho I)	5'-TTTTTTTctcgagGGGCCCGGTACCTTTCTCTT
RJ03107	PUF6 fw (Sac I)	5'-TTTTTTTgagctcATGGCACCTTTAACCAAGAAG
RJ02855	PUF6 fw (Spe I)	5'-TTTTTTTactagtATGGCACCTTTAACCAAGAAG
RJ03108	PUF6 rev (Xho I)	5'-TTTTTTTctcgagTTTTAACAATTTAGCCAAAAG
RJ02854	SHE2 fw (Spe I)	5'-TTTTTTTactagtATGAGCAAAGACAAAGATATC
RJ03101	SHE2 ORF236 rev (Stu I)	5'-TTTTTTTaggcctcaTTTGTTCATGCCATTTAGTAGC
RJ03102	SHE2 ORF226 rev (Stu I)	5'-TTTTTTTaggcctcaCAAGGCGCTCAGCTTACCATC
RJ03103	SHE2 ORF216 rev (Stu I)	5'-TTTTTTTaggcctcaGTGCCACGCAGCTGACAAGGT
RJ03104	SHE2 ORF206 rev (Stu I)	5'-TTTTTTTaggcctcaTTCTTCCGAGTTGACAGGAAG
RJ03164	STP1 region I fw (Xba I)	5'-TTTTTTTtctagaCCCCCGGGCCCCCATGCCCTCTACCA CGCTACTG
RJ03154	STP1 region I fw (Xho I)	5'-TTTTTTTctcgagATGCCCTCTACCACGCTACTG
RJ03165	STP1 region I rev (Xba I)	5'-TTTTTTTtctagaATAATGATGACTTAGATCTGG
RJ03155	STP1 region I rev (Xho I)	5'-TTTTTTTctcgagGGGGGGCCCCGGGGGATAATGATGACTT AGATCTGG
RJ03388	stpA fw (Bam H I)	5'-TTTTTTTggtaccATGTCCGTAATGTTACAAAGT
RJ03389	stpA +Stop rev (Xho I)	5'-TTTTTTTctcgagTTAGATCAGGAAATCGTCGAG
RJ03390	stpA -Stop rev (Xho I)	5'-TTTTTTTctcgagGATCAGGAAATCGTCGAGAGA

4.4.7. Oligonucleotides for site-directed mutagenesis

RJ03133	1100_1 st Kpn I to Xho I fw	5'-AGACACTTAAAAATGctcgagTCGGACCAGGATAAT
RJ03134	1100_1 st Kpn I to Xho I rev	5'-ATTATCCTGGTCCGActcgagCATTTTTTAAGTGTCT
RJ03135	1100_2 nd Kpn I to Apa I fw	5'-GATCCCCCGGGCCCCCGggGCcAGCAAAGACAAAGATATC
RJ03136	1100_2 nd Kpn I to Apa I rev	5'-GATATCTTTGTCTTTGCTggGCcGGGGGGCCCCGGGGGAT
RJ03152	1101_Kpn I to Xho I fw	5'-AGACACTTAAAAATGctcgagAGCAAAGACAAAGATA
RJ03153	1101_Kpn I to Xho I rev	5'-TATCTTTGTCTTTGCTctcgagCATTTTTTAAGTGTCT

4.5. Buffers – Media

4.5.1. General Buffers

10× PBS(T)

(phosphate-buffered saline)(Tween)

1.37 M (80 g) NaCl
27 mM (2.0 g) KCl
20 mM (2.4 g) KH₂PO₄
10 mM (17.8 g) Na₂HPO₄·2 H₂O
PBST: 0.1% (v/v) (1 ml 100%) Tween-20
ad 1 l water
store @ RT

1 M PK_i pH 7.5

(inorganic potassium phosphate)

86.6 ml 1 M K₂HPO₄
13.4 ml 1 M KH₂PO₄
adjust pH
store @ RT

1 M PNa_i pH 7.0 (inorganic sodium phosphate)

57.7 ml 1 M Na₂HPO₄
42.3 ml 1 M NaH₂PO₄
adjust pH
store @ RT

20× SSC (saline-sodium citrate)

3 M (175,3 g) NaCl
0.3 M (88,2 g) sodium citrate
ad 1000 ml water
store @ RT

10× TBS (Tris-buffer saline)

1.37 M (80 g) NaCl
27 mM (2.0 g) KCl
125 mM (125 ml 1 M) Tris pH 7.4
ad 1 l water
store @ RT

4.5.2. Media (plates supplemented with 20 g/l Bacto™ Agar)

Yeast media were prepared as described (Adams, 1998), sometimes with minor changes in composition. *E. coli* media were prepared as described previously (Sambrook & Russell, 2001).

LB (Luria-Bertani Broth)

10 g Bacto™ Tryptone
5 g Bacto™ Yeast Extract
10 g NaCl
ad 1 l water
autoclave
before use add respective antibiotic, if needed

Presporulation (plates only!)

5 g glucose
3 g nutrient broth
1 g yeast extract
ad 100 ml water
autoclave
store @ 4°C and use within 2 weeks

SDC dropout (Synthetic Dextrose Complete)

6.7 g YNB
dropout mix as required
ad 900 ml water
autoclave
before use add 100 ml 20%(w/v) glucose

SGC dropout (Synthetic Galactose Complete)

6.7 g YNB
dropout mix as required
ad 900 ml water
autoclave
before use add 100 ml 20%(w/v) galactose

SOB (Super Optimal Broth)

20 g Bacto™ Trypton
5 g Bacto™ Yeast Extract
8.55 mM (0.5 g) NaCl
2.5 mM (2.5 ml 1 M) KCl
ad 1.0 l water (adjust pH to 7 (with NaOH))
autoclave
before use add 10 mM (5 ml 2 M) MgCl₂

SOC (Super Optimal Broth with Catabolite

Repression)

See SOB
before use add 20 mM (10 ml 2.2 M) Glc
store 15 ml aliquots @ -20°C

Materials

Sporulation (plates)

10 g potassium acetate
1 g yeast extract
2 g synthetic complete mix
2.5 ml 20% (w/v) glucose
ad 500 ml water
autoclave

SRC dropout (Synthetic Raffinose Complete)

6.7 g YNB
dropout mix as required
ad 900 ml water
autoclave
before use add 100 ml

YP (Yeast Extract Peptone)

11 g Bacto™ Yeast Extract
22 g Bacto™ Peptone
55 mg adenine hemisulfate
ad 900 ml water
autoclave
before use add 100 ml 20% (w/v)
of respective sugar (YPD – Glc, YPG – Gal, YPR – Raf)

Sporulation (solution)

1 g potassium acetate
0.05 g zinc acetate
ad 100 ml water
autoclave

TBYE (Tryptone Broth Yeast Extract)

10 g Bacto™ Tryptone
5 g Bacto™ Yeast Extract
5 g NaCl
ad 1 l water
20% (w/v) raffinose autoclave
before use add respective antibiotic, if needed

4.5.3. Consumables

Name	Supplier
Calmodulin Affinity Resin	Stratagene
Econo Column®	Bio-Rad
Filter paper 3MM	Whatman
Gene Pulser® Cuvettes 0.2 cm electrode gap	Bio-Rad
glass beads (∅ 0.2 – 0.3 mm)	Roth
IgG Sepharose™ 6 Fast Flow	Amersham
mini Quick Spin Columns	Roche Applied Science
Mobicols	MoBiTec
NuPAGE® Novex 4-12% Bis-Tris Gel (1.0 mm)	Invitrogen
Positive™ Membrane	Qbiogene
Sterile Filter units (0.45 µm, 0.22 µm)	Millipore
SW40 polycarbonate tubes	Beranek

4.5.4. Devices

Name	Supplier
Biofuge fresco	Heraeus
Electroporation device Micropulser™	Bio-Rad
Fluorescence Image Reader LAS-3000	Fujifilm
Fluorescence Microscope BX60	Olympus
Gradient Station	BioComp Instruments
Mini Hybridization Oven	MWG Biotech

Materials

SE Mighty Small II gel electrophesis system	Hoefer
Sequi-Gen® GT Nucleic Acid Electrophoresis Cell (21×40 cm)	Bio-Rad
Thermocycler	MJ Research
Thermomixer compact	Eppendorf
Typhoon™ Variable Mode Imager	Amersham
UV Stratalinker	Stratagene
Vibrax VXR basic	IKA

4.5.5. Commercial Kits

Name	Supplier
Colloidal Blue Staining Kit	Invitrogen
FastPlasmid™ Mini Kit	Eppendorf
Prime-It® II Random Primer Labeling Kit	Stratagene
QuikChange® Site-Directed Mutagenesis Kit	Stratagene
QIAquick® Gel Extraction Kit	Qiagen
QIAquick® PCR Purification Kit	Qiagen
QIAprep® Spin Miniprep Kit	Qiagen
SilverQuest™ Silver Staining Kit	Invitrogen
TOPO TA Cloning Kit	Invitrogen

4.5.6. Stockists

Company	Contact
A. Hartenstein Laborbedarf GmbH	www.laborversand.de
abcam	www.abcam.com
Ambion, Inc.	www.ambion.com
Amersham (now GE Healthcare)	www.gehealthcare.com
Axon Labortechnik	www.axon-lab.de
Beranek Laborgeräte	www.laborgeraete-beranek.de
BioComp Instruments, Inc. (via Science Services GmbH)	www.scienceservices.de
Bio-Rad	www.bio-rad.com
Carl Roth	www.carl-roth.de
Covance	www.covance.com
Eppendorf AG	www.eppendorf.de
Fermentas Life Sciences	www.fermentas.com
Fluka (via Sigma-Aldrich)	www.sigmaaldrich.com
Gentaur Molecular Products	www.gentaur.com
Heraeus (via VWR)	www.vwr.com
Hoefer®, Inc.	www.hoeferinc.com
IKA® Labortechnik	www.ika.de
Invitrogen Corporation	www.invitrogen.com
Jackson ImmunoResearch Europe, Ltd.	www.jireurope.com

Materials

Millipore	www.millipore.com
MJ Research, Inc. (now Bio-Rad)	www.bio-rad.com
MoBiTec	www.mobitec.de
Molecular Probes® (Invitrogen)	www.invitrogen.com
MWG Biotech (now eurofins MWG Operon)	www.eurofinsdna.com
New England Biolabs	www.neb.com
Olympus Deutschland	www.olympus.de
Promega GmbH	www.promega.com/de
Qbiogene (now MP Biomedicals)	www.qbiogene.com
QIAGEN AG	www.qiagen.com
Roche Applied Science	www.roche-applied-science.com
Santa Cruz Biotechnology, Inc.	www.scbt.com
SEIKAGAKU Biobusiness Corp.	www.seikagaku.co.jp/english
Sigma-Aldrich®	www.sigmaaldrich.com
Stratagene (Agilent Technologies)	www.stratagene.com
WERNER BioAgents	www.webioage.com
Whatman (now GE Healthcare)	www.gehealthcare.com

(...) sic coquantur: (...)

M. Gavius Apicius,
De re coquinaria, 5,1,1.

5. Methods

5.1. Methods in molecular biology

5.1.1. Agarose gel electrophoresis

5.1.1.1. Standard agarose gel electrophoresis

Agarose gel electrophoresis is used to separate DNA fragments of different lengths. The method is described in detail in Sambrook & Russell, 2001. In this work electrophoresis was performed routinely with 1.0% (w/v) agarose gels containing 0.2 µg/ml ethidium bromide, with 1×TAE as electrophoresis buffer. To assay the length of the fragments, 250 ng of a DNA ladder (see section 4.1.4) was used.

6× loading dye (LD)

40% (w/v) Sucrose
0.25% (w/v) Bromophenol blue
0.25% (w/v) Xylene cyanol FF
store aliquots @ -20°C

50× TAE

2 M (121 g) Tris
100 mM EDTA pH 8,0
1 M acetic acid
autoclave
store @ RT

5.1.1.2. Preparative agarose gel electrophoresis

For purification of DNA fragments after digestion with restriction endonucleases (section 5.1.2), 1.0% gels were cast with broad lanes, enabling loading of up to 100 µl of the digestion sample per lane.

5.1.2. Digestion of DNA with restriction endonucleases

In this work, a variety of prokaryotic restriction endonucleases were used to digest DNA in order to prepare defined fragments for cloning or to check cloned plasmids for presence and correct orientation of inserted DNA fragments. The reactions were generally set up in 1.5 ml tubes as test digests to control cloning (20 µl reaction mix) or as preparative digests (100 µl reaction mix).

Table 3 | Setup for digestion of DNA with restriction endonucleases.

	20 µl reaction	100 µl reaction
sterile water	15.5 / 15.3 µl	57.5 / 56.5 µl
10× restriction enzyme buffer	2 µl	10 µl
100× BSA	0 / 0.2 µl	0 / 1 µl
restriction enzyme	0.5 µl (2.5 – 10 U)	2.5 µl (12.5 – 120 U)
plasmid preparation	2 µl	30 µl

20 µl reactions were incubated for 2 h at the respective temperature, 100 µl reactions were for 5 h to overnight. Preparative digests were additionally incubated with Calf Intestine Alkaline Phosphatase (CIAP) for 30 min at 37°C. The different restriction enzyme activity is due to different concentrations provided by the manufacturer.

10 µl of the 20 µl reactions were analyzed on a 1.0% agarose gel (see section 5.1.1.1); the 100 µl reactions were loaded entirely onto broad lanes, and the bands of interest were cut out after the gel course.

5.1.3. Purification of DNA fragments from agarose gels

DNA fragments of interest were cut out from agarose gels and purified using the commercial QIAquick® gel extraction kit, following the manual provided by the manufacturer.

5.1.4. Ligation of DNA fragments

Ligation of digested DNA fragments was carried out with T4 DNA Ligase either according to the protocol from the Quick Ligation™ Kit or according to the protocol provided with the enzyme. For a standard ligation reaction, 1 µl vector was mixed with 9 µl insert (depending on concentration), 2 µl 10× ligation buffer, and 7 µl sterile water. After addition of 1 µl of ligase the mixture was incubated for at least 30 min at room temperature.

5.1.5. Polymerase chain reaction (PCR)

Using the polymerase chain reaction (PCR) fragments of DNA can rapidly be amplified and subsequently used for cloning. The principles are described in detail in Sambrook & Russell, 2001. The program for all PCR reactions in this work was described previously (Janke et al., 2004, see Table 4). 10 µl of each sample were analyzed on a 1.0% agarose gel after the end of amplification. All PCR products for further use were subsequently purified using the QIAGEN® PCR purification kit, eluted in 30 µl of sterile water and stored at -20 °C.

Table 4 | PCR program (SJKNOP)

Denaturation	Annealing	Elongation	Number of cycles
3 min 95°C	30 s 54°C	2 min 40 s 68°C	1
1 min 95°C	30 s 54°C	2 min 40 s 68°C	10
1 min 95°C	30 s 54°C	2 min 40 s 68°C	20
		+20 s/cycle	

5.1.5.1. Yeast colony PCR

A small amount of yeast cells was suspended in 100 μ l 0.02 M NaOH in a safe-lock 1.5 ml tube, 250 μ l glass beads (\varnothing 0.2 – 0.3 mm) were added, and the mixture was incubated for 5 min at 99°C and 1400 rpm (thermomixer). Glass beads and cell debris were spun down and 5 μ l of the supernatant were used as template for PCR. For each 50 μ l reaction the respective volumes of the following components were mixed in a 0.2 ml tube:

28.14 μ l sterile water
 5 μ l 25 mM MgCl₂
 5 μ l 10× PCR buffer
 1 μ l DMSO
 3 μ l dNTPmix (2.5 mM each)
 1.28 μ l 25 μ M forward (fw) primer
 1.28 μ l 25 μ M reverse (rev) primer
 5 μ l template DNA
 0.3 μ l Taq polymerase

5.1.5.2. Proof-reading PCR for cloning

Proof-reading PCR was carried out using Herculase[®] II or a 2:1 mixture of Taq polymerase and Vent Polymerase. Pipetting schemes are shown in Table 5.

Table 5 | Proof-reading PCR

	Herculase [®]	Taq/Vent mixture
sterile water	32 μ l	33.4 μ l
polymerase buffer	10 μ l 5×	5 μ l 10×
25 mM MgCl ₂	0	2.5 μ l
dNTP mix (2.5 mM each)	5 μ l	5 μ l
25 μ M fw primer	0.5 μ l	1 μ l
25 μ M rev primer	0.5 μ l	1 μ l
template DNA	1 μ l	1 μ l
polymerase	1 μ l	0.6 μ l

5.1.6. Extraction and ethanol precipitation of nucleic acids

In this study, DNA and RNA for various purposes have been purified via classical phenol-chloroform extraction (Sambrook & Russell, 2001). Simple extraction was done by addition of one volume of phenol/chloroform/isoamylalcohol (PCI) (25:24:1) (pH acidic for RNA extraction) to the sample, vortexing 10 s, and centrifuging 5 min at full speed and 4°C in a microfuge. For nucleic acids of higher purity, three rounds of extraction were performed, the first with phenol only, the second with the PCI mix, and the third with chloroform only.

Subsequently, nucleic acids were precipitated by adding 0.1 volumes of 3 M sodium acetate pH 5.2 and 2.2 volumes of ethanol to the sample, which was then incubated at -20°C for 30 min to complete precipitation before being centrifuged for 10 min at maximum speed in a microfuge at room temperature. After removal of the supernatant, the pellet was washed once in 70% (v/v) ethanol and dried for about 15 min at room temperature. It was then dissolved in water or a buffer used for subsequent reactions.

5.1.7. RNA extraction for Northern Blots

For Northern Blots from yeast total RNA (section 5.1.9), a modified protocol was used for RNA extraction (Cross & Tinkelenberg, 1991). 200 μl small glass beads, 400 μl PCI mix, and 500 μl Cross buffer 1 were added to frozen cell pellets in 1.5 ml safe-lock tubes. Tubes were incubated on a vibrax for 10 min at 2000 rpm, centrifuged (5 min at maximum speed and 4°C), the supernatant was transferred to new tubes and ethanol precipitated.

Cross buffer 1

0.3 M NaCl
10 mM Tris/HCl pH 7.5
1 mM EDTA pH 8.0
0.2% (w/v) SDS

5.1.8. Sequencing of DNA

DNA samples were sent to MWG Biotech for sequencing in a concentration of 150 ng/ μl .

5.1.9. Northern Blot

5.1.9.1. Capillary transfer

Transfer of RNAs onto positively charged membranes (Northern Blot) was performed essentially as described (Sambrook & Russell, 2001). Purified RNA was loaded onto a 1.2% denaturing agarose gel, which was run at 80 V for about 4 h.

The gel and a piece of positively charged membrane were equilibrated 10 min in water and 10 min in $10\times$ SSC, then the capillary transfer sandwich was assembled in a buffer reservoir containing $10\times$ SSC (from bottom to top): gel tray (upside down), one layer Whatman 3MM paper (bridge to buffer reservoir), one layer Whatman 3MM paper in the size of the gel, the membrane, the gel with pockets oriented downwards, three layers Whatman 3MM paper, a 10 cm stack of paper towels, and a glass plate with a filled 1 l bottle on top. After blotting overnight at

room temperature, the sandwich was disassembled, the membrane was shaken 1 min in 2× SSC, dried at room temperature, and crosslinked with UV light (30 s 1200 μJ/cm²). To control for efficient transfer, the membrane was stained with methylene blue, destained with water, dried and stored at room temperature.

10× MOPS buffer

0.2 M MOPS pH 7.0
20 mM sodium acetate
10 mM EDTA pH 8.0

Methylene blue solution

0.4 M sodium acetate
0.4 M acetic acid
0.2% (w/v) Methylene blue

1.2% denaturing agarose gel (150 ml)

1.8 g agarose
131.5 ml DEPC-treated water
(boil, cool to ≈60°C)
3.5 ml 37% formaldehyde
15 ml 10× MOPS

RNA loading dye

50% (v/v) glycerol
1 mM EDTA pH 8.0
few grains Bromophenol blue
few grains Xylene cyanol FF

5.1.9.2. Synthesis of radiolabeled probes

25 ng PCR product comprising a fragment of the gene of interest were used for labeling with α-[³²P]-dCTP. The procedure was carried out with a commercial kit following the manufacturer's protocol.

5.1.9.3. Hybridization

Before actual hybridization, the dried membrane was pre-hybridized with 8.7 ml pre-hybridization solution per 100 cm² membrane for at least one hour at 65°C in a hybridization oven. Subsequently, radiolabeled probe was added and hybridized to the membrane overnight at 65°C in a hybridization oven. The membrane was washed twice briefly in 2× SSC, 0.1% SDS, twice for 20 min in 0.5× SSC, 0.1% SDS at 43°C and once briefly in 3 mM Tris/HCl pH 8.0, before being exposed to a PhosphorImager screen overnight and analyzed with a Typhoon™ imager.

20× Scp

2 M NaCl
0.6 M Na₂HPO₄
0.02 M EDTA
adjust pH to 6.2 (HCl)
autoclave
store @ RT

Scp/Sarc/DS

20 g dextran sulfate
60 ml 20× Scp
ad 101 ml DEPC-treated water
(heat gently)
7 ml 30% (v/v) sodium-lauroyl-sarcosine
store @ RT

Pre-hybridization solution

0.46 volumes DEPC-treated water
0.54 volumes Scp/Sarc/DS
0.0046 volumes 10 mg/ml herring sperm DNA

5.1.10. Mapping of 2'-O-methylated nucleotides and Ψ residues

Primer extension was performed to map 2'-O-methylated nucleotides and pseudouridine (Ψ) residues essentially as described before (Ganot et al., 1999;

Massenet et al., 1999), with some modifications. First, total RNA was extracted from a logarithmically growing yeast culture as described in section 5.1.7.

5.1.10.1. Reaction of RNA with CMC

10 μg of dried total RNA were used for reaction with *N*-cyclohexyl-*N'*- β -(4-methylmorpholinium)-ethylcarbodiimide *p*-tosylate (CMC) as described (Bakin & Ofengand, 1993). In brief, 30 μl CMC buffer were added to the RNA, and the mixture was incubated for 20 minutes at 37°C (water bath). The reaction was stopped by addition of 100 μl buffer A and 700 μl 100% ethanol. Samples were incubated 5 minutes in a pre-cooled metal block at -80°C to precipitate RNA, before being centrifuged 5 min at full speed and 4°C in a microfuge. The pellet was washed once with 70% ethanol, and the precipitation with buffer A and ethanol was repeated once. Then, the pellet was air-dried and dissolved in 40 μl 50 mM SCB buffer, and incubated for 3 hours at 37°C. After precipitation of the RNA with buffer A and ethanol, the pellet was washed twice with 70% ethanol, air-dried and dissolved in 20 μl DEPC-treated water.

CMC buffer

170 mM CMC
50 mM Bicine pH 8.3
4 mM EDTA pH 8.0
7 M Urea

SCB buffer pH 10.4

8 ml 0.1 M Na_2CO_3
2 ml 0.1 M NaHCO_3
10 ml DEPC-treated water

Buffer A

300 mM sodium acetate pH 5.3
0.1 mM EDTA pH 8.0

5.1.10.2. Primer extension

Primer extension was performed in 20 μl samples with a Thermocycler. 5 μg RNA preparation (either total or CMC-treated RNA) were diluted with DEPC-treated water to a final volume of 9 μl . 2 μl of 10 μM 5'-FAM labeled primer (see section 4.4.1.2) were added, and samples were incubated 5 minutes at 70°C and subsequently cooled to 4°C. After addition of 4 μl 5 \times reaction buffer, 2 μl nucleotide mix, 1 μl RNasin, and 5 minutes at 37°C, 2 μl M-MuLV reverse transcriptase were added, and the complete extension reaction mixes were incubated for one hour at 42°C, before being heat-inactivated (10 min at 70°C). Different nucleotide mixtures were used for mapping of Ψ residues, ribose-methylated nucleotides, and sequencing ladders. For Ψ detection, a standard 2.5 mM each dNTP mix was used. For detection of 2'-O-methylations, dNTPs were used at a concentration of 0.004 mM each (positive control reaction: 1 mM each

dNTP; Maden et al., 1995). For sequencing ladders, dNTP/ddXTP mixtures were used, with three dNTPs at 2.5 mM each, the fourth at 1.6 mM plus 0.9 mM of the corresponding ddNTP.

With the reactions completed, 180 μ l DEPC-treated water, 20 μ l 3 M sodium acetate pH 5.2, and 440 μ l ethanol were added to the samples, DNAs were precipitated for at least two hours at -20°C, centrifuged, washed with 70% (v/v) ethanol, and the resulting pellet was taken up in 10 μ l loading buffer without dyes (bromophenol blue and xylene cyanol quench fluorescence).

Loading buffer

50% (v/v) formamide
5 mM EDTA pH 8.0

5 \times reaction buffer

provided with M-MuLV RT

5.1.10.3. Electrophoresis

Samples were loaded onto a 17 \times 40 cm 7% denaturing sequencing gel with 1 \times TBE as running buffer. Before loading, the gel was pre-run for one hour at 3000 V and 45 W to warm it up. The actual run was performed for about 80 minutes at 3000 V and 45 W. Gels were analyzed with a Typhoon™ imager.

7% denaturing sequencing gel (50 ml)

21.0 g Urea (fluorescence-free)
8.75 ml 40% Acrylamide/Bisacrylamide (19:1) (fluorescence-free)
5 ml 10 \times TBE
50 μ l TEMED
120 μ l 10% (w/v) APS
water ad 50 ml

5.2. Biochemical methods

5.2.1. SDS-PAGE

Sodium dodecyl sulfate polyacrylamide gel electrophoresis (SDS-PAGE) was carried out as described (Sambrook & Russell, 2001), routinely using 8%-12% polyacrylamide mini-gels (PAGs). For separation of purified complexes (e.g. TAP, see section 5.2.5) and mass spectrometry (MS), precast 4-12% Bis-Tris gradient gels were used.

Standard gels were run at 25 mA and 150 V, gradient gels according to the manufacturer's manual.

Gels were routinely stained with Coomassie Blue (Sambrook & Russell, 2001), gradient gels with Colloidal Blue, and for maximal sensitivity silver staining was used.

4× Lower Tris

1.5 M Tris
0.4% (w/v) SDS
adjust pH to 8.8
store @ RT

10× Tris glycine electrophoresis buffer

250 mM Tris
1.9 M Glycine
1% (w/v) SDS
store @ RT

Coomassie staining solution

0,25% (w/v) Coomassie Brilliant Blue R-250
0.1% (w/v) Coomassie Brilliant Blue G-250
30% (v/v) ethanol
10% (v/v) acetic acid
store @ RT

4× Sample Loading Buffer

0.2 M Tris pH 6.8
40% (v/v) glycerol
8% (w/v) SDS
0.43 M β -mercaptoethanol
few grains Bromophenol Blue
store aliquots @ -20°C

4× Upper Tris

0.5 M Tris
0.4% (w/v) SDS
adjust pH to 6.8
store @ RT

20× MOPS electrophoresis buffer

1 M MOPS
1 M Tris
2% (w/v) SDS
10 mM EDTA
store dark @ RT

Coomassie destaining solution

30% (v/v) ethanol
10% (v/v) acetic acid
store @ RT

5.2.2. Denaturing protein extraction

Denaturing protein extraction from yeast cells was carried out essentially as described (Knop et al., 1996). In brief, a small amount of cells from plate was suspended in 1 ml cold water, 150 μ l of pre-treatment solution were added, and the mixture was incubated for 15 min on ice. After addition of 150 μ l 55%(v/v) trichloroacetic acid (TCA) and a further 10 min incubation on ice, tubes were centrifuged for 10 min at maximum speed at 4°C in a microfuge. The supernatant was discarded completely, cells were resuspended in 100 μ l buffer HU (and neutralized with 1 M Tris base, if indicator turned yellow) and incubated for 10 min at 65°C and 600 rpm in a thermomixer. After 5 min centrifugation at maximum speed, the supernatant was loaded onto a PAG.

Buffer HU

5% (w/v) SDS
0.2 M (4 ml 0.5 M) Tris pH 6.8
8 M (4.8 g) Urea
0.2 M β -mercaptoethanol
1 mM EDTA pH 8.0
few grains Bromophenol Blue
store aliquots @ -20°C

pre-treatment solution

7.5%(v/v) β -mercaptoethanol
1.85 M NaOH
store aliquots @ -20°C

5.2.3. Western Blot

5.2.3.1. Protein transfer

To detect proteins on SDS-PAGs, the stacking gel was removed after the course, and the gel was equilibrated for ≥ 10 min in 1× blotting buffer. A sandwich consisting of (from bottom to top) three layers Whatman 3MM paper soaked with 1× blotting buffer, equilibrated PVDF membrane, equilibrated SDS-PAG, and three layers Whatman 3MM paper soaked with 1× blotting buffer was assembled in a semidry blotting device. To equilibrate the PVDF membrane, it was plunged briefly in methanol, incubated 5 min in water and ≥ 10 min in 1× blotting buffer. Proteins were transferred either at 1.0 mA/cm² for 2 h or overnight at 5 V. Successful transfer was controlled by Ponceau S staining.

5.2.3.2. Protein detection

After blotting, the membrane was blocked for at least 1 h in 1× PBS, 5% (w/v) milk powder. Antibody incubations were done in 1× PBST, 0.5% milk powder. Usually, the membrane was shrink-wrapped and incubated for 3 h at room temperature or overnight at 4°C with the primary antibody, and 1 h at room temperature with the secondary antibody, respectively. After each antibody incubation, the membrane was washed three times with 1× PBST, 0.5% milk powder.

Signals were detected using a chemiluminescence kit and either films or a fluorescent image reader.

Table 6 | Antibody combinations for Western blots used in this study.

primary antibody	dilution	secondary antibody	dilution
mouse α - actin	1:1000	HRP goat α -mouse	1:5000
mouse α -myc (9E10)	1:1000	HRP goat α -mouse	1:5000
PAP	1:2000	–	–
rabbit α -She2	1:1000	HRP goat α -rabbit	1:5000
rat α -HA (3F10)	1:1000	HRP goat α -rat	1:5000
rat α -tubulin	1:1000	HRP goat α -rat	1:5000

5.2.4. Sucrose density gradient centrifugation

5.2.4.1. Preparation of total RNA from yeast

To collect UV profiles of ribosomal RNA, total RNA was isolated from yeast cells under low-salt conditions as described (Baßler et al., 2001). An overnight culture of the respective yeast strain was diluted and grown in full medium to $OD_{600} \approx 0.5$. 50 ml of the culture were transferred to a tube, cycloheximide (CHX, 10 mg/ml) was added to a final concentration of 0.1 mg/ml, and the tube was incubated for 10 min at 30°C in a water bath. Cells were centrifuged, suspended in 500 µl polysome buffer supplemented with 0.1 mg/ml CHX, 1 mM DTT, and 5 U Suprase-In, transferred to a 1.5 ml tube containing 250 µl small glass beads, and lysed by incubating 5 min on a vibrax (2000 rpm, 4°C). After centrifugation (5 min, maximum speed, 4°C) in a microfuge, the clear supernatant was transferred to a new tube, RNA concentration was measured, and 250–500 µg were loaded onto linear sucrose gradients.

10× polysome buffer

200 mM HEPES/KOH pH 7.5
750 mM KCl
25 mM MgCl₂
10 mM EDTA pH 8.0
adjust pH to 7.5
filter sterilize

5.2.4.2. Preparation of gradients

Linear 7–47% (w/v) sucrose gradients were prepared in SW40 tubes with a Gradient Master™ gradient making station (BioComp). Tubes were filled to a defined mark with light (7%) sucrose solution, then heavy (47%) sucrose solution was added at the bottom of the tube using a syringe.

Light sucrose solution

1× polysome buffer
7% (w/v) sucrose
1 mM DTT
0.1 mg/ml CHX

Heavy sucrose solution

1× polysome buffer
47% (w/v) sucrose
1 mM DTT
0.1 mg/ml CHX

5.2.4.3. Collection of UV profiles and fractionation

Loaded gradients were centrifuged for 2 h at 38000 rpm and 4°C in a SW40 swing-out rotor. UV profile collection and fractionation was done with a Piston Gradient Fractionator™ (BioComp). UV profiles were collected measuring absorption at 254 nm (A_{254}) at a sensitivity of 0.1 with WINDAQ software. Facultative fractionation was carried out with a fraction size of 0.2 min/tube (piston speed: 0.29), yielding approx. 15 fractions per gradient.

5.2.5. Tandem affinity purification

Tandem affinity purification (TAP) was carried out after tagging the respective ORF with the TAP-tag at the N- or C-terminus (see section 5.4.3) according to the original protocol (Puig et al., 2001; Rigaut et al., 1999), with some modifications.

5.2.5.1. Yeast culture

Cells were grown in 2 l YPD to late logarithmic phase ($OD_{600} \approx 3.5$), harvested by centrifugation, washed once with water and frozen in 50 ml tubes in liquid nitrogen for storage at -80°C .

5.2.5.2. Cell lysis

Pellets were thawed on ice, and one pellet volume of lysis buffer (LB), supplemented with protease inhibitors, was added. After addition of two pellet volumes of small glass beads, cells were lysed using a bead beater (3×4 min, 510 rpm). Glass beads were removed by filtering, and the cell lysate was pre-cleared by centrifugation at 3000 g and 4°C for 10 min, transferred to SW32 tubes and centrifuged for 1 h at 100,000 g (27000 rpm, SW32 swing out rotor). If the protein of interest pelleted under these conditions, centrifugation was done at 60,000 g or 20,000 g, respectively. Following centrifugation, the fatty top layer was removed with a water jet pump. The clear supernatant was transferred to a 50 ml tube, and frozen in liquid nitrogen after addition of glycerol to 5% (v/v).

5.2.5.3. Purification

For routine purifications, 200 μl packed IgG sepharose beads and 250 μl of Calmodulin beads were used. Beads were equilibrated in cold LB (for Calmodulin beads supplemented with 2 mM CaCl_2 and 1 mM DTT), and IgG beads were added to the thawed cell lysate. After a 1 h slow rotation at 4°C , beads were spun down and transferred to prepared Mobicols, and washed with 10 ml LB + 0.5 mM DTT. To cleave protein complexes bound to the resin, Tobacco etch virus (TEV) protease was added (4 μl 1 mg/ml in 150 μl LB + 0.5 mM DTT) to the beads, and the mixture was incubated 2 h at 16°C with rotation. Spinning for 1 min at 2000 rpm and 4°C in a microfuge eluted cleaved complexes. 150 μl of this eluate was transferred to a second Mobicol containing equilibrated Calmodulin beads, mixed and rotated for 1 h at 4°C . After washing the beads with 15 ml LB + 2 mM CaCl_2 , purified protein complexes were eluted by a 10 min incubation with elution buffer and subsequent centrifugation. To increase protein concentration, proteins were precipitated by

addition of trichloroacetic acid ($c_f=10\%$ (v/v), 15 min on ice). Pellets were collected by centrifugation and dissolved in 1× SDS sample loading buffer (section 5.2.1).

10× TAP lysis buffer (LB)

1 M NaCl
0.5 M Tris
15 mM MgCl₂
1.5% (v/v) IGEPAL CA-630
store @ 4°C

Elution buffer

10 mM Tris/HCl pH 8.0
5 mM EGTA pH 8.0
prepare freshly

5.2.6. Preparation of glass beads for cell lysis

Glass beads with a diameter of 0.4 to 0.6 mm were plunged into a 5 l flask containing 1 l 0.1 M hydrochloric acid and shaken for 30 min. After several washes with water to neutralize the pH, beads were washed for 30 min with 70% (v/v) ethanol. Beads were then briefly washed with 95% ethanol, dried completely, and autoclaved in bottles.

5.3. Working with *Escherichia coli*

5.3.1. Transformation of chemical competent *Escherichia coli* TOP10

The basic principles of this widely used method are described in Sambrook & Russell, 2001.

5.3.1.1. Preparation of competent cells

Chemical competent *E. coli* TOP10 cells were prepared as described previously (Pope & Kent, 1996). In brief, 100 ml LB medium were inoculated with 1 ml of an overnight culture of *E. coli* TOP10; this culture was grown with vigorous aeration at 130 rpm and 37°C for about 3 h, until the OD₆₀₀ reached a value between 0.7 and 0.8. Then, the culture was chilled on ice for 15 min before being centrifuged for 15 min at 5000 rpm and 4°C in a GS3 rotor. Centrifugation was repeated in a SS-34 rotor after resuspension of the pellet in 50 ml ice-cold, sterile 0.1 M CaCl₂ and 30 min incubation on ice. The washed pellet was resuspended in 5 ml cold, sterile 0.1 M CaCl₂/10% (v/v) glycerol, and 50–100 µl aliquots were stored at –80°C.

5.3.1.2. Transformation of competent cells

Routinely, one aliquot of chemical competent *E. coli* cells was added to 1 µl of a diluted plasmid preparation or 10 µl ligation sample in a 1.5 ml tube. The mixture was incubated for ≥5 min on ice, plated onto selection plates and incubated overnight at 37°C (Pope & Kent, 1996).

5.3.2. Isolation of plasmids from *E. coli*

To isolate plasmids from *Escherichia coli* liquid cultures, commercial Miniprep Kits were used, following the manual provided by the manufacturer. The final elution was reduced to 30 μ l.

5.3.3. Overexpression and purification of His₆-tagged proteins

Overnight cultures of *E. coli* carrying an inducible plasmid were diluted 1:100 in the respective selection medium and incubated at 37°C and 140 rpm until they reached an OD₆₀₀≈0.6. Then, isopropyl- β -D-1-thiogalactopyranoside (IPTG) was added to a final concentration of 1 mM, and cultures were further incubated at 37°C, 140 rpm for 3 hours.

Cells were harvested by centrifugation, resuspended in lysis buffer and stored at -20°C until needed after shock-freezing in liquid nitrogen. Cells lysed by sonication, centrifuged, and the supernatant was applied to a column containing Ni-NTA agarose pre-equilibrated with respective purification buffer (PB). The column was closed and incubated for one hour at 4°C. Subsequently, excess liquid was allowed to drop out by gravity flow. The resin was washed with 5 ml PB, 1 ml PB supplemented with 1 M NaCl, 1 ml PB supplemented with 10 mM imidazole. His-tagged proteins were eluted with 800 μ l PB, 300 mM imidazole.

(example) Lysis buffer

50 mM Tris/HCl pH 7.5
500 mM NaCl
2 mM β -mercaptoethanol
1 \times Protease Inhibitor Cocktail

(example) Purification buffer (PB)

50 mM Tris/HCl pH 7.5
150 mM NaCl
2 mM β -mercaptoethanol

5.3.4. *in vivo* RNA chaperone assay

To test a possible RNA chaperone activity of Loc1, I tried to establish an assay using a ribozyme folding trap as described (Prenninger et al., 2006).

5.3.4.1. Preparation of *E. coli* cultures

2 ml TBYE_{Amp/Cla} were inoculated with a single colony of a strain transformed with the respective plasmids. After overnight incubation at 37°C with shaking, 100 ml TBYE_{Amp/Cla} were inoculated with 500 μ l of this culture, protein expression was induced by adding IPTG to a final concentration of 1 mM, and cells were grown to an OD₆₀₀ of approximately 0.5. Cultures were harvested by centrifugation (5 min, 2300 g, 4°C) and the pellet was resuspended in 1 ml TM buffer. The suspension was transferred to 1.5 ml tubes, spun down, and the pellet was stored at -80°C.

5.3.4.2. Preparation of RNA

Pellets were suspended on ice in freshly prepared solution A, and cells were disrupted by three freeze-thaw cycles (freeze: liquid nitrogen; thaw: 30°C water bath). Subsequently, 20 µl fresh solution B were added and the mixture was incubated for 45-60 min on ice. After addition of 20 µl solution C and 5 min at room temperature, 200 µl phenol were added, and highly pure RNA was extracted as described in section 5.1.6.

TM buffer

10 mM Tris/HCl pH 7.0

10 mM MgCl₂

Solution A

150 µl TE (10/1)

1.5 µl 1 M DTT

0.75 µl RNasin

4 µl 10 mg/ml lysozyme

0.75 µl DEPC-treated water

Solution B

4 µl 1 M magnesium acetate

3.5 µl RQ1 DNase

0.1 µl RNasin

12.4 µl DEPC-treated water

Solution C

0.1 M acetic acid

5% (w/v) SDS

5.3.4.3. Poisoned primer assay

1 µl 4.5× hybridization buffer and 1 µl (5 pmol) end-labeled NBS-2 primer were added to 10 µg total RNA in a volume of 2.5 µl. The mixture was heated to 95°C for 1 minute, then slowly cooled down to 42°C in a PCR block (11s/°C). Following addition of 2.3 µl extension mix, samples were incubated at 42°C for one hour. Then, extension was stopped by adding 7 µl 2× stop solution and 60 µl 100% ethanol, and nucleic acids were precipitated at -20°C. After centrifugation (20 min, 16000 rpm, 4°C), pellets were resuspended in 5 µl loading dye and loaded onto a 12% TBE/7 M Urea PAG, which was run at 35 mA and 50W until the bromophenol blue band reached the bottom. Bands were visualized with a Typhoon reader.

Hybridization buffer

225 mM HEPES/KOH pH 7

450 mM KCl

Extension mix

0.67 µl 10× extension buffer

0.33 µl poisoned dNTP mix

0.3 µl AMV reverse transcriptase

1 µl sterile water

2× Stop solution

300 mM sodium acetate

10 mM EDTA pH 8.0

10× Extension buffer

500 mM Tris/HCl pH 8.0

50 mM MgCl₂

50 mM DTT

Poisoned dNTP mix

3 µl each of 10 mM dATP, dCTP, dGTP, dTTP

25 µl 5 mM ddTTP

TBE loading dye

1× TBE

7 M urea

few grains bromophenol blue & xylene cyanol FF

5.4. Yeast techniques

5.4.1. Dot test

Dot tests are widely used to assay growth of yeast clones on e.g. different selective media or different temperatures (in the case of temperature sensitive mutants). The test was carried out as follows. Cells were suspended in 1 ml sterile medium and OD₆₀₀ was adjusted to 0.2. From this suspension, a 1:10 dilution series was prepared with medium. 10 µl of each dilution were then dropped onto respective selection plates.

5.4.2. Transformation of plasmids into yeast

Transformation of yeast strains with plasmids amplified in *E. coli* was carried out as described (Chen et al., 1992). In brief, a small amount of cells was scraped off a plate, suspended in 1 ml sterile water, and spun down. The pellet was resuspended in 100 µl one-step buffer and vortexed vigorously, before 10 µl salmon sperm DNA (2 mg/ml) supplemented with ≥100 ng of plasmid DNA was added. The mixture was incubated for 30 min at 45°C (temperature sensitive strains 25 min room temperature, 5 min 37°C). Then, 1 ml full medium was added, cells were spun down, resuspended in medium and plated onto respective selection plates.

One-step buffer

0.2 M lithium acetate
40% (w/v) PEG 4000
0.1 M DTT
filter sterilize
store aliquots @ -20°C

5.4.3. Gene disruption and epitope-tagging

To disrupt genes or tag genes of interest with epitopes at the C- or N-terminus, homologous recombination of PCR products was used (Baudin et al., 1993).

5.4.3.1. Preparation of competent cells

The applied protocol is described in detail in Knop et al., 1999. In brief, 50 ml of medium were inoculated with the respective strain, grown to an OD₆₀₀ of 0.5 to 0.7 at 30°C, and harvested by centrifugation at 2000 g for 5 min. All centrifugations were carried out at room temperature. Cells were washed once with 0.5 volumes sterile water and once with 0.1 volumes LitSorb. Subsequently, the pellet was resuspended in 360 µl LitSorb, and 40 µl of salmon sperm DNA, which had been denatured for 10 min at 100°C and rapidly cooled down on ice before. After

mixing, 50 µl aliquots are stored at -80°C (without shock-freezing in liquid nitrogen).

TELit pH 8.0

0.1 M lithium acetate
10 mM Tris pH 8.0
1 mM EDTA pH 8.0
adjust pH to 8.0 (acetic acid)
autoclave
store @ RT

LitSorb

1 M Sorbitol
ad 50 ml TELit pH 8.0
filter sterilize
store @ RT

5.4.3.2. Transformation

For transformation of plasmid DNA, 10 µl of competent cells were used, whereas 50 µl were used for transformation of PCR products. The DNA was placed in 1.5 ml tubes (2 µl plasmid DNA and 10 µl PCR product, respectively) prior to addition of the thawed competent cells. After thorough mixing, 6 volumes LitPEG were added to the samples, which were then, after again mixing them well, incubated for 30 min at room temperature. 1/9 volume DMSO was added before placing the cells for 15 min in a water bath at 42°C (temperature sensitive strains: 5 min at 37°C). Cells were centrifuged at 2000 rpm in a microfuge, resuspended in 100 µl medium, and plated onto selection plates. With this method, it was possible to disrupt genes, tag genes at the C-terminus and at the N-terminus (under control of heterologous promoters) with published marker cassettes (e.g. Janke et al., 2004; Knop et al., 1999; Puig et al., 2001; Wach et al., 1997; Wach et al., 1994). For N-terminal tags under the control of the endogenous promoter, a second step had to be carried out. After tagging, cells were transformed with a plasmid expressing *cre* recombinase (Güldener et al., 1996), that can use loxP sites in tagging cassettes to loop out the heterologous promoter and selection marker (Gauss et al., 2005; Puig et al., 2001).

LitPEG

40% (w/v) PEG 3350
ad 50 ml TELit pH 8.0
filter sterilize
store @ 4°C

5.4.4. Mating of yeast strains

To mate two haploid yeast strains, an equal amount of cells of either strain from overnight cultures was transferred to a 1.5 ml tube containing 1 ml YPD. After mixing and several hours incubation at 30°C without shaking, cells were spun down, washed with water, and spread onto plates selecting for diploids.

5.4.5. Sporulation and tetrad dissection

To sporulate a diploid strain, a single colony from a fresh plate was transferred directly onto a sporulation plate (see section 4.5.2). For strains that are difficult to sporulate (e.g. BY background), a colony was streaked out onto a presporulation plate, which was incubated overnight at 30°C. Subsequently, one inoculation loop of cells was streaked out onto a sporulation plate or used to inoculate 2 ml of sporulation medium. Sporulation was monitored with a light microscope.

For dissection of tetrads, a small amount of sporulated cells was suspended in 100 µl sterile water. 10 µl of 5 mg/ml Zymolyase 20T solution in 1 M sorbitol was added, and after 5 min incubation at 30°C (water bath) 5 µl of the suspension were carefully dropped on the top left side of a rich medium plate. The drop was allowed to run down the plate and dry, and tetrads were dissected using a tetrad microscope.

5.4.6. *in vivo* pulse labeling

Pulse labeling of RNA was carried out as described (Ferreira-Cerca et al., 2005). In brief, 3 ml of a logarithmic yeast culture were pelleted and resuspended in 1 ml prewarmed YPD containing 20 µCi 5', 6'-[³H] -uracil (Amersham) and incubated for 15 min at 30°C. Cultures were rapidly cooled down in ice-water, pelleted, and RNA was extracted by three rounds phenol-chloroform extraction (phenol only, phenol/chloroform/isoamylalcohol 25:24:1, and chloroform only). After ≥ 1 h ethanol precipitation RNA was dissolved in 50% deionized formamide with dyes (bromophenol blue and xylene cyanol FF). Quality and amount of the RNA were checked on a 1% TAE agarose gel, incorporated radioactivity by scintillation counting, then equal amounts of radioactivity were loaded onto a denaturing agarose gel (section 5.1.9.1). Northern Blot was performed as described above, and signals were visualized using a PhosphorImager Screen.

5.4.7. Time course for combined Western/Northern Blot

In order to follow *ASH1* expression on RNA and protein level, a time course with galactose-inducible strains and subsequent Northern and Western blot analysis was performed.

Strains were grown overnight in raffinose-containing medium, diluted to 100 ml $OD_{600}=0.3$ and grown to $OD_{600}=0.8-1.0$ at 30°C. Before *ASH1* expression was induced by adding 20% (w/v) galactose to a final concentration of 4%, 2 50 ml tubes per strain and time point were filled with 20 ml ice and chilled on ice. An equal number of 2 ml safe-lock tubes were chilled on ice as well. For each strain and time point, two times 20 OD_{600} were harvested in the ice-containing 50 ml tubes (3 min, 3600 rpm, 4°C). Supernatant and residual ice was discarded, pellets were resuspended in 1 ml ice-cold water, transferred to the 2 ml tubes, spun down, snap-frozen in liquid nitrogen, and stored at -80°C.

To extract proteins for Western blotting, pellets were suspended in 400 μ l breaking buffer, and the cells were lysed twice for 4 minutes on a vibrax with 2 minutes pause on ice after addition of 200 μ l glass beads. Piercing the bottom of the tubes with a hot 25G needle and centrifuging them in 15 ml tubes removed cell debris. The clear lysate was transferred to 1.5 ml tubes and centrifuged for 15 minutes at maximum speed in a microfuge at 4°C. Protein concentration was determined photometrically, and 1 OD_{280} was loaded onto a SDS-PAGE. Transfer and antibody incubation were performed as described above (section 5.2.3).

Extraction of RNA and Northern blotting was performed as described in sections 5.1.7 and 5.1.9, respectively.

Breaking buffer

50 mM Tris/HCl pH 7.5

1 mM EDTA pH 8.0

20 mM DTT

1× Protease Inhibitor Cocktail

5.4.8. Long-term storage of cultures

To store yeast cultures for longer periods, 1 ml of a cell suspension was mixed with 0.5 ml 50% (v/v) sterile glycerol in a labelled storage tube (with screw cap and air-tight gasket) and stored at -80°C. For bacterial cultures, the procedure was performed in the same way (see Sambrook & Russell, 2001).

5.5. Microscopy

5.5.1. Live cell imaging

5.5.1.1. GFP

Yeast cells from a plate (of a strain with a GFP-tagged protein) were grown overnight in liquid medium, diluted to $OD_{600}=0.2$ and grown to $OD_{600}\approx 0.8$. 1 ml of the culture was transferred to a 1.5 ml tube, centrifuged, and resuspended in 100 – 200 μ l minimal medium to reduce autofluorescence. To immobilize cells on the slide, agarose (approx. 2% (w/v)) was dissolved in minimal medium by heating and dropped onto 3-well-slides which were immediately covered with a plain slide to distribute the agarose evenly as a slim layer over the wells. After removal of the plain slide, 5 μ l of the concentrated cell suspension were dropped onto the agarose in the wells, covered with a cover slip, and analyzed under the microscope (filter: GFP BP or FITC).

5.5.1.2. Calcofluor White

The protocol for Calcofluor White staining was adapted from a published one (Ni & Snyder, 2001). In brief, a diluted overnight culture was grown to $OD_{600}\approx 4.0$. 1 ml of the culture was transferred to a 1.5 ml tube, centrifuged, washed once with 1 \times PBS, and resuspended in 1 ml 1 \times PBS containing 2 μ g/ml Calcofluor White. After a 10-minute incubation at room temperature, cells were washed three times with 1 \times PBS, resuspended in 100 – 200 μ l 1 \times PBS, and 5 μ l were spotted onto agarose-coated 3-well-slides as described above. Analysis was carried out using the DAPI filter of the microscope.

5.5.2. Indirect immunofluorescence

5.5.2.1. Preparation of slides

0.02% (w/v) poly-L-lysine was used to coat multi-well slides. After dropping the solution onto each well, slides were incubated at room temperature for 5 min and washed three times with deionized water.

5.5.2.2. Preparation of cells

Cells of respective strains were grown overnight in appropriate selective medium at the appropriate temperature, diluted to $OD_{600}\approx 0.2$, and further grown for about two generations ($OD_{600}=0.7 - 1.0$). 37% Formaldehyde was added to a final concentration of 3.7%(v/v), and after 1 h fixation cells were harvested and resuspended in 1 ml spheroplasting premix. After transfer of the suspension to 1.5

ml tubes, cells were washed twice with 1 ml spheroplasting premix and then carefully resuspended in 500 μ l spheroplasting solution. Cells were incubated at 30°C in a water bath for 15 – 60 min, centrifuged for 3 min at 3000 rpm in a microfuge, washed once with 1 ml spheroplasting premix, and resuspended carefully in 100 – 300 μ l spheroplasting premix. Aliquots were snap-frozen in liquid nitrogen and stored at –80°C.

Spheroplasting premix	Spheroplasting solution
1.2 M Sorbitol	0.1 mg lyophilized Zymolyase 100T
0.1 M PK _i pH 7.5	1 ml spheroplasting premix
0.5 mM MgCl ₂	28 mM β -mercaptoethanol
autoclave	
store @ RT	

5.5.2.3. Immunofluorescence

Immunofluorescence was carried out essentially as described (Gorsch et al., 1995). 5 μ l cell suspension was dropped onto each well. After 5 min incubation at room temperature, wells were blocked with blocking solution before applying the primary antibody (30 μ l per well, diluted in blocking solution) and incubating the slide in a humid chamber for 2 h at room temperature. The slide was washed three times with 1 \times TBS, 0.1% BSA, 0.1% (w/v) NP-40, the fluorescent secondary antibody (30 μ l per well, diluted in blocking solution) was applied and the slide was incubated 2 h in a humid chamber in the dark. After three times washing the slide with 1 \times TBS, 0.1% BSA, 0.1% NP-40, nuclei were stained by 15 min incubation at room temperature with 10 μ l DAPI solution per well. DAPI was aspirated off, 1 μ l mounting solution was pipetted onto each well, and the slide was covered with a cover slip and sealed with nail polish.

Blocking solution	Mounting solution
1 \times TBS	80% (v/v) glycerol
0.1% (w/v) BSA	1 \times PBS

Table 7 | Primary antibodies used in indirect immunofluorescence.

primary antibody	dilution in blocking solution
mouse α -HA (clone 16B12)	1:1000
mouse α -myc (clone 9E10)	1:1000
mouse α -fibrillarlin (clone 28F2)	1:2000
rabbit α -She2 (323/4, E12, #7)	1:1000
rat α -HA (clone 3F10)	1:200

Table 8 | Fluorescent secondary antibodies used in indirect immunofluorescence.

secondary antibody	dilution in blocking solution
Alexa Fluor® 488 goat α -mouse	1:250
Alexa Fluor® 488 goat α -rabbit	1:300
Alexa Fluor® 488 goat α -rat	1:100
Alexa Fluor® 594 rabbit α -mouse	1:1000

5.5.3. Fluorescent *in situ* hybridization

5.5.3.1. Preparation of Cy3-labeled *ASH1* probes

For fluorescent *in situ* hybridization (FISH) of *ASH1* mRNA, a mixture of five oligonucleotides directly labeled with Cy3 (see section 4.4.1.1) was used. A stock of the mixture was prepared with 10 μ l DEPC-treated water and 2 μ l of each oligonucleotide ($V_f=20\mu$ l, $c_{f/oligo}= 10 \mu$ M). 1 μ l of the stock mixture was diluted with 79 μ l DEPC-treated water, 10 μ l 10 mg/ml tRNA, and 10 μ l 10 mg/ml herring sperm DNA ($V_f=100\mu$ l, $c_{f/oligo}= 100$ nM). This solution was divided into 10 10 μ l aliquots, which were dried in a speed vac.

5.5.3.2. Preparation of DIG-labeled probes

IST2 mRNA and *WSC2* mRNA were detected with digoxigenin (DIG)-labeled oligonucleotides. For each mRNA, four DNA fragments (each approx. 250 bp) spanning the complete ORF were amplified by PCR (see section 5.1.5), purified with a PCR purification kit, phenol-chloroform-extracted and precipitated in 100% ethanol for ≥ 2 h. Subsequent labeling with DIG-UTP was carried out with roughly 1 μ g of each concentrated PCR product as template for *in vitro* transcription with T7 MEGAscript™ kit according to the manufacturer's protocol. Labeled RNA was purified first through mini Quick Spin™ RNA columns, then by three rounds of phenol-chloroform extraction (phenol only, phenol/chloroform/isoamylalcohol 25:24:1, and chloroform only) before overnight precipitation in 100% ethanol. The pellet was resuspended in 15 μ l DEPC-treated water, and 10 μ l aliquots containing ≈ 125 ng of each probe (500 ng in total) were stored at -80°C .

5.5.3.3. Preparation of cells

Cells were grown and fixed as described above (section 5.5.2.2). After harvesting, cells were resuspended in 1 ml buffer B, transferred to a 1.5 ml tube, and washed three times with 1 ml buffer B. The pellet was then resuspended carefully in 250 μ l

freshly prepared Oxalyticase solution, incubated for 10 min at 30°C in a water bath, washed once in 1× buffer B and finally resuspended in 100 – 200 µl buffer B on ice. 5 to 10 µl of the spheroplast suspension was spotted per well on poly-L-lysine coated slides (see section 5.5.2.1). Following a 30 min incubation on ice, the suspension was diluted with one large drop of 1× buffer B, aspirated off with a water jet pump, and plunged into a jar containing 70% ethanol pre-cooled to –20°C for storage at –20°C.

1× Buffer B

1.2 M Sorbitol
0.1 M PK_i pH 7.5
autoclave
store @ RT

Oxalyticase solution

0.1 mg lyophilized oxalyticase
720 µl buffer B
100 µl 200 mM Ribonucleoside Vanadyl complex
3.5 µl 5 mM AEBSF
3 µl RNasin
2 µl 1 M DTT
ad 1 ml DEPC-treated water

5.5.3.4. *in situ* hybridization with Cy3-labeled probes

For hybridization, two probe aliquots per slide are needed. The protocol was adapted from Long et al., 1997. 15 µl hybridization solution 1 were added to each tube at room temperature, and after 3 min incubation at 80°C and 300 rpm and addition of 15 µl hybridization solution 2 on ice, the tubes were spun for 15 min at maximum speed and 4°C. Cells were rehydrated 5 min in 2× SSC and 5 min in 2× SSC, 40% formamide, before 5 µl probe were transferred to each well. The slide was covered with a cover slip and incubated overnight at 37°C in a dark humid chamber.

Slides were washed subsequently twice for 15 min in prewarmed 2× SSC, 40% formamide at 37°C, in 2× SSC, 0.1% Triton X-100 at room temperature, and in 1× SSC, also at room temperature. DAPI-staining of nuclei and mounting was carried out as described above (section 5.5.2.3).

Hybridization solution 1

49.3 µl formamide
0.63 µl 1 M PNa_i
11.7 µl DEPC-treated water

Hybridization solution 2

12.3 µl 20 mg/ml BSA
36.2 µl DEPC-treated water
12.3 µl 20× SSC
0.75 µl RNasin

5.5.3.5. *in situ* hybridization with DIG-labeled probes

Hybridization of spheroplasts with DIG-labeled probes against IST2 mRNA and WSC2 mRNA, respectively, was performed as described previously (Münchow et al., 1999). Cells were rehydrated for 5 min in 5× SSC, pre-hybridized with 40 ml HybMix in a jar for 1 h at room temperature, before 20 µl probe diluted 1:20 in

HybMix ($c_i=5$ ng/ μ l) were dropped onto each well. The slide was covered with a cover slip and incubated overnight at 37°C in a dark humid chamber.

Subsequently, slides were washed once with prewarmed 2×SSC, 40% formamide at 37°C and twice with blocking solution at room temperature (all washes 15 min, \approx 80 rpm). Incubation with the primary antibody (mouse α -DIG, dilution 1:250) was done for 2 h. All antibody incubations were done at room temperature in a dark humid chamber, and antibodies were diluted in blocking solution. After three 1 min washes with 1× PBS, 0.1% BSA, the slides were incubated with the secondary antibody (Alexa Fluor® 488 rabbit α -mouse IgG, dilution 1:2000) for 1 h. The tertiary antibody (Alexa Fluor® 488 goat α -rabbit IgG, dilution 1:10000) was applied for 1 h after three 1 min washes with 1× PBS, 0.1% BSA. Following three final washes, DAPI staining and mounting were carried out as described above.

HybMix

50%(v/v) formamide
5× SSC
5 mM (0.4 ml 0.5 M) EDTA pH 8.0
0.1% (v/v) Tween-20
1× Denhardt's
0.1% (0.4 ml 10%) CHAPS
0.1 mg/ml herring sperm DNA
0.1 mg/ml heparin
ad 40 ml DEPC-treated water

Blocking solution

1× PBS
10% fetal calf serum (FCS)
0.1% (v/v) Triton X-100
ad 100 ml DEPC-treated water

50× Denhardt's reagent

1% (w/v) BSA
1% (w/v) Ficoll
1% (w/v) polyvinylpyrrolidone (PVP)

5.5.4. Statistical analysis

For experiments where statistical analysis was necessary, at least 100 cells were counted in independent experiments. Counting was performed double blind, i.e. without knowing strain identities. To evaluate statistical significance, P values were determined using chi-square (χ^2) tests (Preacher, 2001).

Deswegen sind Bücher willkommen, die uns sowohl das neu empirisch aufgefundene als die neu beliebten Methoden darlegen.

Johann Wolfgang Goethe, *Maximen und Reflexionen* 427.

6. References

Adams A (1998) *Methods in yeast genetics : a Cold Spring Harbor Laboratory course manual*, 1997 edn. Cold Spring Harbor, N.Y.: Cold Spring Harbor Laboratory Press.

Adams CC, Jakovljevic J, Roman J, Harnpicharnchai P, Woolford JL, Jr. (2002) Saccharomyces cerevisiae nucleolar protein Nop7p is necessary for biogenesis of 60S ribosomal subunits. *RNA* **8**(2): 150-165

Aguilera A, Klein HL (1990) HPR1, a novel yeast gene that prevents intrachromosomal excision recombination, shows carboxy-terminal homology to the Saccharomyces cerevisiae TOP1 gene. *Mol Cell Biol* **10**(4): 1439-1451

Altschul SF, Madden TL, Schaffer AA, Zhang J, Zhang Z, Miller W, Lipman DJ (1997) Gapped BLAST and PSI-BLAST: a new generation of protein database search programs. *Nucleic Acids Res* **25**(17): 3389-3402

Altschul SF, Wootton JC, Gertz EM, Agarwala R, Morgulis A, Schaffer AA, Yu YK (2005) Protein database searches using compositionally adjusted substitution matrices. *FEBS J* **272**(20): 5101-5109

Andreasson C, Ljungdahl PO (2004) The N-terminal regulatory domain of Stp1p is modular and, fused to an artificial transcription factor, confers full Ssy1p-Ptr3p-Ssy5p sensor control. *Mol Cell Biol* **24**(17): 7503-7513

Aronov S, Gelin-Licht R, Zipor G, Haim L, Safran E, Gerst JE (2007) mRNAs encoding polarity and exocytosis factors are cotransported with the cortical endoplasmic reticulum to the incipient bud in Saccharomyces cerevisiae. *Mol Cell Biol* **27**(9): 3441-3455

Bakin A, Ofengand J (1993) Four newly located pseudouridylylate residues in Escherichia coli 23S ribosomal RNA are all at the peptidyltransferase center: analysis by the application of a new sequencing technique. *Biochemistry* **32**(37): 9754-9762

Bartel B, Wunning I, Varshavsky A (1990) The recognition component of the N-end rule pathway. *EMBO J* **9**(10): 3179-3189

Baßler J, Grandi P, Gadal O, Leßmann T, Petfalski E, Tollervey D, Lechner J, Hurt E (2001) Identification of a 60S preribosomal particle that is closely linked to nuclear export. *Mol Cell* **8**(3): 517-529

Baudin A, Ozier-Kalogeropoulos O, Denouel A, Lacroute F, Cullin C (1993) A simple and efficient method for direct gene deletion in Saccharomyces cerevisiae. *Nucleic Acids Res* **21**(14): 3329-3330

Beggs JD (2005) Lsm proteins and RNA processing. *Biochem Soc Trans* **33**(Pt 3): 433-438

Bobola N, Jansen RP, Shin TH, Nasmyth K (1996) Asymmetric accumulation of Ash1p in postanaphase nuclei depends on a myosin and restricts yeast mating-type switching to mother cells. *Cell* **84**(5): 699-709

Böhl F (2001) Identifizierung der Funktion von She2p bei der zytoplasmatischen mRNA-Lokalisation in Saccharomyces cerevisiae. Dr. rer. nat. Thesis, Zentrum für Molekulare Biologie, Universität Heidelberg, Heidelberg

Böhl F, Kruse C, Frank A, Ferring D, Jansen RP (2000) She2p, a novel RNA-binding protein tethers ASH1 mRNA to the Myo4p myosin motor via She3p. *EMBO J* **19**(20): 5514-5524

Boisvert FM, van Koningsbruggen S, Navascues J, Lamond AI (2007) The multifunctional nucleolus. *Nat Rev Mol Cell Biol* **8**(7): 574-585

Bond VC, Wold B (1993) Nucleolar localization of myc transcripts. *Mol Cell Biol* **13**(6): 3221-3230

Bousquet-Antonelli C, Henry Y, G'Elugne J P, Caizergues-Ferrer M, Kiss T (1997) A small nucleolar RNP protein is required for pseudouridylation of eukaryotic ribosomal RNAs. *EMBO J* **16**(15): 4770-4776

Bousquet-Antonelli C, Vanrobays E, Gelugne JP, Caizergues-Ferrer M, Henry Y (2000) Rrp8p is a yeast nucleolar protein functionally linked to Gar1p and involved in pre-rRNA cleavage at site A2. *RNA* **6**(6): 826-843

References

- Boyne JR, Whitehouse A (2006) Nucleolar trafficking is essential for nuclear export of intronless herpesvirus mRNA. *Proc Natl Acad Sci U S A* **103**(41): 15190-15195
- Briggs MW, Burkard KT, Butler JS (1998) Rrp6p, the yeast homologue of the human PM-Scl 100-kDa autoantigen, is essential for efficient 5.8 S rRNA 3' end formation. *J Biol Chem* **273**(21): 13255-13263
- Brodsky AS, Silver PA (2000) Pre-mRNA processing factors are required for nuclear export. *RNA* **6**(12): 1737-1749
- Burkhalter MD, Sogo JM (2004) rDNA enhancer affects replication initiation and mitotic recombination: Fob1 mediates nucleolytic processing independently of replication. *Mol Cell* **15**(3): 409-421
- Carmo-Fonseca M, Mendes-Soares L, Campos I (2000) To be or not to be in the nucleolus. *Nat Cell Biol* **2**(6): E107-112
- Chao FC (1957) Dissociation of macromolecular ribonucleoprotein of yeast. *Arch Biochem Biophys* **70**(2): 426-431
- Chao FC, Schachman HK (1956) The isolation and characterization of a macro-molecular ribonucleoprotein from yeast. *Arch Biochem Biophys* **61**(1): 220-230
- Chartrand P, Meng XH, Singer RH, Long RM (1999) Structural elements required for the localization of ASH1 mRNA and of a green fluorescent protein reporter particle in vivo. *Curr Biol* **9**(6): 333-336
- Chen DC, Yang BC, Kuo TT (1992) One-step transformation of yeast in stationary phase. *Curr Genet* **21**(1): 83-84
- Colau G, Thiry M, Leduc V, Bordonne R, Lafontaine DL (2004) The small nucle(ol)ar RNA cap trimethyltransferase is required for ribosome synthesis and intact nucleolar morphology. *Mol Cell Biol* **24**(18): 7976-7986
- Cole C, Barber JD, Barton GJ (2008) The Jpred 3 secondary structure prediction server. *Nucleic Acids Res* **36**(Web Server issue): W197-201
- Coleman KG, Steensma HY, Kaback DB, Pringle JR (1986) Molecular cloning of chromosome I DNA from *Saccharomyces cerevisiae*: isolation and characterization of the CDC24 gene and adjacent regions of the chromosome. *Mol Cell Biol* **6**(12): 4516-4525
- Collins SR, Kemmeren P, Zhao XC, Greenblatt JF, Spencer F, Holstege FC, Weissman JS, Krogan NJ (2007) Toward a comprehensive atlas of the physical interactome of *Saccharomyces cerevisiae*. *Mol Cell Proteomics* **6**(3): 439-450
- Condeelis J, Singer RH (2005) How and why does beta-actin mRNA target? *Biol Cell* **97**(1): 97-110
- Cramer P, Armache KJ, Baumli S, Benkert S, Brueckner F, Buchen C, Damsma GE, Dengl S, Geiger SR, Jasiak AJ, Jawhari A, Jennebach S, Kamenski T, Kettenberger H, Kuhn CD, Lehmann E, Leike K, Sydow JF, Vannini A (2008) Structure of eukaryotic RNA polymerases. *Annu Rev Biophys* **37**: 337-352
- Cross FR, Tinkelenberg AH (1991) A potential positive feedback loop controlling CLN1 and CLN2 gene expression at the start of the yeast cell cycle. *Cell* **65**(5): 875-883
- D'Amours D, Stegmeier F, Amon A (2004) Cdc14 and condensin control the dissolution of cohesin-independent chromosome linkages at repeated DNA. *Cell* **117**(4): 455-469
- Dahm R, Macchi P (2007) Human pathologies associated with defective RNA transport and localization in the nervous system. *Biol Cell* **99**(11): 649-661
- Decatur WA, Fournier MJ (2003) RNA-guided nucleotide modification of ribosomal and other RNAs. *J Biol Chem* **278**(2): 695-698
- Deng Y, Singer RH, Gu W (2008) Translation of ASH1 mRNA is repressed by Puf6p-Fun12p/eIF5B interaction and released by CK2 phosphorylation. *Genes Dev* **22**(8): 1037-1050
- Denman R, Colgan J, Nurse K, Ofengand J (1988) Crosslinking of the anticodon of P site bound tRNA to C-1400 of E.coli 16S RNA does not require the participation of the 50S subunit. *Nucleic Acids Res* **16**(1): 165-178

References

- Dez C, Houseley J, Tollervey D (2006) Surveillance of nuclear-restricted pre-ribosomes within a subnucleolar region of *Saccharomyces cerevisiae*. *EMBO J* **25**(7): 1534-1546
- Dez C, Tollervey D (2004) Ribosome synthesis meets the cell cycle. *Curr Opin Microbiol* **7**(6): 631-637
- Dihanich ME, Najarian D, Clark R, Gillman EC, Martin NC, Hopper AK (1987) Isolation and characterization of MOD5, a gene required for isopentenylation of cytoplasmic and mitochondrial tRNAs of *Saccharomyces cerevisiae*. *Mol Cell Biol* **7**(1): 177-184
- Dragon F, Gallagher JE, Compagnone-Post PA, Mitchell BM, Porwancher KA, Wehner KA, Wormsley S, Settlege RE, Shabanowitz J, Osheim Y, Beyer AL, Hunt DF, Baserga SJ (2002) A large nucleolar U3 ribonucleoprotein required for 18S ribosomal RNA biogenesis. *Nature* **417**(6892): 967-970
- Du T-G (2007) Role of nuclear RNP assembly in cytoplasmic mRNA localization. Dr. rer. nat. Thesis, Gene Center Munich and Institute for Biochemistry, Ludwig-Maximilians-Universität München, Munich
- Du TG, Jellbauer S, Müller M, Schmid M, Niessing D, Jansen RP (2008) Nuclear transit of the RNA-binding protein She2 is required for translational control of localized *ASH1* mRNA. *EMBO Rep* **9**(8): 781-787
- Dujon B, Alexandraki D, Andre B, Ansorge W, Baladron V, Ballesta JP, Banrevi A, Bolle PA, Bolotin-Fukuhara M, Bossier P, et al. (1994) Complete DNA sequence of yeast chromosome XI. *Nature* **369**(6479): 371-378
- Dundr M, Leno GH, Hammarskjöld ML, Rekosh D, Helga-Maria C, Olson MO (1995) The roles of nucleolar structure and function in the subcellular location of the HIV-1 Rev protein. *J Cell Sci* **108** (Pt 8): 2811-2823
- Emmott E, Hiscox JA (2009) Nucleolar targeting: the hub of the matter. *EMBO Rep* **10**(3): 231-238
- Entian KD, Schuster T, Hegemann JH, Becher D, Feldmann H, Guldener U, Gotz R, Hansen M, Hollenberg CP, Jansen G, Kramer W, Klein S, Kotter P, Kricke J, Launhardt H, Mannhaupt G, Maierl A, Meyer P, Mewes W, Munder T, Niedenthal RK, Ramezani Rad M, Rohmer A, Romer A, Hinnen A, et al. (1999) Functional analysis of 150 deletion mutants in *Saccharomyces cerevisiae* by a systematic approach. *Mol Gen Genet* **262**(4-5): 683-702
- Farina KL, Singer RH (2002) The nuclear connection in RNA transport and localization. *Trends Cell Biol* **12**(10): 466-472
- Fatica A, Cronshaw AD, Dlakic M, Tollervey D (2002) Ssf1p prevents premature processing of an early pre-60S ribosomal particle. *Mol Cell* **9**(2): 341-351
- Fatica A, Tollervey D (2002) Making ribosomes. *Curr Opin Cell Biol* **14**(3): 313-318
- Ferreira-Cerca S, Poll G, Gleizes PE, Tschochner H, Milkereit P (2005) Roles of eukaryotic ribosomal proteins in maturation and transport of pre-18S rRNA and ribosome function. *Mol Cell* **20**(2): 263-275
- Fink AL (2005) Natively unfolded proteins. *Curr Opin Struct Biol* **15**(1): 35-41
- Fontana F. (1781) *Traité sur le venin de la vipère, sur les poisons américains, sur le laurier-cerise et sur quelques autres poisons végétaux*. Gibelin, Firenze.
- Fromont-Racine M, Senger B, Saveanu C, Fasiolo F (2003) Ribosome assembly in eukaryotes. *Gene* **313**: 17-42
- Furic L, Maher-Laporte M, DesGroseillers L (2008) A genome-wide approach identifies distinct but overlapping subsets of cellular mRNAs associated with Stauf1- and Stauf2-containing ribonucleoprotein complexes. *RNA* **14**(2): 324-335
- Gabus C, Mazroui R, Tremblay S, Khandjian EW, Darlix JL (2004) The fragile X mental retardation protein has nucleic acid chaperone properties. *Nucleic Acids Res* **32**(7): 2129-2137
- Ganot P, Jady BE, Bortolin ML, Darzacq X, Kiss T (1999) Nucleolar factors direct the 2'-O-ribose methylation and pseudouridylation of U6 spliceosomal RNA. *Mol Cell Biol* **19**(10): 6906-6917
- Garí E, Piedrafita L, Aldea M, Herrero E (1997) A set of vectors with a tetracycline-regulatable promoter system for modulated gene expression in *Saccharomyces cerevisiae*. *Yeast* **13**(9): 837-848
- Gauss R, Trautwein M, Sommer T, Spang A (2005) New modules for the repeated internal and N-terminal epitope tagging of genes in *Saccharomyces cerevisiae*. *Yeast* **22**(1): 1-12

References

- Gavin AC, Aloy P, Grandi P, Krause R, Boesche M, Marzioch M, Rau C, Jensen LJ, Bastuck S, Dumpelfeld B, Edelmann A, Heurtier MA, Hoffman V, Hoefert C, Klein K, Hudak M, Michon AM, Schelder M, Schirle M, Remor M, Rudi T, Hooper S, Bauer A, Bouwmeester T, Casari G, Drewes G, Neubauer G, Rick JM, Kuster B, Bork P, Russell RB, Superti-Furga G (2006) Proteome survey reveals modularity of the yeast cell machinery. *Nature* **440**(7084): 631-636
- Gavin AC, Bosche M, Krause R, Grandi P, Marzioch M, Bauer A, Schultz J, Rick JM, Michon AM, Cruciat CM, Remor M, Hofert C, Schelder M, Brajenovic M, Ruffner H, Merino A, Klein K, Hudak M, Dickson D, Rudi T, Gnau V, Bauch A, Bastuck S, Huhse B, Leutwein C, Heurtier MA, Copley RR, Edelmann A, Querfurth E, Rybin V, Drewes G, Raida M, Bouwmeester T, Bork P, Seraphin B, Kuster B, Neubauer G, Superti-Furga G (2002) Functional organization of the yeast proteome by systematic analysis of protein complexes. *Nature* **415**(6868): 141-147
- Gerber AP, Herschlag D, Brown PO (2004) Extensive association of functionally and cytologically related mRNAs with Puf family RNA-binding proteins in yeast. *PLoS Biol* **2**(3): E79
- Gerbi SA, Borovjagin AV, Lange TS (2003) The nucleolus: a site of ribonucleoprotein maturation. *Curr Opin Cell Biol* **15**(3): 318-325
- Ghaemmaghami S, Huh WK, Bower K, Howson RW, Belle A, Dephoure N, O'Shea EK, Weissman JS (2003) Global analysis of protein expression in yeast. *Nature* **425**(6959): 737-741
- Gietz RD, Sugino A (1988) New yeast-Escherichia coli shuttle vectors constructed with in vitro mutagenized yeast genes lacking six-base pair restriction sites. *Gene* **74**(2): 527-534
- Giorgi C, Moore MJ (2007) The nuclear nurture and cytoplasmic nature of localized mRNPs. *Semin Cell Dev Biol* **18**(2): 186-193
- Goethe JW (1996) Goethes Werke · Hamburger Ausgabe, Band 12. 16. Aufl., C. H. Beck, München
- Gonsalvez GB, Lehmann KA, Ho DK, Stanitsa ES, Williamson JR, Long RM (2003) RNA-protein interactions promote asymmetric sorting of the ASH1 mRNA ribonucleoprotein complex. *RNA* **9**(11): 1383-1399
- Gorsch LC, Dockendorff TC, Cole CN (1995) A conditional allele of the novel repeat-containing yeast nucleoporin RAT7/NUP159 causes both rapid cessation of mRNA export and reversible clustering of nuclear pore complexes. *J Cell Biol* **129**(4): 939-955
- Gorski SA, Dundr M, Misteli T (2006) The road much traveled: trafficking in the cell nucleus. *Curr Opin Cell Biol* **18**(3): 284-290
- Grandi P, Rybin V, Bassler J, Petfalski E, Strauss D, Marzioch M, Schafer T, Kuster B, Tschochner H, Tollervey D, Gavin AC, Hurt E (2002) 90S pre-ribosomes include the 35S pre-rRNA, the U3 snoRNP, and 40S subunit processing factors but predominantly lack 60S synthesis factors. *Mol Cell* **10**(1): 105-115
- Grosshans H, Deinert K, Hurt E, Simos G (2001) Biogenesis of the signal recognition particle (SRP) involves import of SRP proteins into the nucleolus, assembly with the SRP-RNA, and Xpo1p-mediated export. *J Cell Biol* **153**(4): 745-762
- Gu W, Deng Y, Zenklusen D, Singer RH (2004) A new yeast PUF family protein, Puf6p, represses ASH1 mRNA translation and is required for its localization. *Genes Dev* **18**(12): 1452-1465
- Guldener U, Heck S, Fielder T, Beinhauer J, Hegemann JH (1996) A new efficient gene disruption cassette for repeated use in budding yeast. *Nucleic Acids Res* **24**(13): 2519-2524
- Gunasekaran K, Tsai CJ, Kumar S, Zanuy D, Nussinov R (2003) Extended disordered proteins: targeting function with less scaffold. *Trends Biochem Sci* **28**(2): 81-85
- Haarer BK, Petzold A, Lillie SH, Brown SS (1994) Identification of MYO4, a second class V myosin gene in yeast. *J Cell Sci* **107** (Pt 4): 1055-1064
- Hachet O, Ephrussi A (2004) Splicing of oskar RNA in the nucleus is coupled to its cytoplasmic localization. *Nature* **428**(6986): 959-963
- Halic M, Beckmann R (2005) The signal recognition particle and its interactions during protein targeting. *Curr Opin Struct Biol* **15**(1): 116-125

References

- Handwerger KE, Gall JG (2006) Subnuclear organelles: new insights into form and function. *Trends Cell Biol* **16**(1): 19-26
- Harnpicharnchai P, Jakovljevic J, Horsey E, Miles T, Roman J, Rout M, Meagher D, Imai B, Guo Y, Brame CJ, Shabanowitz J, Hunt DF, Woolford JL, Jr. (2001) Composition and functional characterization of yeast 66S ribosome assembly intermediates. *Mol Cell* **8**(3): 505-515
- Hasegawa Y, Irie K, Gerber AP (2008) Distinct roles for Khd1p in the localization and expression of bud-localized mRNAs in yeast. *RNA* **14**(11): 2333-2347
- Henras AK, Soudet J, Gerus M, Lebaron S, Caizergues-Ferrer M, Mouglin A, Henry Y (2008) The post-transcriptional steps of eukaryotic ribosome biogenesis. *Cell Mol Life Sci* **65**(15): 2334-2359
- Heuck A, Du TG, Jellbauer S, Richter K, Kruse C, Jaklin S, Muller M, Buchner J, Jansen RP, Niessing D (2007) Monomeric myosin V uses two binding regions for the assembly of stable translocation complexes. *Proc Natl Acad Sci U S A* **104**(50): 19778-19783
- Hibbett DS, Binder M, Bischoff JF, Blackwell M, Cannon PF, Eriksson OE, Huhndorf S, James T, Kirk PM, Lucking R, Thorsten Lumbsch H, Lutzoni F, Matheny PB, McLaughlin DJ, Powell MJ, Redhead S, Schoch CL, Spatafora JW, Stalpers JA, Vilgalys R, Aime MC, Aptroot A, Bauer R, Begerow D, Benny GL, Castlebury LA, Crous PW, Dai YC, Gams W, Geiser DM, Griffith GW, Gueidan C, Hawksworth DL, Hestmark G, Hosaka K, Humber RA, Hyde KD, Ironside JE, Koljalg U, Kurtzman CP, Larsson KH, Lichtwardt R, Longcore J, Miadlikowska J, Miller A, Moncalvo JM, Mozley-Standridge S, Oberwinkler F, Parmasto E, Reeb V, Rogers JD, Roux C, Ryvarden L, Sampaio JP, Schussler A, Sugiyama J, Thorn RG, Tibell L, Untereiner WA, Walker C, Wang Z, Weir A, Weiss M, White MM, Winka K, Yao YJ, Zhang N (2007) A higher-level phylogenetic classification of the Fungi. *Mycol Res* **111**(Pt 5): 509-547
- Hilleren P, McCarthy T, Rosbash M, Parker R, Jensen TH (2001) Quality control of mRNA 3'-end processing is linked to the nuclear exosome. *Nature* **413**(6855): 538-542
- Hiscox JA (2007) RNA viruses: hijacking the dynamic nucleolus. *Nat Rev Microbiol* **5**(2): 119-127
- Horkheimer M, Adorno TW (1969) Dialektik der Aufklärung. Limitierte Sonderausgabe, Fischer Taschenbuch Verlag, Frankfurt a. M.
- Horsey EW, Jakovljevic J, Miles TD, Harnpicharnchai P, Woolford JL, Jr. (2004) Role of the yeast Rrp1 protein in the dynamics of pre-ribosome maturation. *RNA* **10**(5): 813-827
- Huh WK, Falvo JV, Gerke LC, Carroll AS, Howson RW, Weissman JS, O'Shea EK (2003) Global analysis of protein localization in budding yeast. *Nature* **425**(6959): 686-691
- Hüttelmaier S, Zenklusen D, Lederer M, Dichtenberg J, Lorenz M, Meng X, Bassell GJ, Condeelis J, Singer RH (2005) Spatial regulation of beta-actin translation by Src-dependent phosphorylation of ZBP1. *Nature* **438**(7067): 512-515
- Ideue T, Azad AK, Yoshida J, Matsusaka T, Yanagida M, Ohshima Y, Tani T (2004) The nucleolus is involved in mRNA export from the nucleus in fission yeast. *J Cell Sci* **117**(Pt 14): 2887-2895
- Irie K, Tadauchi T, Takizawa PA, Vale RD, Matsumoto K, Herskowitz I (2002) The Khd1 protein, which has three KH RNA-binding motifs, is required for proper localization of ASH1 mRNA in yeast. *EMBO J* **21**(5): 1158-1167
- Jäger AV, De Gaudenzi JG, Cassola A, D'Orso I, Frasch AC (2007) mRNA maturation by two-step trans-splicing/polyadenylation processing in trypanosomes. *Proc Natl Acad Sci U S A* **104**(7): 2035-2042
- Jäger S, Strayle J, Heinemeyer W, Wolf DH (2001) Cic1, an adaptor protein specifically linking the 26S proteasome to its substrate, the SCF component Cdc4. *EMBO J* **20**(16): 4423-4431
- Jambhekar A, DeRisi JL (2007) Cis-acting determinants of asymmetric, cytoplasmic RNA transport. *Rna* **13**(5): 625-642
- Jambhekar A, McDermott K, Sorber K, Shepard KA, Vale RD, Takizawa PA, DeRisi JL (2005) Unbiased selection of localization elements reveals cis-acting determinants of mRNA bud localization in *Saccharomyces cerevisiae*. *Proc Natl Acad Sci U S A* **102**(50): 18005-18010

References

- Janke C, Magiera MM, Rathfelder N, Taxis C, Reber S, Maekawa H, Moreno-Borchart A, Doenges G, Schwob E, Schiebel E, Knop M (2004) A versatile toolbox for PCR-based tagging of yeast genes: new fluorescent proteins, more markers and promoter substitution cassettes. *Yeast* **21**(11): 947-962
- Jansen RP (2001) mRNA localization: message on the move. *Nat Rev Mol Cell Biol* **2**(4): 247-256
- Jansen RP, Dowzer C, Michaelis C, Galova M, Nasmyth K (1996) Mother cell-specific HO expression in budding yeast depends on the unconventional myosin myo4p and other cytoplasmic proteins. *Cell* **84**(5): 687-697
- Jellbauer S, Jansen RP (2008) A putative function of the nucleolus in the assembly or maturation of specialized messenger ribonucleoprotein complexes. *RNA Biol* **5**(4): 225-229
- Jensen TH, Patricio K, McCarthy T, Rosbash M (2001) A block to mRNA nuclear export in *S. cerevisiae* leads to hyperadenylation of transcripts that accumulate at the site of transcription. *Mol Cell* **7**(4): 887-898
- Jentsch S, McGrath JP, Varshavsky A (1987) The yeast DNA repair gene RAD6 encodes a ubiquitin-conjugating enzyme. *Nature* **329**(6135): 131-134
- Johnston M, Hillier L, Riles L, Albermann K, Andre B, Ansorge W, Benes V, Bruckner M, Delius H, Dubois E, Dusterhoft A, Entian KD, Floeth M, Goffeau A, Hebling U, Heumann K, Heuss-Neitzel D, Hilbert H, Hilger F, Kleine K, Kotter P, Louis EJ, Messenguy F, Mewes HW, Hoheisel JD, et al. (1997) The nucleotide sequence of *Saccharomyces cerevisiae* chromosome XII. *Nature* **387**(6632 Suppl): 87-90
- Jüschke C, Ferring D, Jansen RP, Seedorf M (2004) A novel transport pathway for a yeast plasma membrane protein encoded by a localized mRNA. *Curr Biol* **14**(5): 406-411
- Kadowaki T, Chen S, Hitomi M, Jacobs E, Kumagai C, Liang S, Schneider R, Singleton D, Wisniewska J, Tartakoff AM (1994) Isolation and characterization of *Saccharomyces cerevisiae* mRNA transport-defective (mtr) mutants. *J Cell Biol* **126**(3): 649-659
- Kadowaki T, Schneider R, Hitomi M, Tartakoff AM (1995) Mutations in nucleolar proteins lead to nucleolar accumulation of polyA⁺ RNA in *Saccharomyces cerevisiae*. *Mol Biol Cell* **6**(9): 1103-1110
- Kalderon D, Roberts BL, Richardson WD, Smith AE (1984) A short amino acid sequence able to specify nuclear location. *Cell* **39**(3 Pt 2): 499-509
- Kasper M (1997) Reclams Lateinisches Zitateslexikon. 2. Aufl., Philipp Reclam jun., Stuttgart
- Kiebler MA, Jansen RP, Dahm R, Macchi P (2005) A putative nuclear function for mammalian Staufen. *Trends Biochem Sci* **30**(5): 228-231
- Kim M, Bellini M, Ceman S (2009) Fragile X mental retardation protein FMRP binds mRNAs in the nucleus. *Mol Cell Biol* **29**(1): 214-228
- Kim SH, Ryabov EV, Kalinina NO, Rakitina DV, Gillespie T, MacFarlane S, Haupt S, Brown JW, Taliansky M (2007) Cajal bodies and the nucleolus are required for a plant virus systemic infection. *EMBO J* **26**(8): 2169-2179
- Kiss T (2002) Small nucleolar RNAs: an abundant group of noncoding RNAs with diverse cellular functions. *Cell* **109**(2): 145-148
- Knop M, Finger A, Braun T, Hellmuth K, Wolf DH (1996) Der1, a novel protein specifically required for endoplasmic reticulum degradation in yeast. *EMBO J* **15**(4): 753-763
- Knop M, Siegers K, Pereira G, Zachariae W, Winsor B, Nasmyth K, Schiebel E (1999) Epitope tagging of yeast genes using a PCR-based strategy: more tags and improved practical routines. *Yeast* **15**(10B): 963-972
- Komili S, Farny NG, Roth FP, Silver PA (2007) Functional specificity among ribosomal proteins regulates gene expression. *Cell* **131**(3): 557-571
- Krautz H-W (Hg.) (1985) Epikur - Briefe Sprüche Werkfragmente (Griechisch/Deutsch). Philipp Reclam jun., Stuttgart
- Kress TL, Yoon YJ, Mowry KL (2004) Nuclear RNP complex assembly initiates cytoplasmic RNA localization. *J Cell Biol* **165**(2): 203-211

References

- Krogan NJ, Cagney G, Yu H, Zhong G, Guo X, Ignatchenko A, Li J, Pu S, Datta N, Tikuisis AP, Punna T, Peregrin-Alvarez JM, Shales M, Zhang X, Davey M, Robinson MD, Paccanaro A, Bray JE, Sheung A, Beattie B, Richards DP, Canadien V, Lalev A, Mena F, Wong P, Starostine A, Canete MM, Vlasblom J, Wu S, Orsi C, Collins SR, Chandran S, Haw R, Rilstone JJ, Gandhi K, Thompson NJ, Musso G, St Onge P, Ghanny S, Lam MH, Butland G, Altaf-Ul AM, Kanaya S, Shilatifard A, O'Shea E, Weissman JS, Ingles CJ, Hughes TR, Parkinson J, Gerstein M, Wodak SJ, Emili A, Greenblatt JF (2006) Global landscape of protein complexes in the yeast *Saccharomyces cerevisiae*. *Nature* **440**(7084): 637-643
- Lam KB, Marmur J (1977) Isolation and characterization of *Saccharomyces cerevisiae* glycolytic pathway mutants. *J Bacteriol* **130**(2): 746-749
- Larkin MA, Blackshields G, Brown NP, Chenna R, McGettigan PA, McWilliam H, Valentin F, Wallace IM, Wilm A, Lopez R, Thompson JD, Gibson TJ, Higgins DG (2007) Clustal W and Clustal X version 2.0. *Bioinformatics* **23**(21): 2947-2948
- Lécuyer E, Yoshida H, Parthasarathy N, Alm C, Babak T, Cerovina T, Hughes TR, Tomancak P, Krause HM (2007) Global analysis of mRNA localization reveals a prominent role in organizing cellular architecture and function. *Cell* **131**(1): 174-187
- Liang XH, Xu YX, Michaeli S (2002) The spliced leader-associated RNA is a trypanosome-specific sn(o) RNA that has the potential to guide pseudouridine formation on the SL RNA. *RNA* **8**(2): 237-246
- Linding R, Jensen LJ, Diella F, Bork P, Gibson TJ, Russell RB (2003) Protein disorder prediction: implications for structural proteomics. *Structure* **11**(11): 1453-1459
- Liu Y, Liang S, Tartakoff AM (1996) Heat shock disassembles the nucleolus and inhibits nuclear protein import and poly(A)⁺ RNA export. *EMBO J* **15**(23): 6750-6757
- Long RM, Gu W, Meng X, Gonsalvez G, Singer RH, Chartrand P (2001) An exclusively nuclear RNA-binding protein affects asymmetric localization of ASH1 mRNA and Ash1p in yeast. *J Cell Biol* **153**(2): 307-318
- Long RM, Singer RH, Meng X, Gonzalez I, Nasmyth K, Jansen RP (1997) Mating type switching in yeast controlled by asymmetric localization of ASH1 mRNA. *Science* **277**(5324): 383-387
- Longtine MS, McKenzie A, 3rd, Demarini DJ, Shah NG, Wach A, Brachet A, Philippsen P, Pringle JR (1998) Additional modules for versatile and economical PCR-based gene deletion and modification in *Saccharomyces cerevisiae*. *Yeast* **14**(10): 953-961
- Macchi P, Brownawell AM, Grunewald B, DesGroseillers L, Macara IG, Kiebler MA (2004) The brain-specific double-stranded RNA-binding protein Stauf2: nucleolar accumulation and isoform-specific exportin-5-dependent export. *J Biol Chem* **279**(30): 31440-31444
- Maden BE, Corbett ME, Heeney PA, Pugh K, Ajuh PM (1995) Classical and novel approaches to the detection and localization of the numerous modified nucleotides in eukaryotic ribosomal RNA. *Biochimie* **77**(1-2): 22-29
- Maggi LB, Jr., Weber JD (2005) Nucleolar adaptation in human cancer. *Cancer Invest* **23**(7): 599-608
- Maier R (Hg.) (1991) Das römische Kochbuch des Apicius (Lateinisch/Deutsch). Philipp Reclam jun., Stuttgart
- Martin KC, Ephrussi A (2009) mRNA localization: gene expression in the spatial dimension. *Cell* **136**(4): 719-730
- Massenet S, Motorin Y, Lafontaine DL, Hurt EC, Grosjean H, Branlant C (1999) Pseudouridine mapping in the *Saccharomyces cerevisiae* spliceosomal U small nuclear RNAs (snRNAs) reveals that pseudouridine synthase pus1p exhibits a dual substrate specificity for U2 snRNA and tRNA. *Mol Cell Biol* **19**(3): 2142-2154
- Matera AG, Terns RM, Terns MP (2007) Non-coding RNAs: lessons from the small nuclear and small nucleolar RNAs. *Nat Rev Mol Cell Biol* **8**(3): 209-220
- Michienzi A, Cagnon L, Bahner I, Rossi JJ (2000) Ribozyme-mediated inhibition of HIV 1 suggests nucleolar trafficking of HIV-1 RNA. *Proc Natl Acad Sci U S A* **97**(16): 8955-8960
- Miki T, Takano K, Yoneda Y (2005) The role of mammalian Stauf on mRNA traffic: a view from its nucleocytoplasmic shuttling function. *Cell Struct Funct* **30**(2): 51-56
- Misteli T (2001) The concept of self-organization in cellular architecture. *J Cell Biol* **155**(2): 181-185

References

- Moss T, Stefanovsky VY (2002) At the center of eukaryotic life. *Cell* **109**(5): 545-548
- Mumberg D, Muller R, Funk M (1994) Regulatable promoters of *Saccharomyces cerevisiae*: comparison of transcriptional activity and their use for heterologous expression. *Nucleic Acids Res* **22**(25): 5767-5768
- Münchow S, Sauter C, Jansen RP (1999) Association of the class V myosin Myo4p with a localised messenger RNA in budding yeast depends on She proteins. *J Cell Sci* **112 (Pt 10)**: 1511-1518
- Nash RS, Volpe T, Fitcher B (2001) Isolation and characterization of WHI3, a size-control gene of *Saccharomyces cerevisiae*. *Genetics* **157**(4): 1469-1480
- Ni L, Snyder M (2001) A genomic study of the bipolar bud site selection pattern in *Saccharomyces cerevisiae*. *Mol Biol Cell* **12**(7): 2147-2170
- Niessing D, Huttelmaier S, Zenklusen D, Singer RH, Burley SK (2004) She2p is a novel RNA binding protein with a basic helical hairpin motif. *Cell* **119**(4): 491-502
- Nissan TA, Bassler J, Petfalski E, Tollervey D, Hurt E (2002) 60S pre-ribosome formation viewed from assembly in the nucleolus until export to the cytoplasm. *EMBO J* **21**(20): 5539-5547
- Olivier C, Poirier G, Gendron P, Boisgontier A, Major F, Chartrand P (2005) Identification of a conserved RNA motif essential for She2p recognition and mRNA localization to the yeast bud. *Mol Cell Biol* **25**(11): 4752-4766
- Olson MO, Dundr M, Szebeni A (2000) The nucleolus: an old factory with unexpected capabilities. *Trends Cell Biol* **10**(5): 189-196
- Pan F, Huttelmaier S, Singer RH, Gu W (2007) ZBP2 facilitates binding of ZBP1 to beta-actin mRNA during transcription. *Mol Cell Biol* **27**(23): 8340-8351
- Paquin N, Menade M, Poirier G, Donato D, Drouet E, Chartrand P (2007) Local activation of yeast ASH1 mRNA translation through phosphorylation of Khd1p by the casein kinase Yck1p. *Mol Cell* **26**(6): 795-809
- Politz JC, Lewandowski LB, Pederson T (2002) Signal recognition particle RNA localization within the nucleolus differs from the classical sites of ribosome synthesis. *J Cell Biol* **159**(3): 411-418
- Politz JC, Polena I, Trask I, Bazett-Jones DP, Pederson T (2005) A nonribosomal landscape in the nucleolus revealed by the stem cell protein nucleostemin. *Mol Biol Cell* **16**(7): 3401-3410
- Pope B, Kent HM (1996) High efficiency 5 min transformation of *Escherichia coli*. *Nucleic Acids Res* **24**(3): 536-537
- Preacher KJ. (2001) Calculation for the chi-square test: An interactive calculation tool for chi-square tests of goodness of fit and independence [Computer software]. Lawrence, KS, Vol. 2009.
- Prenninger S, Schroeder R, Semrad K (2006) Assaying RNA chaperone activity in vivo in bacteria using a ribozyme folding trap. *Nat Protoc* **1**(3): 1273-1277
- Puig O, Caspary F, Rigaut G, Rutz B, Bouveret E, Bragado-Nilsson E, Wilm M, Seraphin B (2001) The tandem affinity purification (TAP) method: a general procedure of protein complex purification. *Methods* **24**(3): 218-229
- Rajavel M, Philip B, Buehrer BM, Errede B, Levin DE (1999) Mid2 is a putative sensor for cell integrity signaling in *Saccharomyces cerevisiae*. *Mol Cell Biol* **19**(6): 3969-3976
- Rajkowitsch L, Semrad K, Mayer O, Schroeder R (2005) Assays for the RNA chaperone activity of proteins. *Biochem Soc Trans* **33**(Pt 3): 450-456
- Raška I, Shaw PJ, Cmarko D (2006) Structure and function of the nucleolus in the spotlight. *Curr Opin Cell Biol* **18**(3): 325-334
- Reichow SL, Hamma T, Ferre-D'Amare AR, Varani G (2007) The structure and function of small nucleolar ribonucleoproteins. *Nucleic Acids Res* **35**(5): 1452-1464
- Rigaut G, Shevchenko A, Rutz B, Wilm M, Mann M, Seraphin B (1999) A generic protein purification method for protein complex characterization and proteome exploration. *Nat Biotechnol* **17**(10): 1030-1032
- Rippel P (Hg.)(1986) Niccolò Macchiavelli - Il principe (Italienisch/Deutsch). Philipp Reclam jun., Stuttgart

References

- Rotenberg MO, Moritz M, Woolford JL, Jr. (1988) Depletion of *Saccharomyces cerevisiae* ribosomal protein L16 causes a decrease in 60S ribosomal subunits and formation of half-mer polyribosomes. *Genes Dev* **2**(2): 160-172
- Sambrook J, Russell DW (2001) *Molecular cloning : a laboratory manual*, 3rd edn. Cold Spring Harbor, N.Y.: Cold Spring Harbor Laboratory Press.
- Sanchez-Diaz A, Kanemaki M, Marchesi V, Labib K (2004) Rapid depletion of budding yeast proteins by fusion to a heat-inducible degron. *Sci STKE* **2004**(223): PL8
- Saveanu C, Namane A, Gleizes PE, Lebreton A, Rousselle JC, Noaillac-Depeyre J, Gas N, Jacquier A, Fromont-Racine M (2003) Sequential protein association with nascent 60S ribosomal particles. *Mol Cell Biol* **23**(13): 4449-4460
- Saveanu C, Rousselle JC, Lenormand P, Namane A, Jacquier A, Fromont-Racine M (2007) The p21-activated protein kinase inhibitor Skb15 and its budding yeast homologue are 60S ribosome assembly factors. *Mol Cell Biol* **27**(8): 2897-2909
- Schäfer T, Strauß D, Petfalski E, Tollervy D, Hurt E (2003) The path from nucleolar 90S to cytoplasmic 40S pre-ribosomes. *EMBO J* **22**(6): 1370-1380
- Schmid M, Jaedicke A, Du TG, Jansen RP (2006) Coordination of endoplasmic reticulum and mRNA localization to the yeast bud. *Curr Biol* **16**(15): 1538-1543
- Schneiter R, Kadowaki T, Tartakoff AM (1995) mRNA transport in yeast: time to reinvestigate the functions of the nucleolus. *Mol Biol Cell* **6**(4): 357-370
- Schroeder R, Barta A, Semrad K (2004) Strategies for RNA folding and assembly. *Nat Rev Mol Cell Biol* **5**(11): 908-919
- Segref A, Sharma K, Doye V, Hellwig A, Huber J, Luhrmann R, Hurt E (1997) Mex67p, a novel factor for nuclear mRNA export, binds to both poly(A)+ RNA and nuclear pores. *Embo J* **16**(11): 3256-3271
- Seiser RM, Sundberg AE, Wollam BJ, Zobel-Thropp P, Baldwin K, Spector MD, Lycan DE (2006) Ltv1 is required for efficient nuclear export of the ribosomal small subunit in *Saccharomyces cerevisiae*. *Genetics* **174**(2): 679-691
- Sellers JR (2000) Myosins: a diverse superfamily. *Biochim Biophys Acta* **1496**(1): 3-22
- SGDproject. *Saccharomyces Genome Database*. www.yeastgenome.org; March 2009
- Shen Z, Paquin N, Forget A, Chartrand P (2009) Nuclear Shuttling of She2p Couples ASH1 mRNA Localization to its Translational Repression by Recruiting Loc1p and Puf6p. *Mol Biol Cell*
- Shepard KA, Gerber AP, Jambhekar A, Takizawa PA, Brown PO, Herschlag D, DeRisi JL, Vale RD (2003) Widespread cytoplasmic mRNA transport in yeast: identification of 22 bud-localized transcripts using DNA microarray analysis. *Proc Natl Acad Sci U S A* **100**(20): 11429-11434
- Sidebottom E, Harris H (1969) The role of the nucleolus in the transfer of RNA from nucleus to cytoplasm. *J Cell Sci* **5**(2): 351-364
- Smirnov MN, Smirnov VN, Budowsky EI, Inge-Vechtomov SG, Serebrjakov NG (1967) Red pigment of adenine-deficient yeast *Saccharomyces cerevisiae*. *Biochem Biophys Res Commun* **27**(3): 299-304
- Spahn CM, Beckmann R, Eswar N, Penczek PA, Sali A, Blobel G, Frank J (2001) Structure of the 80S ribosome from *Saccharomyces cerevisiae*--tRNA-ribosome and subunit-subunit interactions. *Cell* **107**(3): 373-386
- Spassov DS, Jurecic R (2003) The PUF family of RNA-binding proteins: does evolutionarily conserved structure equal conserved function? *IUBMB Life* **55**(7): 359-366
- Sträßer K, Masuda S, Mason P, Pfannstiel J, Oppizzi M, Rodriguez-Navarro S, Rondon AG, Aguilera A, Struhl K, Reed R, Hurt E (2002) TREX is a conserved complex coupling transcription with messenger RNA export. *Nature* **417**(6886): 304-308
- Takizawa PA, DeRisi JL, Wilhelm JE, Vale RD (2000) Plasma membrane compartmentalization in yeast by messenger RNA transport and a septin diffusion barrier. *Science* **290**(5490): 341-344

References

- Tarassov K, Messier V, Landry CR, Radinovic S, Serna Molina MM, Shames I, Malitskaya Y, Vogel J, Bussey H, Michnick SW (2008) An in vivo map of the yeast protein interactome. *Science* **320**(5882): 1465-1470
- Thiry M, Lafontaine DL (2005) Birth of a nucleolus: the evolution of nucleolar compartments. *Trends Cell Biol* **15**(4): 194-199
- Thomsen R, Libri D, Boulay J, Rosbash M, Jensen TH (2003) Localization of nuclear retained mRNAs in *Saccharomyces cerevisiae*. *RNA* **9**(9): 1049-1057
- Tolerico LH, Benko AL, Aris JP, Stanford DR, Martin NC, Hopper AK (1999) *Saccharomyces cerevisiae* Mod5p-II contains sequences antagonistic for nuclear and cytosolic locations. *Genetics* **151**(1): 57-75
- Tong AH, Evangelista M, Parsons AB, Xu H, Bader GD, Page N, Robinson M, Raghibizadeh S, Hogue CW, Bussey H, Andrews B, Tyers M, Boone C (2001) Systematic genetic analysis with ordered arrays of yeast deletion mutants. *Science* **294**(5550): 2364-2368
- Torres-Rosell J, Machin F, Jarmuz A, Aragon L (2004) Nucleolar segregation lags behind the rest of the genome and requires Cdc14p activation by the FEAR network. *Cell Cycle* **3**(4): 496-502
- Trumtel S, Leger-Silvestre I, Gleizes PE, Teulieres F, Gas N (2000) Assembly and functional organization of the nucleolus: ultrastructural analysis of *Saccharomyces cerevisiae* mutants. *Mol Biol Cell* **11**(6): 2175-2189
- Urbinati CR, Gonsalvez GB, Aris JP, Long RM (2006) Loc1p is required for efficient assembly and nuclear export of the 60S ribosomal subunit. *Mol Genet Genomics* **276**(4): 369-377
- Venema J, Tollervey D (1999) Ribosome synthesis in *Saccharomyces cerevisiae*. *Annu Rev Genet* **33**: 261-311
- Verna J, Lodder A, Lee K, Vagts A, Ballester R (1997) A family of genes required for maintenance of cell wall integrity and for the stress response in *Saccharomyces cerevisiae*. *Proc Natl Acad Sci U S A* **94**(25): 13804-13809
- Wach A, Brachat A, Alberti-Segui C, Rebischung C, Philippsen P (1997) Heterologous HIS3 marker and GFP reporter modules for PCR-targeting in *Saccharomyces cerevisiae*. *Yeast* **13**(11): 1065-1075
- Wach A, Brachat A, Pohlmann R, Philippsen P (1994) New heterologous modules for classical or PCR-based gene disruptions in *Saccharomyces cerevisiae*. *Yeast* **10**(13): 1793-1808
- Wang SS, Hopper AK (1988) Isolation of a yeast gene involved in species-specific pre-tRNA processing. *Mol Cell Biol* **8**(12): 5140-5149
- Warner JR (1999) The economics of ribosome biosynthesis in yeast. *Trends Biochem Sci* **24**(11): 437-440
- Werner-Washburne M, Stone DE, Craig EA (1987) Complex interactions among members of an essential subfamily of hsp70 genes in *Saccharomyces cerevisiae*. *Mol Cell Biol* **7**(7): 2568-2577
- Wharton RP, Aggarwal AK (2006) mRNA regulation by Puf domain proteins. *Sci STKE* **2006**(354): pe37
- Wilhelm JE, Smibert CA (2005) Mechanisms of translational regulation in *Drosophila*. *Biol Cell* **97**(4): 235-252
- Wilmes GM, Bergkessel M, Bandyopadhyay S, Shales M, Braberg H, Cagney G, Collins SR, Whitworth GB, Kress TL, Weissman JS, Ideker T, Guthrie C, Krogan NJ (2008) A genetic interaction map of RNA-processing factors reveals links between Sem1/Dss1-containing complexes and mRNA export and splicing. *Mol Cell* **32**(5): 735-746
- Wolin SL, Wurtmann EJ (2006) Molecular chaperones and quality control in noncoding RNA biogenesis. *Cold Spring Harb Symp Quant Biol* **71**: 505-511
- Yoo CJ, Wolin SL (1994) La proteins from *Drosophila melanogaster* and *Saccharomyces cerevisiae*: a yeast homolog of the La autoantigen is dispensable for growth. *Mol Cell Biol* **14**(8): 5412-5424
- Zhang A, Derbyshire V, Salvo JL, Belfort M (1995) *Escherichia coli* protein StpA stimulates self-splicing by promoting RNA assembly in vitro. *RNA* **1**(8): 783-793
- Zuk D, Belk JP, Jacobson A (1999) Temperature-sensitive mutations in the *Saccharomyces cerevisiae* MRT4, GRC5, SLA2 and THS1 genes result in defects in mRNA turnover. *Genetics* **153**(1): 35-47

Qui dedit beneficium, taceat.
Narret, qui accepit.

L. Annaeus Seneca, *De beneficiis* 2,11,2.

Acknowledgements

Ich bedanke mich ganz herzlich bei allen, die zum Gelingen dieser Arbeit beigetragen haben.

Zuallererst möchte ich meinem Doktorvater Ralf-Peter Jansen danken: für ein Thema, das erst nach und nach eine definierte Form annahm, aber immer fordernd, spannend und auch kompetitiv war und darüber hinaus die Gelegenheit bot, mit anderen im Team zusammenzuarbeiten. Er stattete mich mit einem hohen Maß an wissenschaftlicher Freiheit aus, indem er Anregungen statt Anweisungen gab, und ermöglichte mir den Besuch wissenschaftlicher Konferenzen sowie die Mitarbeit in einem Doktorandenprogramm des Elitenetzwerks Bayern.

Roland Beckmann danke ich für die Erstellung des Zweitgutachtens und fruchtbare Diskussionen über Loc1.

Ohne Euch, Claus und Dengl, wären die vergangenen vier Jahre um einiges ärmer gewesen. Das Kaffeeritual um halb zwölf, mit aufmunternden Gesprächen über Projektrückschläge, Institutspolitik und nicht zuletzt Fußball hat mir an vielen Tagen geholfen, den Spaß nicht zu verlieren. Nach Claus' Weggang konnte der Mediator Mob mit Laurent, Martin, Christian und Larissa einen guten Teil der Lücke schließen.

Vielen Dank, Tung, für die harmonische und erfolgreiche Zusammenarbeit auf dem She2-Nucleolus-Projekt. Mit Dir, Maria, konnte ich die bayerische Kultur und Sprachfärbung im Labor aufrechterhalten. Susi, Dir danke ich für die ausgezeichnete Organisation im Labor und dafür, dass uns dank Deines großartigen Verhandlungsgeschicks nie das Geld ausgegangen ist. Danke, Gonçalo, für Dein sonniges Gemüt und gemeinsame Feiern. Vielen Dank auch Dir, Heidrun, für geteiltes Leid an der Gradientenmaschine, Gespräche über Räder und TransAlp und dafür, dass Du nun als Letzte die Münchner Jansen-Fahne hochhältst.

Mein Dank gilt auch Euch, Emanuel und Lina, für ausschweifende Diskussionen über unsere Zukunft. Eli, bei Dir bedanke ich mich für die Hilfe bei den Sequenziergelen, bei Dir, Marisa, für die gegenseitigen Anregungen und Aufmunterungen.

Philipp Milkereit und Sébastien Ferreira-Cerca danke ich für die Einladung nach Regensburg, um dort Experimente durchzuführen, sowie für hilfreiche Vorschläge, mein Projekt weiterzuentwickeln.

Dem Doktorandenprogramm „Protein Dynamics in Health and Disease“ des Elitenetzwerks Bayern danke ich für die großzügige Unterstützung, meinen Mitdoktoranden im Programm für interessante Seminare, Retreats und den guten Zusammenhalt.

Kathrin, bei Dir bedanke ich mich sehr herzlich, dass Du in den vergangenen Jahren für mich da warst, für die Chauffeurdienste und die erholsamen Ausflüge nach Würth a. D. zum Rothfischer-Clan.

Schließlich möchte ich ganz besonders meiner Familie danken, vor allem meinen Eltern, die während meiner langen Ausbildung alles getan haben, um mich bestmöglich zu unterstützen.

Curriculum Vitae

Name	Stephan Jellbauer
Geburtsdatum	31.01.1979
Geburtsort	München
Nationalität	deutsch
Familienstand	ledig

Ausbildung

seit 04.2005	Promotion “The nucleolus – a nuclear compartment with impact on cytoplasmic RNA localization” bei Prof. Dr. R.-P. Jansen, Genzentrum, Ludwig-Maximilians-Universität (LMU) München
10.2002 – 07.2003	Auslandsaufenthalt bei Prof. Dr. M. Cresti, Università degli Studi di Siena, Italien
11.1999 – 02.2005	Studium Diplom-Biochemie Abschluss: Dipl.-Biochem. Univ. Universität Regensburg Hauptfächer: Biochemie, Organische Chemie, Molekularbiologie
09.1989 – 06.1998	Gymnasium Abschluss: Allgemeine Hochschulreife Luitpold-Gymnasium München (09.1996 – 06.1998) Michaeli-Gymnasium München (09.1989 – 08.1996)
09.1985 – 07.1989	Grundschule Grundschule an der Grafinger Str. 71, München

Auszeichnungen

seit 04.2007	Internationales Doktorandenprogramm „Protein Dynamics in Health & Disease“ im Rahmen des Elitenetzwerks Bayern (ENB)
11.2002 – 06.2003	Jahresstipendium des Deutschen Akademischen Austauschdienstes (DAAD)
11.1999 – 10.2002 07.2003 – 09.2004	Stipendium nach dem Bayerischen Begabtenförderungs- gesetz (BayBFG)

Übersetzungen der fremdsprachigen Zitate:

- Summary: Man muss erkennen, dass eine kurze wie eine lange Erklärung auf dasselbe abzielen.
- Results: (...) ich könnte kein größeres Geschenk machen, als die Gelegenheit zu geben, in kürzester Zeit in all das Einblick zu nehmen, was ich in so vielen Jahren und unter so vielen Unannehmlichkeiten erfahren und verstanden habe.
- Discussion: Niemals sagt die Natur das eine, die Weisheit das andere.
- Methods: So kocht man das: (...)
- Acknowledgements: Wer eine Wohltat erwiesen hat, soll schweigen. Der soll (davon) erzählen, der sie empfangen hat.
-